

Sampling and extraction methods for soil inorganic N determination to calibrate the EM38 in irrigated fields

by

Diandra Steenekamp

Submitted in fulfilment of the requirements in respect of the
Master's Degree Magister Scientiae Agriculturae in the
Department of Soil, Crop and Climate Sciences in the
Faculty of Natural and Agricultural Sciences at the
University of the Free State Bloemfontein, South Africa

26 June 2019

Supervisor: Prof LD van Rensburg

Co-supervisors: Prof CC du Preez & Dr JH Barnard

DECLARATION

I, Diandra Steenekamp, declare that:

- the Master's Degree research dissertation that I herewith submit for the Master's Degree qualification Magister Scientiae Agriculturae at the University of the Free State is my own independent work, and that I have not previously submitted it for a qualification at another institution of higher education.
- I also agree that the University of the Free State has the sole right to the publication of this dissertation.

Diandra Steenekamp

A handwritten signature in black ink, appearing to read 'Diandra Steenekamp', is written over a horizontal line. The signature is stylized and cursive.

Signature

TABLE OF CONTENTS

ACKNOWLEDGEMENTS	vi
LIST OF FIGURES	vii
LIST OF TABLES	ix
LIST OF APPENDICES	x
ABSTRACT	xi
CHAPTER 1. MOTIVATION, OBJECTIVES AND LAYOUT	1
1.1 Motivation and objectives	1
1.2 Organization of the dissertation	3
CHAPTER 2. LITERATURE REVIEW	4
2.1 Introduction	4
2.2 Soil sampling for nutrient level determination	4
2.2.1 Traditional sampling approach	4
2.2.2 Site specific sampling approach.....	6
2.2.2.1 Grid sampling method	6
2.2.2.2 Management zone sampling method.....	9
2.2.2.3 Geostatistical software-based sampling method.....	10
2.2.3 Perspective on site-specific soil sampling	10
2.2.4 Choosing a suitable site-specific sampling method	12
2.2.5 Soil sample collection for inorganic N determination	14
2.2.5.1 Sampling time	14
2.2.5.2 Sampling depth	15
2.2.5.3 Sample drying	16
2.2.5.4 Sample storage	18
2.3 Extraction and determination methods for soil inorganic N	19
2.3.1 Extraction of inorganic N	19
2.3.1.1 Extraction of nitrate	19
2.3.1.2 Extraction of ammonium.....	19
2.3.1.3 Simultaneous extraction of ammonium and nitrate	20
2.3.1.4 Saturated paste extraction.....	20
2.3.1.5 Important aspects of the extraction procedure.....	20
<i>Soil to extractant ratio</i>	20
<i>Leaching versus equilibrium extraction</i>	21

<i>Extraction duration</i>	21
<i>Filtration</i>	21
2.3.2 Determination of ammonium and nitrate.....	22
2.3.2.1 Colorimetric methods	22
<i>Manual ammonium determination</i>	22
<i>Manual nitrate determination</i>	23
<i>Automated analysis of ammonium and nitrate</i>	24
<i>Ultraviolet adsorption difference</i>	24
2.3.2.2 Ion chromatography	25
2.3.2.3 Ion specific electrode.....	25
<i>Electrodes for ammonium</i>	25
<i>Electrodes for nitrate</i>	26
2.3.2.4 Steam distillation	27
2.3.2.5 Micro diffusion	28
2.4 EMI sensor and EC _a measurements	29
2.4.1 EMI sensor function	29
2.4.2 Principles of the EC _a measurements	31
2.4.3 EC _a data application.....	32
2.4.3.1 Geostatistics.....	32
2.4.3.2 Software directed soil sampling	33
2.4.3.3 Salinity modelling and assessment.....	33
2.4.3.4 Inferring soil properties from EC _a	34
2.4.4 EC _a data to predict inorganic N	35
2.4.4.1 Relationship between soil electrical conductivity and inorganic N.....	35
2.4.4.2 EC _a to predict inorganic N in literature	36
2.5 Statistics for method-comparison studies	39
2.6 Conclusion	42
CHAPTER 3. MATERIALS AND METHODS.....	44
3.1 Study site description	44
3.1.1 Study site locations	44
3.1.2 Weather	46
3.1.3 Topography.....	47
3.1.4 Soils.....	49
3.1.5 Management practices	52
3.2 Soil sampling and EC _a data collection	52
3.3 Soil property analysis	57

3.4 Data analysis	59
3.4.1 Inorganic N concentrations.....	59
3.4.2 Comparing single and composite soil samples.....	59
3.4.3 Comparing 2.0 M KCl and the saturated paste extraction methods	60
3.4.4 EM38 correlation.....	60
CHAPTER 4. RESULTS AND DISUSSION: SINGLE VS. COMPOSITE SOIL SAMPLES FOR INORGANIC N DETERMINATION	62
4.1 Results.....	62
4.1.1 Inorganic N concentrations in single and composite samples.....	62
4.1.2 Comparing single and composite samples	66
4.1.2.1 NH ₄ ⁺ -N concentration	66
4.1.2.2 NO ₃ ⁻ -N concentration	68
4.1.2.3 TIN concentration	70
4.2 Discussion.....	72
CHAPTER 5. RESULTS AND DISUSSION: KCL EXTRACTION VS. SAT_E FOR INORGANIC N DETERMINATION	74
5.1 Results.....	74
5.1.1 Inorganic N concentrations in different extractions	74
5.1.2 Comparing SAT _E and 2.0 M KCl extractions	77
5.1.2.1 NH ₄ ⁺ -N concentrations	77
5.1.2.2 NO ₃ ⁻ -N concentrations	79
5.2 Discussion.....	81
CHAPTER 6. RESULTS AND DISCUSSION: APPLYING EC_a DATA FOR INDIRECT MEASUREMENT OF SOIL INORGANIC N	83
6.1 Results.....	83
6.1.1 Single and average EM38 measurements.....	83
6.1.2 Inorganic N prediction models.....	85
6.2 Discussion.....	86
6.2.1 Single and average EM38 measurements.....	86
6.2.2 Inorganic N prediction models.....	87
CHAPTER 7. CONCLUSIONS AND RECOMMENDATIONS	89
REFERENCES	91
APPENDICES.....	100

ACKNOWLEDGEMENTS

- ❖ First and foremost my utmost gratitude to the God who granted me the ability and will to finish this dissertation.
- ❖ To my parents for supporting and motivating me in every way for the last 26 years and for giving me all the possible opportunities to complete my studies.
- ❖ To Pieter, thank you for your understanding, support and encouragement through these few years of my studies.
- ❖ I would like to acknowledge the Water Research Commission for the financial support and the use of the data collected in the WRC-K5/2499//4 project.
- ❖ I would like to thank the University of the Free State through the Department of Soil-, Crop- and Climate Sciences and the Post Graduate school for financial and personal support
- ❖ I would like to thank SENWES LTD for offering me financial assistance.
- ❖ Thank you to my supervisor Prof L.D. van Rensburg and co-supervisors Prof C.C. du Preez and Dr J.H. Barnard for their efforts and contributions to the successful completion of this dissertation.
- ❖ I must thank the technicians Mr R. Smit and Mr S. van Stade for their valuable assistance with electromagnetic induction surveys of crop fields and soil sampling.
- ❖ To all the lab staff at Van's Lab and the Institute of Groundwater Studies, thank you for your help with experiments and analysis.
- ❖ I am very thankful for Prof R. Schall who helped me in identifying the most suitable statistical analysis methods and interpreting the results.
- ❖ Thank you to Anneline Bothma for her time, effort and contribution in editing and proofreading my work
- ❖ I would like to acknowledge Mr F. Lesoetsa who conducted the soil surveys.
- ❖ Special thanks to my friends and colleagues who have assisted me in any way with profound inputs.

LIST OF FIGURES

Figure 2.1 Illustration of a) random-, b) stratified random and c) systematic designs in which the traditional sampling approach is often categorized (Franzen & Cihacek, 1998; Peters & Laboski, 2013).	5
Figure 2.2 Illustration of the difference between grid-cell and grid-point sampling designs (Jones <i>et al.</i> , 2014; Rains <i>et al.</i> , 2016).	7
Figure 2.3 Sampling according to a grid-cell design may be done a) randomly or b) systematically. Concentrating samples in c) a particular area or d) along crop rows should be avoided (Knowles & Dawson, 2018).	7
Figure 2.4 Different grid-point sampling designs: a) regular systematic, b) systematic unaligned, c) staggered start systematic and d) diamond/triangle/hexagon systematic (Franzen & Cihacek, 1998; Peters & Laboski, 2013).	8
Figure 2.5 Flow diagram developed from literature showing approaches, methods, designs and patterns with respect to soil sampling for determination of plant nutrient levels.	11
Figure 2.6 The operating principle of the EMI sensor (Grisso <i>et al.</i> , 2009).	29
Figure 2.7 The EM38 in the a) horizontal mode with the coils parallel to the soil surface and b) vertical orientation with the coils perpendicular to the soil surface.	30
Figure 2.8 A mobile EMI soil survey unit for continuous soil measurement (photo courtesy of Van's Lab Limited).	30
Figure 2.9 Relationship between soil extract NO_3^- and EC (Patriquin <i>et al.</i> , 1993).	35
Figure 2.10 The Bland-Altman plot with the mean difference, limits of agreement and line of equality (Giavarina, 2015).	41
Figure 3.1 Location of the four study sites in South Africa.	44
Figure 3.2 Study sites, outlined in red, situated near a) Douglas, b) Luckhoff, c) Hofmeyr and d) Empangeni.	45
Figure 3.3 Elevation maps of the fields at a) Douglas, b) Luckhoff, c) Hofmeyr and d) Empangeni.	48
Figure 3.4 Maps of the soil forms identified at a) Douglas, b) Luckhoff, c) Hofmeyr and d) Empangeni.	50
Figure 3.5 Clay percentage for the different soil depth intervals at sites of a) Douglas, b) Luckhoff, d) Hofmeyr and d) Empangeni.	51
Figure 3.6 Route maps of transects driven by the mobile sensor unit showing EMI measuring points and soil sampling points at the a) Douglas, b) Luckhoff, c) Hofmeyr and d) Empangeni study sites.	53
Figure 3.7 Spatial variability of EC_a to a depth of 1500 mm and soil sampling points at a) Douglas, b) Luckhoff, c) Hofmeyr and d) Empangeni study sites.	54
Figure 3.8 Orientation of the EM38-MK2 for EC_a readings and sampling positions at a soil sampling location in a selected field.	56
Figure 3.9 Soil samples collected from the four corners of the 1 m ² cleared area in a selected field to prepare a composite sample.	56
Figure 3.10 Filtration of the 2.0 M KCl soil extracts.	57
Figure 4.1 2.0 M KCl extracted NH_4^+ -N concentrations in single and composite soil samples of the depth intervals for the study sites.	63
Figure 4.2 A 2.0 M KCl extracted NO_3^- -N concentrations in single and composite soil samples of the depth intervals for the study sites.	64
Figure 4.3 Calculated TIN concentrations in single and composite soil samples of the depth intervals for the study sites.	65
Figure 4.4 Regression plot for comparison of single vs. composite soil sampling in determining NH_4^+ -N concentrations in soil samples.	67
Figure 4.5 A Bland-Altman plot of NH_4^+ -N concentrations in single and composite soil samples.	67

Figure 4.6 Regression of NO_3^- -N concentrations in single soil samples and composite soil samples with a line of equality.....	69
Figure 4.7 A Bland-Altman plot of NO_3^- -N concentrations in single and composite soil samples.	69
Figure 4.8 Regression line ($R^2=0.70$) and line of equality ($R^2=1$) of log transformed TIN concentrations in single and composite samples.....	71
Figure 4.9 A Bland-Altman plot of TIN concentrations in single and composite soil samples.	71
Figure 5.1 NH_4^+ -N concentrations determined in extracts of 2.0 M KCl and SATe in all samples collected at the four study sites.	75
Figure 5.2 NO_3^- -N concentrations determined in extracts of 2.0 M KCl and SATe in all samples collected at the four study sites.	76
Figure 5.3 Scatterplot for log transformed concentrations of NH_4^+ -N in 2.0 KCl extracts against the saturated paste extract.	78
Figure 5.4 Bland-Altman plot for \log_e transformed values of NH_4^+ -N extraction methods....	78
Figure 5.5 Regression of NO_3^- -N concentrations in extracts of 2.0 M KCl and SATe, with a line of equality.	80
Figure 5.6 Bland-Altman plot for concentrations of NO_3^- -N in 2.0 M KCl and SATe.....	80
Figure 6.1 Scatterplot of single against composite EC_a measurements.	84
Figure 6.2 Bland-Altman plot for EC_a readings.	84

LIST OF TABLES

Table 2.1 Advantages and disadvantages of using a whole-field composite sample for fertilizer recommendations (Franzen & Cihacek, 1998; Anonymous, 2005).....	6
Table 2.2 Reasons for the justification of grid sampling, management zone sampling or geostatistical based sampling (ESAP-RSSD).....	13
Table 2.3 Steam distillation methods for determining different forms of inorganic N (Mulvaney, 1996)	27
Table 2.4 Abbreviations of variables and equations related to Bland-Altman analysis (Bland & Altman, 1986)	41
Table 3.1 Summary of weather data for 2016 at each study site (ARC-ISCW, 2017).....	46
Table 3.2 Soil forms and corresponding horizons identified at the four study sites.....	49
Table 3.3 Agronomic practices applied on the four study sites during 2016 when soil samples were taken	52
Table 3.4 GPS coordinates of the sampling points for the different study sites	55
Table 4.1 Bland-Altman statistics for log and anti-log transformed NH_4^+ -N data	66
Table 4.2 Bland-Altman statistics for log and anti-log transformed NO_3^- -N data	68
Table 4.3 Bland-Altman statistics for log and anti-log transformed TIN data	70
Table 5.1 Bland-Altman statistics for log transformed data of NH_4^+ -N for the two extraction methods as well as back transformation (anti-log) for interpretation purposes	77
Table 5.2 Bland-Altman statistics for log and anti-log transformed NO_3^- -N data	79
Table 6.1 Calculated Bland-Altman statistics	83
Table 6.2 Multiple regression model statistics Douglas.....	85
Table 6.3 Multiple regression model statistics Luckhoff	86
Table 6.4 Multiple regression model statistics Hofmeyr	86

LIST OF APPENDICES

Appendix 1 Study site weather data.....	100
Appendix 2 Inorganic N concentrations in single and composite soil samples	102
Appendix 3 Inorganic N concentrations in 2.0 M KCl and SATe soil extracts	106
Appendix 4 Single and composite EC _a measurements	113
Appendix 5 EC _a measurements, geometric mean and elevation data used for model development	114
Appendix 6 Inorganic N stock (kg/ha) in samples taken at Douglas, Luckhoff and Hofmeyr	115

Sampling and extraction methods for soil inorganic N determination to calibrate the EM38 in irrigated fields

by

Diandra Steenekamp

ABSTRACT

Precise management of N variability in crop fields are required to increase yields and ensure sustainable and economic crop production, whilst not having a negative impact on the environment. A popular type of sensor for characterizing soil variability is the EM38-MK2 that measures apparent electrical conductivity (EC_a), operating on the principle of electromagnetic induction (EMI). After analysis, inorganic N results can be calibrated to EC_a measurements. It has been established that NH_4^+ -N and NO_3^- -N can be predicted from EC_a .

This study presented three main research aims to: i) compare single and composite samples for the determination of NH_4^+ -N, NO_3^- -N, and total inorganic N (TIN), ii) determine if the saturated paste extract (SATE) could replace the standard 2.0 M KCl extraction for determination of NH_4^+ -N and NO_3^- -N, and iii) determine what combination of single or composite EC_a measurements and inorganic N at different sampling depths would produce the most statistically significant inorganic N prediction model.

EMI surveys were conducted on four study sites under centre pivots, located on commercial irrigation farms in the districts of Douglas, Luckhoff, Hofmeyr and Empangeni. Using EC_a data with the “Electrical Conductivity Sampling Assessment and Prediction” (ESAP) software and it’s featured “Response Surface Sampling Design” (RSSD) sampling methodology, soil sampling points were identified based on the degree of EC_a variability. Before sample collection, additional EC_a readings were taken at each sampling point, one in the centre and one on each corner of a 1 m² area. Afterwards soil samples were collected in the same manner in 300 mm depth increments up to 1500 mm. Samples collected in the centre were considered single, while those from the corners were composited. Concentrations of NH_4^+ -N and NO_3^- -N in KCl and SATE soil extracts were simultaneously determined colorimetrically.

For the first aim, inorganic N concentrations in KCl extracts was \log_e transformed and pooled to compare sampling methods irrespective of study site, sampling point, and depth. For the second aim, data of inorganic N concentrations determined in KCl and SATe extracts were transformed and pooled for comparison, irrespective of site, sampling point, sampling method, and depth. The third aim was divided into three parts, determining agreement between single and composite EC_a measurements, determining what inorganic N values to use, i.e. what sampling method and extract, and finally model calibration.

Statistical analysis focused on assessing agreement using the Bland-Altman method for assessing agreement on a 95% confidence interval and multiple-linear regression calibration models were developed in Microsoft Excel.

Results revealed poor agreement between single and composite samples for NO_3^- -N and TIN. A composite sample taken in a 1 m² area was more suitable when investigating NO_3^- -N or TIN. Good agreement was found for NH_4^+ -N and a single sample proved sufficient. Agreement between the two extracts was poor for both NH_4^+ -N and NO_3^- -N and it was concluded that SATe cannot replace KCl for inorganic N determination. Agreement between single and composite EC_a measurements was good and one EC_a measurement was sufficient per 1 m² sampling location.

Based on the conclusions from the previous research questions, inorganic N results used for model development were those from composite samples extracted using KCl and an average between the single and composite EC_a measurements was used.

Values of inorganic N, EC_a and elevation were \log_e transformed. Results showed that the majority of the calibration models were statistically insignificant except for one sampling depth (900 to 1200 mm) at Douglas (EC_a 0 to 750 mm; $R^2=0.54$ and EC_a 0 to 1500 mm; $R^2=0.57$). It was concluded that for the sites investigated, inorganic N was not the dominant soil property influencing EC_a .

Keywords: Nitrogen, nitrate, ammonium, ESAP (Electrical Conductivity Sampling Assessment and Prediction), RSSD (Responce Surface Sampling Design), soil sampling, extraction, 2.0 M KCl, saturated paste extract (SATe), EMI, EC_a , Bland-Altman analysis

CHAPTER 1. MOTIVATION, OBJECTIVES AND LAYOUT

1.1 Motivation and objectives

Through precision agriculture, also known as site-specific management, soil can be managed to meet the exact needs of the crop by adjusting practices to field variability (Hanquet *et al.*, 2002). An important nutrient that requires precise management in plant production is nitrogen (N), specifically nitrate (NO_3^-) and ammonium (NH_4^+). Excess amounts of N in the soil can be avoided by applying exact amounts of fertilizers through precise management strategies (Jurisic *et al.*, 2013). This promotes sustainable agriculture and environmental conservation through less pollution, which in turn increases productivity and profitability (Stafford, 2000).

One method of identifying soil variability is by using soil sensors that can provide a large amount of accurate and precise spatial data (Stafford, 2000; Hendriks, 2011). A popular type of sensor for soil characterization is apparent electrical conductivity (EC_a) sensors. Non-contact proximal EC_a soil sensors operate close to the soil and are based on the principle of electromagnetic induction (EMI) (Hanquet *et al.*, 2002; Grisso *et al.*, 2009; Adamchuk, 2010).

Measurements of EC_a may be used together with “Electrical Conductivity Sampling Assessment and Prediction” (ESAP) software to identify soil sampling points using a sampling methodology known as “response surface sampling design” (RSSD) (Corwin & Lesch, 2003).

For the current study, soil samples were taken from fields involved in a salinity management project of the Water Research Commission (WRC project K5/2499//4) and the ESAP-RSSD sampling method was used. Study sites chosen for this dissertation included center pivot irrigated fields near Douglas, Luckhoff, Hofmeyr and Empangeni.

An important aspect that is always considered for any soil sampling design is the collection of representative soil samples. The ESAP-RSSD identified sampling points can be sampled according to the preference of the researcher and his or her objectives and available resources. The researcher needs to decide whether to take just single samples or composite samples at each sampling point. While composite samples could give a more accurate estimation of nutrients levels in the soil, single samples would be much less time consuming.

Therefore, with the determination of inorganic N in mind, the first research question was if a composite sample taken in a 1 m² area at a sampling location identified by the ESAP-RSSD software would agree well with results found in a single sample, regardless of the study site or sampling depth.

After the collection of soil samples, samples need to be analysed to accurately determine concentrations of NH₄⁺ and NO₃⁻. Soil analysis can be divided into two steps, firstly extraction of a nutrient from a sample and secondly the determination of the nutrient concentration in the extract solution. Many methods exist for the extraction of either NO₃⁻ or NH₄⁺, but the most common extractant used for both these forms of inorganic N is 2.0 M KCl (Maynard *et al.*, 2007). However, chemicals used can become expensive when a large number of samples are to be analysed. For this reason, an alternative to the 2.0 M KCl extraction was investigated, namely saturated paste extraction (SATE). The reason for testing SATE was because the determination of electrical conductivity of the saturated extract (EC_e) and calibration of EC_e with EC_a data is a standard analysis conducted after an EM soil survey. It would therefore be convenient if the SATE could also be used for determination of inorganic N. Thus, the second research question was if a SATE would agree well with the reference 2.0 M KCl in extracting NO₃⁻ and NH₄⁺ from soil samples.

After laboratory analysis of soil samples, analysis results and EC_a measurements can be used to create prediction models for target soil properties. In the case of a high correlation, the model can be used to estimate, map and manage the soil property in question (Corwin & Lesch, 2003; Corwin *et al.*, 2006). If the soil property is inorganic N, its spatial analysis and site-specific management can help to maximize N use efficiency, improve yield and yield quality and also minimize the impact that N has on the environment (Haberle *et al.*, 2004; Jurisic *et al.*, 2013).

It has already been established that inorganic N can be predicted from EC_a measurements (Eigenberg & Nienaber, 1998; Eigenberg *et al.*, 2002; Corwin *et al.*, 2003a; Korsath, 2005; Wienhold & Doran, 2008). Therefore, the third research question asked was what combination of i) single or composite EC_a measurements and ii) inorganic N in different soil depths would produce the most statistically significant model for prediction of NO₃⁻, NH₄⁺ and total inorganic nitrogen (TIN). For this, the third aim was divided into three parts. Agreement between single and composite EC_a measurements needed to be determined first. Secondly, conclusions drawn from the first two research questions would be used to decide between using single or composite soil samples and 2.0 M KCl or the SATE for calibration analysis. Further, multiple-linear regression calibration models were developed by using Microsoft Excel so that elevation data could be incorporated as an x-variable in

addition to EC_a . The reason for incorporating elevation is because levels of inorganic N in soil are highly related to topography due the internal movement of water as well as surface runoff (Franzen & Kitchen, 1999), making topography an important factor that needs to be considered in the site-specific management of inorganic N.

Considering the above motivation, three main research aims can be summarized: i) compare single and composite samples for the determination of NH_4^--N , NO_3^--N , and TIN, ii) determine if the SATe could replace the standard 2.0 M KCl extraction for determination of NH_4^--N and NO_3^--N , and iii) determine what combination of single or composite EC_a measurements and inorganic N at different sampling depths would produce the most statistically significant inorganic N prediction model. As an additional research aim it was important to conduct a thorough literature review so to fully understand the research topic and to identify possibly gaps in knowledge.

1.2 Organization of the dissertation

Regarding the layout of this dissertation, it is organized into 5 chapters as described below:

Chapter 1: Provides background information and the objectives of the study. Here the scope and organization of each chapter is also described.

Chapter 2: Contains the literature review and it is divided into four main topics, namely soil sampling methods, extraction and determination methods for inorganic N, use of EMI sensors and EC_a data and lastly statistical methods for method comparison studies.

Chapter 3: Here the overall material and methods are provided. All study sites are described as well as the collection of EC_a data, taking of soil samples and laboratory analysis. Also described is the statistical analysis for each research question.

Chapter 4, 5 and 6: These chapters respectively contain the results and discussions for each of the aims.

Chapter 7: In the final chapter conclusions are drawn and recommendations made for each research question.

CHAPTER 2. LITERATURE REVIEW

2.1 Introduction

This literature review covers four main subjects, namely soil sampling methods, soil inorganic N extraction and determination methods, EMI sensors and EC_a data application and lastly appropriate statistical methods for method comparison studies.

The first section reviewed covers different methods of soil sampling for fertilizer recommendations, namely traditional whole-field sampling and site-specific sampling methods. Site-specific sampling methods discussed include grid- and management zone sampling, as well as geostatistical software based methods. This section also gives guidelines related to soil sample collection and handling prior to analysis of NH_4^+ and NO_3^- .

The second section describes the standard KCl extraction for both NH_4^+ and NO_3^- . Important laboratory aspects for extraction are also mentioned and the most basic principles related to different determination methods for NH_4^+ and NO_3^- in soil extracts, are summarized.

Within the third section, the EMI sensor function and EC_a measurements are briefly discussed as well as their usefulness along with geostatistical software for identifying where to sample soils and for estimating measured soil properties, specifically inorganic N.

The final section provides important information and clarity on the statistical methods that should be used in method-comparison studies.

2.2 Soil sampling for nutrient level determination

2.2.1 Traditional sampling approach

The traditional sampling approach for fertilizer recommendation is to make use of a whole-field composite sampling method where many selectively random samples are taken (Franzen & Cihacek, 1998; Peters & Laboski, 2013). The term “selectively random”, means that only relevant areas that represent most of a field are selected for sampling. Irrelevant areas, such as saline zones or manure piles, are avoided. A smaller sampled area is usually better represented by a composite sample.

Samples are often collected randomly which is the simplest design (Figure 2.1a). Sometimes a field is divided into smaller sections and each is sampled separately and is known as stratified random sampling (Figure 2.1b). A systematic sampling design in the form of a zigzag pattern can also be followed (Figure 2.1c). These three sampling designs are dealt with in more detail by Franzen & Cihacek (1998) and Peters & Laboski (2013).

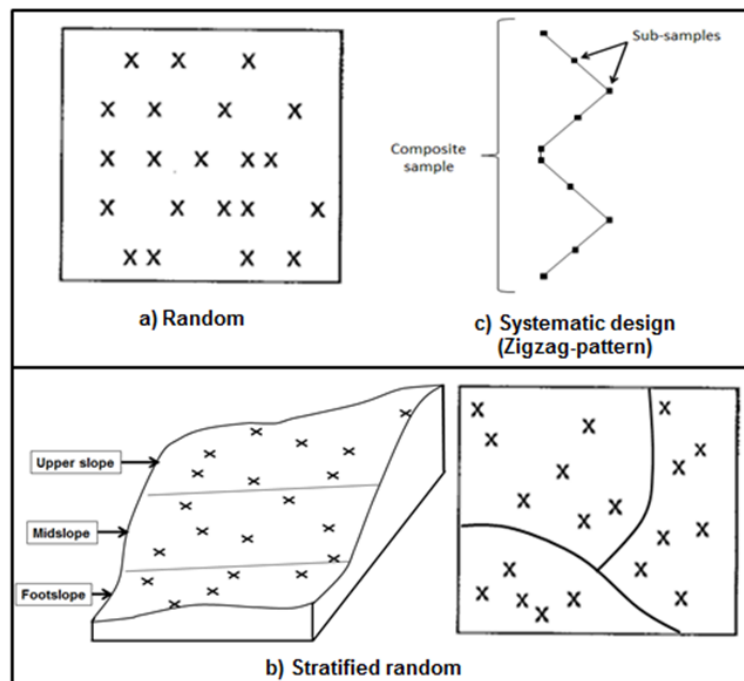


Figure 2.1 Illustration of a) random-, b) stratified random and c) systematic designs in which the traditional sampling approach is often categorized (Franzen & Cihacek, 1998; Peters & Laboski, 2013).

Each of the three traditional sampling designs generates a number of samples for a field or section and compositing the samples are essential for a whole-field approach. Compositing involves gathering and mixing individual samples from various sampling points over a field or section of a field to form a single homogenized sample (Sheppard & Addison, 2007). The average conditions that exist in the sampled area are then represented by the composite sample and the analysis results are used to make a single fertilizer recommendation for the whole field or a section of it (EPA, 2005; Walworth, 2011; Peters & Laboski, 2013).

It is often emphasized that the number of samples needed to make a composite depends on the field's size and uniformity. A larger or less uniform field should be sampled more intensively than a small or homogeneous field (Walworth, 2011). Different recommendations exist on the actual number of samples needed to make a composite. Walworth (2011) suggests a minimum of 5 samples, but preferably 15 to 25. Peters & Laboski (2013) proposes a minimum of 10 samples for a representative composite, while Hartz (2007) recommends at least 12 and Franzen & Cihacek (1998) at least 20. According to Knowles & Dawson (2018), a composite should consist of 15 to 20 samples for a field of 10 ha or less.

Advantages and disadvantages of taking one composite sample for the determination of plant available nutrient levels in a whole field are given in Table 2.1. The main advantage is the relatively low cost involved since only one sample is analysed to represent a field (Franzen & Cihacek, 1998). Unfortunately, one particular disadvantage is that extremes are sometimes not detected due to the diluting effect when soil samples are composited (EPA, 2005). Analysis of a composite sample can show high nutrient levels, but this does not mean

that the whole field requires no fertilizer. Similarly, low nutrient levels do not mean that the entire field needs to be fertilized. To avoid this, it must be carefully considered whether individual samples should be composited or not. Even though cost and time inputs are reduced, any potential for finding ‘nutrient hotspots’ or for the evaluation of soil property variations within a field will be lost if samples are composited (Perkins *et al.*, 2013).

Table 2.1 Advantages and disadvantages of using a whole-field composite sample for fertilizer recommendations (Franzen & Cihacek, 1998; Anonymous, 2005)

Advantages	Disadvantages
Relatively inexpensive and fast.	Extreme nutrient values are sometimes not detected.
Results are mostly reproducible.	Irrelevant areas are difficult to identify.
Results can be tracked from one year to the next.	Irrelevant areas avoided could contribute significantly to the total area in a field.
	Large areas of the field could be over or under fertilized.
	There is a low level of confidence that a high soil test value represents most of the field.

2.2.2 Site specific sampling approach

Site-specific sampling considers in-field variability of nutrient levels and their spatial distribution. The disadvantages of the traditional sampling approach has led to the development of more intelligent site-specific approaches. Global positioning systems are used to record the position of each sample and analysis results can be used to make a variable fertilizer rate application map with the possibility of immediate economic returns if considerable variability is present in a field (Franzen & Cihacek, 1998). For the site-specific approach, use of either grid sampling, management zone sampling or geostatistical based sampling, may be considered.

2.2.2.1 Grid sampling method

The grid sampling method involves sampling soils systematically at fixed intervals (Jones *et al.*, 2014) and each sample is analysed separately (Walworth, 2011). Two sampling designs stem from grid sampling, namely grid-point and grid-cell sampling (Figure 2.2).

In the design of grid-cell sampling one or multiple samples are randomly or systematically collected throughout a cell to prepare a composite sample. For a composite sample, 10 to 15 random soil samples should be collected throughout a cell (Figure 2.3a) or samples should be taken systematically such as in a diagonal pattern (Figure 2.3b) (Dinkins & Jones, 2017; Knowles & Dawson, 2018). It is important, however, to avoid the concentration of samples in

a particular area or along crop rows (Figure 2.3c and d). A field sampled according to the grid-cell design will consist of many cells, each with a different fertilizer recommendation.

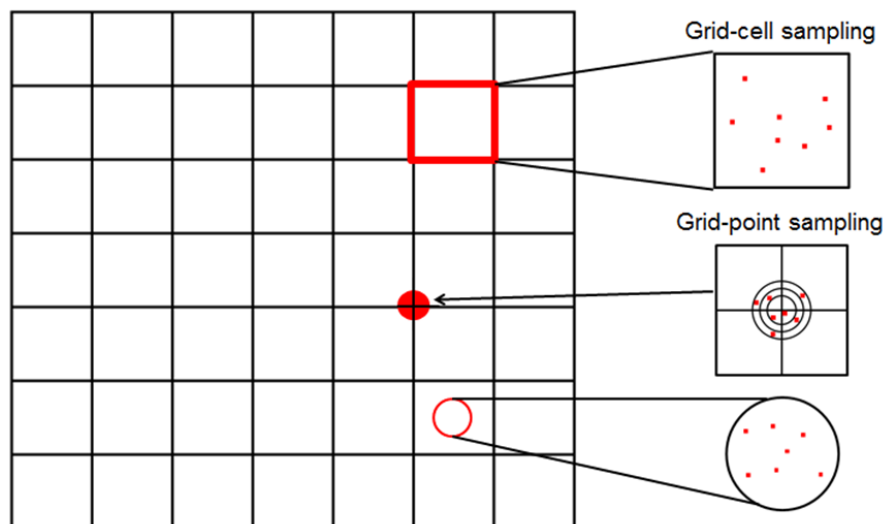


Figure 2.2 Illustration of the difference between grid-cell and grid-point sampling designs (Jones *et al.*, 2014; Rains *et al.*, 2016).

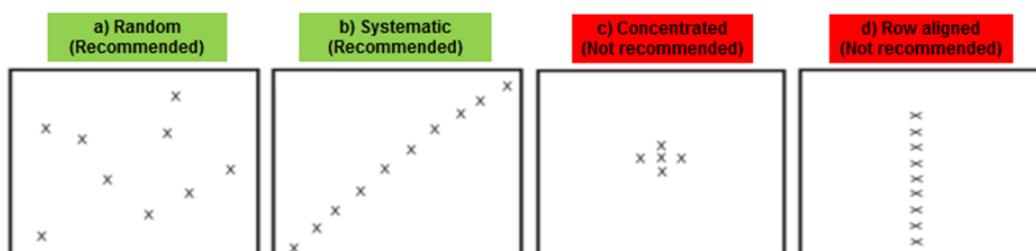


Figure 2.3 Sampling according to a grid-cell design may be done a) randomly or b) systematically. Concentrating samples in c) a particular area or d) along crop rows should be avoided (Knowles & Dawson, 2018).

In grid-point sampling, samples should be taken within a 3 to 6 m radius of the grid point (Franzen & Cihacek, 1998). Further, one or multiple subsamples are collected around a georeferenced point at a grid intersection or inside the grid, as depicted in Figure 2.2 (Dinkins & Jones, 2017). This design is better for identifying variability because samples are taken near georeferenced points and not scattered throughout a cell (Knowles & Dawson, 2018).

In the past, grid-point samples were often collected according to a regular grid (Figure 2.4a). However, this design can easily contain bias if aligned with fertilizer row patterns. Therefore, the use of an unaligned systematic grid-point design is recommended (Figure 2.4b) (Franzen & Cihacek, 1998; Peters & Laboski, 2013). This design also provides the opportunity for greater statistical evaluation through Kriging interpolation techniques. Other systematic grid sampling designs include a staggered start grid and a diamond/triangle/hexagon grid (Franzen & Cihacek, 1998), as illustrated in Figure 2.4c and d.

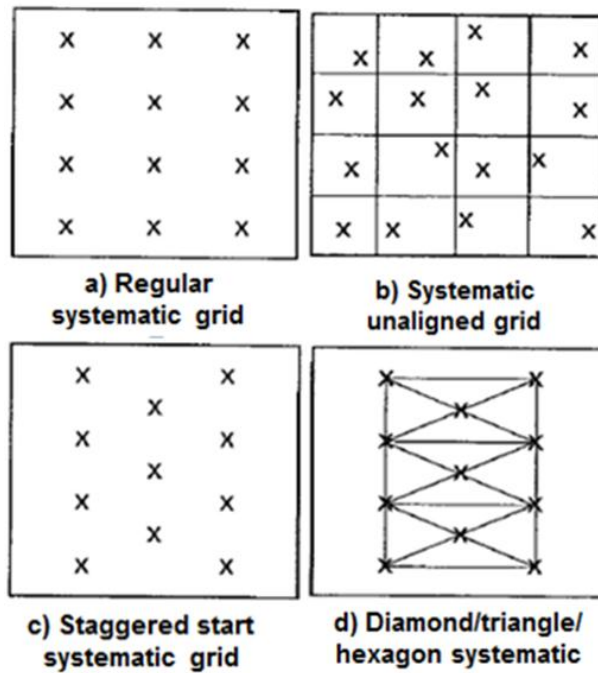


Figure 2.4 Different grid-point sampling designs: a) regular systematic, b) systematic unaligned, c) staggered start systematic and d) diamond/triangle/hexagon systematic (Franzen & Cihacek, 1998; Peters & Laboski, 2013).

Regarding what grid density to use, grid spacing should be determined after considering field uniformity (Franzen & Peck, 1995). The distance between sampling points can be greater on fields with homogeneous soils than on fields with variable soils (Jones *et al.*, 2014). Further considerations include past management of the field, soil types and apparent economic benefit (Knowles & Dawson, 2018).

When creating maps of soil properties or variable nutrient applications, the closer the grid spacing the more reliable the interpolation and correlation between sampling points (Knowles & Dawson, 2018). For mapping by means of Kriging interpolation, the most important factor that determines the accuracy and reliability of the empirical variogram and which can be controlled is the size of the sample on which it is based. Generally, the larger the dataset the greater the accuracy. Variograms that are computed with less than 100 data points are unreliable and it is recommended that the data set be a minimum of 100 to 150 points. Further, for Kriging, the samples should be collected evenly to give even coverage of the field at intervals of less than half the effective range (Oliver & Webster, 2014).

In practice, the grid density used for field crops under irrigation is one sample per hectare and for fruit crops one sample per 0.25 ha (Haarhoff, Personal communication¹). Dryland farmers are generally advised to use a 2 ha grid when sampling the topsoil (0 to 300 mm)

¹ Mr D. Haarhoff, 2018. Chief Agronomist, GWK, Douglas, Northern Cape, South Africa.

and a 4 ha grid for the subsoil (300 to 600 mm) (Van Staden, Personal communication²). Concerning irrigated land, the ideal is a 0.5 ha grid for the topsoil and a 1 ha grid for the subsoil. However, farmers are sometimes forced to sample larger grids under either dryland or irrigation since they cannot afford the analysis of a large number of samples.

2.2.2.2 Management zone sampling method

The variation in plant available soil nutrient levels over fields is the motivation behind the use of management zone sampling, also termed directed soil sampling. With management zone sampling it is assumed that a field consists of different soils, each with unique properties that crops respond differently to. These different soils should therefore be divided into distinct zones that can be sampled and managed separately (Dinkins & Jones, 2017).

Differences useful in delineating management zones include inherent factors like soil texture, drainage, depth and colour, as well as slope. Other forms of variability are caused by management, for instance crop history, yield, fertilization and land shaping (Jones *et al.*, 2014; Knowles & Dawson, 2018). Sometimes information collected by technologies of precision agriculture are implemented to evaluate the spatial distribution of various factors that influence nutrient availability to identify uniform management zones. Such resources include topography or digital elevation maps (DEM), soil survey maps, yield maps, EC_a measurement maps, aerial images and normalized difference vegetation index (NDVI) (Ferguson *et al.*, 2007; Dinkins & Jones, 2017; Peters & Laboski, 2013; Jones *et al.*, 2014).

Once management zones for a specific field have been identified, the sampling design within each zone can be random or systematic. A random sampling design could be both random or random stratified and these samples are then mixed to obtain a composite soil sample for each management zone. Systematic sampling designs within management zones involve the use of predetermined sampling points, for example as displayed in Figure 2.2 a grid-point or grid-cell design (James & Wells, 1990; Peters & Laboski, 2013).

Once again, the recommended number of samples needed to prepare a composite differs from one reference source to the next and from one design to the next. Rains *et al.* (2016) stated that in a management zone, a minimum of two to three randomly selected samples should be sufficient. On the other hand, James & Wells (1990) had indicated that micro-variation in a uniform zone (differences in soil properties between points 0 to 0.5 m from each other) will only be accounted for if the number of samples collected and mixed is sufficient, for example 25 to 30 per composite sample.

² Mr P. van Staden, 2018. Senior Agronomist, Senwes, Klerksdorp, North West, South Africa.

2.2.2.3 Geostatistical software-based sampling method

Geostatistics is a tool that implements information on spatial variability through the detection, estimation and mapping of spatial patterns of soil or plant variables (Haberle *et al.*, 2004). EC_a measurements are a type of supplementary sensor data frequently used to develop soil sampling patterns to identify where to sample soils (Heil & Schmidhalter, 2017) and to help identify, quantify and predict various soil or crop properties (Corwin *et al.*, 2010).

The geostatistical software, ESAP, uses EC_a data as input for conductivity modelling (Amezketá, 2007) and is useful in the improvement of sampling network efficiency to aid researchers in obtaining the maximum amount of information from the fewest number of soil samples (Yates & Warrick, 2002). The software uses EC_a data to direct soil sampling as a means of characterizing spatial variability of those soil properties that correlate with EC_a at a particular study site. Characterizing spatial variability with EC_a -directed soil sampling is based on the notion that when EC_a correlates with a soil property or properties, the spatial EC_a information can be used to identify sampling locations based on the degree of variability in EC_a measurements (Corwin *et al.*, 2010).

Currently, two EC_a -directed sampling designs are used, namely prediction-based (model) sampling and probability-based (design) sampling. Prediction-based sampling designs typically rely upon optimized spatial response surface sampling designs (RSSD) (Corwin *et al.*, 2010) and are explicitly focused towards model estimation (Lesch, 2005). The application of EC_a data through ESAP-RSSD will be discussed in further detail in Section 2.4.

Examples of probability-based sampling designs will not be discussed in depth. These designs include *inter alia* simple random sampling, stratified random sampling, cluster sampling and multistage sampling for geostatistical estimation problems. Probability-based sampling designs are useful for many spatial studies and rely on built-in randomization principles for drawing statistical interpretations. They, however, are not designed for estimating models and avoid incorporating any parametric modelling assumptions (Lesch, 2005; Corwin *et al.*, 2010).

2.2.3 Perspective on site-specific soil sampling

A flow diagram (Figure 2.5) was developed from the literature review to provide context on how the ESAP software fits into the field of site-specific soil sampling relative to other methods.

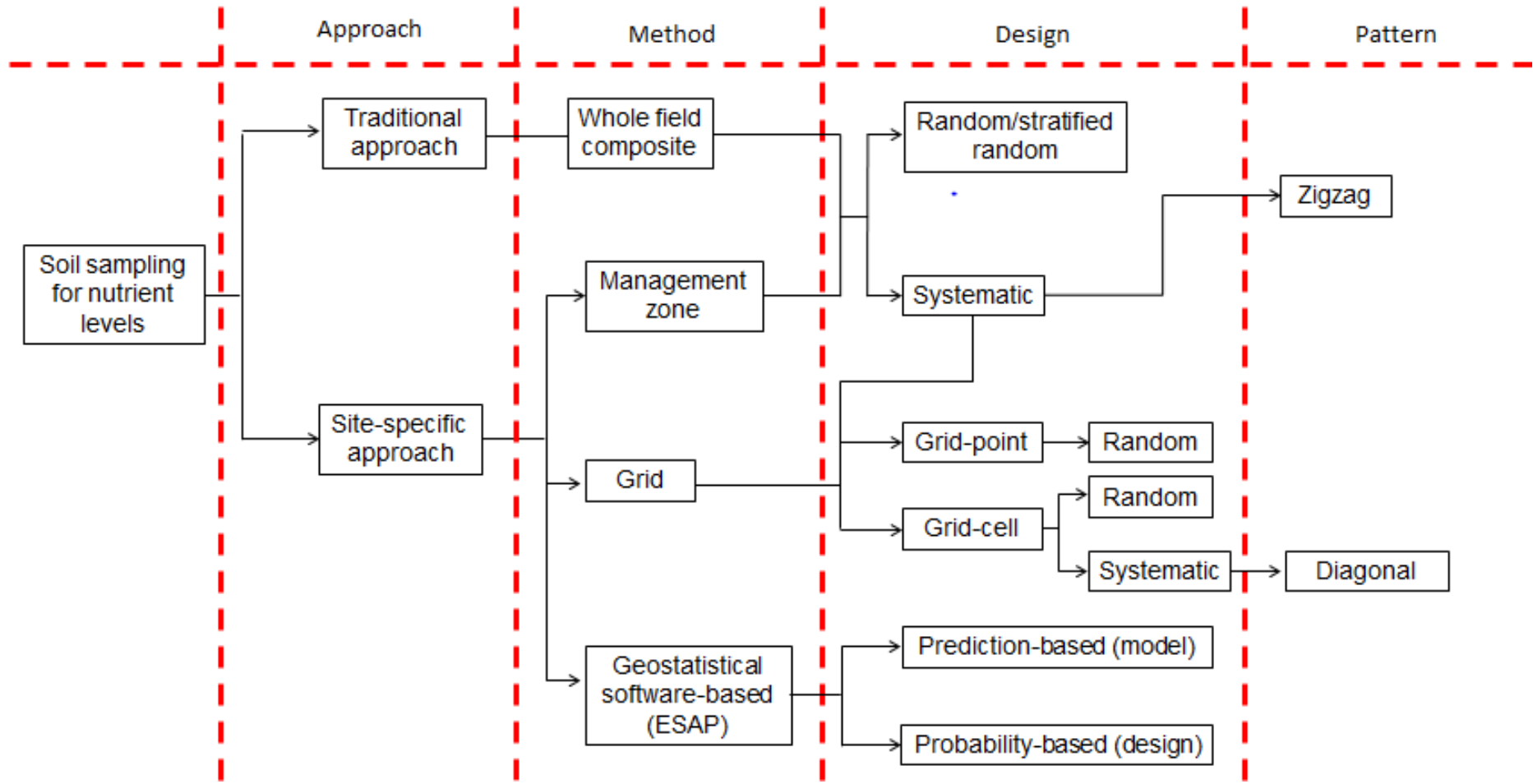


Figure 2.5 Flow diagram developed from literature showing approaches, methods, designs and patterns with respect to soil sampling for determination of plant nutrient levels.

In this diagram the terms “approach”, “method”, “design” and “pattern” was used to provide clarity on the different stages of deciding how and where to sample soils. These terms were chosen since the terminology used in literature on soil sampling for site-specific management may be somewhat confusing and are sometimes used interchangeably. For example, Peters & Laboski (2013) uses the term strategy to distinguish between site-specific sampling and the traditional sampling approach, but also refers to an unaligned grid as a strategy. Peters & Laboski (2013) and Ferguson *et al.* (2007) both refer to management zone sampling and grid sampling as two approaches for site-specific fertilizer management, but Franzen *et al.* (1998), Walworth (2011) and Jones *et al.* (2014) all refer to grid sampling as a method. Peters & Laboski (2013) also states that grid-point sampling is a technique, while Dinkins & Jones (2017) considers grid-point and grid-cell as two types of grid sampling. Also, concerning ESAP-RSSD, Corwin *et al.* (2010) refers to design-based sampling and model-based sampling both as design approaches, but Corwin *et al.* (2006) refers to these only as sampling approaches, while Lesch (2005) calls these strategies.

According to the developed diagram there are two different approaches for sampling soils for the purpose of determining nutrient levels, namely a traditional and a site-specific approach. As described earlier, the traditional approach involves taking a whole-field composite sample using a random design, or a systematic design such as a zigzag pattern. Under the site-specific sampling approach falls grid sampling, management zone sampling and geostatistical based sampling (Ferguson *et al.*, 2007; Dinkins & Jones, 2017; Rains *et al.*, 2016). Designs for grid sampling include mainly grid-point and grid-cell sampling, while designs for management zones include random sampling and systematic designs such as a grid-point, grid-cell design or zigzag design. Concerning geostatistical methods, of specific interest for this study is the ESAP software program that uses EC_a data as input to establish prediction- or probability-based sampling designs.

Irrespective of the sampling approach, method and design used, with the ESAP-RSSD model it is assumed that individual samples taken at a point can be handled separately or as a composite due to the presence of high small-scale variability present in most areas of a field (Franzen & Cihacek, 1998).

2.2.4 Choosing a suitable site-specific sampling method

For site-specific soil sampling, soils can be sampled using a grid, management zone or a geostatistical software based method. Reasons for choosing a particular site-specific sampling method are summarized in Table 2.2 and can be used as a guide for choosing a method depending on the research aim and available resources.

Table 2.2 Reasons for the justification of grid sampling, management zone sampling or geostatistical based sampling (ESAP-RSSD)

Grid sampling ^a	Management zone sampling ^b	Geostatistical software-based (ESAP-RSSD) sampling ^c
Unknown field history.	Unknown field history.	Gathering EC _a data with EMI sensors is fast, easy and relatively inexpensive.
Can provide a soil database that can be used for many years.	Spatial information sources available.	Large volumes of reliable EC _a data available.
Ensures good coverage of the field.	Clear relationship between landscape and yield data or aerial images.	Potential spatial variability determination of soil properties that influence EC _a .
High fertilizer application rates in the past.	Relatively low fertility levels. Low application of non-mobile nutrients in recent years.	RSSD allows assessment of spatiotemporal changes in soil properties.
Investigation of non-mobile nutrients (P, K, Zn).	Investigation and mapping of soil organic matter, pH and mobile nutrients like NO ₃ ⁻ -N.	Automatic selection of sampling points saves time and effort.
History of manure application.	Livestock or manure had little to no influence in the past.	Number of samples needed for calibration can be much lower than for grid sampling.
Allows variable rate fertilizer application.	Allows variable rate fertilizer application.	RSSD permits delineation of site-specific management units (SSMU's) that can be managed separately.
Merger of individual fields with different cropping histories.	High in-field variability.	
Past management significantly altered nutrient levels.	Long cropping history.	
Requires a lower level of interpretive skill compared to zone and RSSD sampling.	Zone delineation is validated by experience of the field.	
	Less expensive than grid sampling.	

^a Franzen & Cihacek, 1998; Bouma *et al.*, 1999; Ferguson & Hergert, 2009; Jones *et al.*, 2014; Rains *et al.*, 2016

^b Franzen & Cihacek, 1998; Ferguson *et al.*, 2007; Dinkins & Jones, 2017; Ferguson & Hergert, 2009; Jones *et al.*, 2014

^c Corwin *et al.*, 2003a; Corwin & Lesch, 2005; Amezketta, 2007; Adamchuk, 2010; Corwin *et al.*, 2010; Doolittle & Brevik, 2014

Various motivations exist for choosing a grid sampling method. Grid sampling is simple to apply and either a map or computer can be used to decide on suitable locations (Franzen & Cihacek, 1998). Further motivations for choosing grid sampling include when investigating non-mobile nutrients and when past management has significantly changed nutrient levels of the field, for example either high irrigation or fertilization applications (Ferguson & Hergert, 2009). If little prior knowledge exists on in-field variability, grid sampling can also provide a soil database that can be used for many years (Bouma *et al.*, 1999; Rains *et al.*, 2016). A disadvantage is that grid sampling is more time consuming and expensive due to the large number of soil samples that needs to be collected and analysed. However, occasionally there are patterns in soil fertility that can only be detected with grid sampling since it ensures better coverage of the field if the grid is dense enough (Ferguson & Hergert, 2009).

With regard to zone sampling, one main consideration for choosing this method is that it is much less expensive than grid sampling. The number of soil samples taken is greatly reduced because individual samples in a zone can be mixed to form one or a few composite samples (Dinkins & Jones, 2017) thereby minimizing laboratory costs (Rains *et al.*, 2016). However, to apply management zone sampling, the soil sampler or supervisor requires a bit more interpretive skill and a higher degree of soil and crop knowledge to identify sampling locations compared to grid sampling. It takes time to review resources that are spatially variable. Aerial images or topography maps are useful to identify spatial patterns and decide on management boundaries and sampling locations (Franzen & Cihacek, 1998).

Sampling based on geostatistical software modelling, specifically ESAP-RSSD that uses EC_a data as input, holds many advantages. This process is cost effective (Amezketta, 2007) since fewer samples are needed for soil property calibration than with systematic grid sampling. The mobile equipment used for the gathering of EC_a data allows fast and easy measurement. Furthermore, an EM survey provides large volumes of reliable EC_a data that is suitable for ESAP-RSSD modelling to select calibration sites (Corwin *et al.*, 2010; Doolittle & Brevik, 2014). A further advantage of using EC_a data to identify sampling locations, is that the spatial variability of the variety of soil properties that influences EC_a could potentially be established. Unfortunately, a greater level of technical knowledge is required for ESAP-RSSD compared to other sampling designs, but software is available (ESAP) that significantly reduces the statistical expertise required (Corwin *et al.*, 2010).

2.2.5 Soil sample collection for inorganic N determination

2.2.5.1 Sampling time

The purpose of the soil analysis determines the most suitable sampling time (Knight, 2006). For example, for fertilization recommendations, it is recommended by the United States Department of Agriculture (USDA-NRCS, 2016) that soil samples be taken after harvest and before planting the following crop. Samples specifically for NO_3^- analysis should be taken as close to planting as possible.

Soil nutrient levels can change slightly during the course of the year and seasonal variations can be expected due to the variation in factors that influence soil mineral depletion and accumulation (James & Wells, 1990). Yet, when deciding on when to collect samples, the main consideration is still convenience (Horneck *et al.*, 2011). However, sampling soils for the determination of inorganic N is an exception (Horneck *et al.*, 2011) and regular analysis of NO_3^- throughout the growing season is highly recommended to retrieve accurate

indications of plant-available levels (Walworth, 2011). Concentrations of NH_4^+ and NO_3^- fluctuate over time depending on soil microbiological activity and the amount of water moving through the soil (Horneck *et al.*, 2011). It is therefore important to be aware of circumstances that could cause changes in the inorganic N content of soils between sampling and planting (USDA-NRCS, 2016). For example, excess precipitation between the time of sampling and planting could result in NO_3^- leaching. If the effective precipitation is higher than 200 mm on clayey soils and 100 mm on sandy soils, losses may have occurred and re-sampling is needed (Ferguson *et al.*, 2007).

2.2.5.2 Sampling depth

Soil nutrient content can vary greatly with depth (Ferguson & Hergert, 2009). The depth at which samples should be taken depends primarily on the specific nutrient of interest, on the crop to be fertilized and on the tillage system.

Soil sampling depth for fertilizer recommendations is most often restricted to the tillage depth, which varies between 150 mm and 200 mm (Ferguson *et al.*, 2007; Hartz, 2007; USDA-NRCS, 2016). This zone is typically sampled for fertilization recommendations since it contains most root activity and also because organic matter and fertilizer applications are generally restricted to this soil zone (Hartz, 2007; USDA-NRCS, 2016).

For the determination of a mobile nutrient such as NO_3^- , soil should be sampled to a minimum depth of 600 mm (Franzen & Cihacek, 1998; Ferguson *et al.* 2007). However, if NO_3^- has been leached to deeper soil layers, for example in more humid regions, sampling up to 1200 mm is recommended (James & Wells, 1990; Franzen & Cihacek, 1998). James & Wells (1990) adds that the recommended depths for NO_3^- sampling ranges from 300 to 1800 mm, but soils are more often sampled from 600 to 1200 mm.

It is also important to take the crop into consideration, Franzen & Cihacek (1998) states that sampling up to 600 mm is sufficient for most crops. Yet, the rooting depths of different crops vary and sampling for mobile nutrients must occur to the depth at which roots can extract water (Jones *et al.*, 2014). Factors influencing water movement and rooting depth include soil type, soil depth, cropping system and obviously the crop (James & Wells, 1990; Jones *et al.*, 2014). For the recommendation of N containing fertilizers in the case of deep-rooted crops (USDA-NRCS, 2016) as well as in semi-arid and some humid regions (James & Wells, 1990), deeper samples from 150 to 600 mm are required (Dahnke & Johnson, 1990; USDA-NRCS, 2016). Many studies have found that the correlation between residual NO_3^- -N and crop yield increases as the sampling depth increases (Dahnke & Johnson, 1990).

Concerning the effect of tillage system on soil N, soils in no-till systems have a greater organic N content compared to conventional tillage. This is because crop residues are largely inaccessible to soil microorganisms, soil temperatures are lower and soil is less oxidized. On the other hand, soils subjected to long term conventional tillage have more N in the inorganic form due to crop residues being accessible to micro-organisms to mineralize under oxidative conditions. The N mineralized under conventional tillage could be subject to leaching causing an increase in NO_3^- in soil layers below the root zone (Hafif, 2014). Therefore, sampling soils for inorganic N in deeper layers is more important for conventionally tilled soils than for no-till soils.

2.2.5.3 Sample drying

It is essential to be aware that soil characteristics are subject to change from the moment samples are collected (Perkins *et al.*, 2013). Determination of exchangeable NH_4^+ and NO_3^- is complicated by the rapid changes that these forms are subject to through ammonification, nitrification and other microbial processes. Especially in wet soils, different forms of inorganic N are subject to transformations by soil microbes that alter nutrient concentrations (Bremner, 1965). Samples taken for determination of inorganic N should be analysed immediately to avoid these changes (Bremner, 1965; Mulvaney, 1996). Moreover, it is recommended to not collect more samples than can be processed the same day (Perkins *et al.*, 2013). However, avoiding delays in analysis is difficult due to samples having to be transported to the laboratory, sieved and possibly stored for a period of time before analysis (Bremner, 1965; Mulvaney, 1996).

Working with wet samples can also cause inaccuracies related to storage and retrieval of subsamples intended for the analysis (Maynard *et al.*, 2007). Therefore, samples are usually dried for easier handling to ensure proper sieving (soil particles of less than 2 mm in diameter) and mixing before analysis (Adepetu *et al.*, 2000; Gelderman & Mallarino, 2012). Drying of soil and the method used can affect mineralizable N (Gelderman & Mallarino, 2012). Ferguson *et al.* (2007) advises that samples be dried within 24 hours after collection when N is to be analysed. Drying soils intended for analysis of inorganic N is often carried out in a well-ventilated room with temperatures at or below 30°C (Mulvaney, 1996). When preservation is necessary, air drying at room temperature is the most reasonable and reliable method according to Knight (2006), especially concerning NO_3^- in soils with low inorganic N content. Still, air drying could possibly result in changes in the amount of extractable NH_4^+ and NO_3^- (Mulvaney, 1996).

In research conducted by Mueller (2015), the effect of drying and drying temperature on various soil analytical test values were studied, two of which were $\text{NH}_4^+\text{-N}$ and $\text{NO}_3^-\text{-N}$. Samples were handled in different ways before analysis. Field moist samples were stored in sealed containers to maintain water content and kept in a refrigerator to await analysis. The rest of the samples were dried at either 25°C, 45°C, 65°C, 85°C or 105°C. Soils were dried for 24 hours in a forced air oven except for the 25°C samples which were kept at room temperature until dry. Main conclusions made were that (i) $\text{NH}_4^+\text{-N}$ is increased by drying temperatures, and (ii) very high drying temperatures (85 to 105°C) should be avoided since it may cause the release of $\text{NH}_4^+\text{-N}$. Further, the clay mineralogy and drying temperatures used may affect $\text{NH}_4^+\text{-N}$ fixation and release. Also, it seems that the $\text{NO}_3^-\text{-N}$ in soils with a high initial $\text{NO}_3^-\text{-N}$ concentration will decrease as drying temperature increases.

Villar *et al.* (2014) also evaluated the effect of drying temperatures on extractable inorganic N. In their experiment soil samples were dried at 30°C, 40°C, or 105°C. Soils were subsequently extracted with 0.01 M CaCl_2 and the NH_4^+ and NO_3^- were determined spectrophotometrically. In this study NH_4^+ showed lower variability than NO_3^- between drying temperatures. The amounts extracted at 105°C were, however, almost double that extracted at 40°C. Regarding NO_3^- , almost no difference was found between drying samples at 30°C and 40°C, but concentrations of NO_3^- was below the spectrophotometer detection limit at 105°C due to denitrification.

In a study by Nina & Sigunga (2012), three field-fresh sampled soils of different C:N ratios intended for inorganic N extraction were dried using five different methods, namely:

- a) Stored at -10°C and later used for inorganic N extraction.
- b) Air dried at room temperature for 2 days then stored at -10°C.
- c) Stored at -10°C and sub-sampled 0, 3, 8, 18 and 38 days after collection. Sub-samples were air dried at room temperature for two days before extraction.
- d) Oven dried at 60°C for two days, cooled in a desiccator and stored at -10°C.
- e) Oven dried at 100°C for two days then cooled in a desiccator and stored at -10°C.

Conclusions drawn from this study was that both air drying and oven drying soils consistently resulted in a significant increase of NH_4^+ released from each soil. This can possibly be attributed to an increase in organic matter decomposition and a release of NH_4^+ from soil clay exchange sites. Soils dried in an oven showed a higher release of NH_4^+ and the higher the drying temperature, the greater the NH_4^+ release was. In contrast, the higher the temperature, the lower the amount of NO_3^- released, indicating that temperatures of 70 and

100°C depressed nitrifying organisms. The first drying method showed significantly lower concentrations of NH_4^+ and NO_3^- than the four other drying methods, leading Nina & Sigunga (2012) to conclude that none of the tested drying methods was suitable as a substitute for the field-fresh sample when determining mineral N in Vertisols.

2.2.5.4 Sample storage

Shortly after taking a soil sample, it is essential to be treated to stop mineralization. This is especially important when samples are taken in winter or late autumn in temperate climates. The most common method is to air dry soils by spreading them out in a thin layer. Other methods include freezing or the addition of a biological inhibitor, but these can be ineffective and inconvenient (Dahnke & Johnson, 1990). For example, Nina & Sigunga (2012) found that storing samples at -10°C depressed nitrification, but did not eliminate it.

Air dried samples should be kept in air tight containers to avoid the adsorption of NH_3 gasses in the laboratory. This is also important in order to avoid contamination of samples with dust. As for the storage room, it should be well ventilated and kept at low temperatures with low relative humidity (Tan, 2005).

When samples are stored for extended periods of time, it is important to know if the parameter of interest has changed during storage. Changes in analytical results after storage depends on the element and the extractant used (Bates, 1993). In general, changes that could occur in air dried samples are usually limited during storage (Tan, 2005). However, as stated by Maynard *et al.* (2007), significant changes may occur in the amounts of NH_4^+ and NO_3^- in air dried soils when stored at room temperature for extended periods. An unpublished study conducted by the Western Enviro-Agricultural Laboratory Association revealed that the NO_3^- content of soils decreased significantly after a 3-year storage of air-dried samples at room temperature. Increases in NH_4^+ content have also been reported (Maynard *et al.*, 2007). It was observed that samples air dried at 40°C for 24 hours release NH_4^+ during storage. Small changes were also reported in the concentrations of NH_4^+ and NO_3^- of samples stored at -5°C for 9 months (Bates, 1993).

2.3 Extraction and determination methods for soil inorganic N

For inorganic N, the laboratory process is divided into two phases, namely the extraction of either NO_3^- or NH_4^+ from the soil, followed by the determination of the concentrations of these ions in the soil extract. Numerous methods exist for the extraction of NH_4^+ and NO_3^- from soil samples and the methods of determination are even more diverse (Maynard *et al.*, 2007). Soil extraction involves the use of a chemical solution that aids in the separation of a plant available nutrient from the soil. After extraction follows determination that entails the measurement of the amount of nutrient in the extract (Peck & Soltanpour, 1990).

2.3.1 Extraction of inorganic N

According to Mulvaney (1996), extractants and coinciding extraction methods should fulfil the following criteria:

- a) Extraction of the N forms in question has to be practically quantitative.
- b) Levels of this N forms should not change due to biological or non-biological reactions.
- c) The extractant used should be matched with the determination method and not contain substances that could cause interference.
- d) The extractant must be stable to ensure safe storage for later use.
- e) The extraction method should be fast and uncomplicated.

2.3.1.1 Extraction of nitrate

A number of extractants can be used for NO_3^- . Some of these include distilled water, saturated $\text{CaSO}_4 \cdot 2\text{H}_2\text{O}$, 0.03 M NH_4F , 0.015 M H_2SO_4 , 0.01 M CaCl_2 , 0.5 M NaHCO_3 at pH 8.5, 0.01 M CuSO_4 with or without Ag_2SO_4 , and 2.0 M KCl (Maynard *et al.*, 2007). According to Berg & Gardner (1978) NO_3^- -N can be extracted with distilled water or a dilute solution free of N. As stated by Patriquin *et al.* (1993) measurements of NO_3^- in water extracts of soils are conducted routinely by a number of laboratories.

2.3.1.2 Extraction of ammonium

Ammonium is a cation that occurs in solute, exchangeable and fixed forms in soil. Unlike NO_3^- , exchangeable NH_4^+ is therefore not extractable with water. Extraction of exchangeable NH_4^+ requires displacement of this cation from adsorbed positions on clay layers by exchange with another cation of a saline solution. On the other hand, the determination of fixed or non-exchangeable NH_4^+ , that cannot be replaced by another cation,

involves the treatment of soil with alkaline KBr (potassium hypobromide) to remove the non-exchangeable NH_4^+ and labile organic-N compounds followed by digestion with a solution of hydrogen fluoride and hydrochloric acid (HF-HCl) (Mulvaney, 1996). Only extraction of exchangeable NH_4^+ will be discussed further.

2.3.1.3 Simultaneous extraction of ammonium and nitrate

The most common extractant for the simultaneous extraction of NH_4^+ and NO_3^- is 2.0 M KCl (Maynard *et al.*, 2007). Research done by Wheatley *et al.* (1989), revealed that for NO_3^- -N extraction, both 2.0 M KCl and distilled water extracted significantly higher amounts than any other extractant tested (e.g. 1.0 M KCl, 4.0 M KCl, 0.05 M K_2SO_4 and 0.01 M CaCl_2). Further, the results showed that the most efficient extractant of NH_4^+ -N is 2.0 M KCl, which significantly extracted more NH_4^+ -N than any of the other extractants. In conclusion the 2.0 M KCl extractant can be used for both NH_4^+ -N and NO_3^- -N (Wheatley *et al.*, 1989). Preparation of the 2.0 M KCl extractant is described in Chapter 3 (Mulvaney, 1996; Maynard *et al.*, 2007; Griffin *et al.*, 2009) and therefore no detailed information is given here.

2.3.1.4 Saturated paste extraction

No information was found in literature where the SATe was used to obtain NH_4^+ and NO_3^- simultaneously in solution. However, Corwin *et al.* (2003a) reported results on saturated extraction of NO_3^- , but not compared to 2.0 M KCl extraction of NO_3^- .

2.3.1.5 Important aspects of the extraction procedure

Soil to extractant ratio

The ratio of soil to extractant is very important since it influences the amount of the nutrient extracted. For either NH_4^+ or NO_3^- , a soil to extractant ratio of 1:10 is recommended. A lower ratio could lead to incomplete extraction of NH_4^+ (Mulvaney, 1996). However, Bremner (1965) reported that estimates of exchangeable NH_4^+ in incubated soils extracted with neutral K salt solutions increased very little with a soil to extractant ratio higher than 1:5.

Wiltshire & Laubscher (1989) compared different soil to extractant ratios for NaCl (1:10 and 1:40) and KCl (1:10). They reported that with a 1:10 soil to extractant ratio, there was no difference between the NaCl and KCl extractants for NH_4^+ and TIN, but this was not the case for NO_3^- . Larger amounts of NO_3^- were extracted with NaCl than with KCl. Linear regressions of 1:40 versus 1:10 soil to extractant ratios showed that a reduction in sample size to 1 g significantly and consistently increased NH_4^+ content with $4 \pm 0.7\%$ and

decreased NO_3^- content with $3 \pm 0.6\%$. On average inorganic N was 1.5 mg/kg larger. None of the extraction procedures gave results that differed more than twice the standard deviation from the mean (Wiltshire & Laubscher, 1989).

Leaching versus equilibrium extraction

To obtain soil extracts, Mulvaney (1996) suggests two methods, namely leaching or equilibration. In leaching, a soil sample is treated with the extractant for a certain time period that could or could not include shaking. Thereafter the soil suspension is filtered, the residue on the filter paper leached with the extractant, and the filtrate brought to a specific volume. With the equilibrium method, a measured volume of extractant is added to the soil sample and shaken for a certain period of time. The soil suspension is then filtered, the residue not leached and the filtrate not made up to volume. The leaching method is supposed to, in theory, be more quantitative, but both methods can give the same results if carried out properly. The equilibrium method is more convenient, easier and a smaller volume of extractant is required, making storage and analysis easier.

Extraction duration

When using KCl to extract NH_4^+ and NO_3^- , it is recommended by Maynard *et al.* (2007) to shake for 30 minutes. Mulvaney (1996) on the other hand, states that not shaking for at least an hour can lead to inadequate extraction of NH_4^+ , but Bremner (1965) reported that NH_4^+ contents in neutral K salt extracts increased very little when shaking more than 15 minutes.

For NO_3^- , the extraction time with KCl can vary from 5 to 30 minutes, but it has been found that shaking for only 5 minutes can give the same results as shaking for 8 hours and that a shaking time of only 2 minutes is sufficient (Gelderman & Beegle, 2012).

In research by Wheatley *et al.* (1989), different extractants were evaluated when soils were shaken for 15, 30, 60 and 120 minutes. Results showed no significant difference in the amounts of either NH_4^+ -N or NO_3^- -N extracted with different extraction durations. Nonetheless, shaking should be carried out under constant conditions, especially when consecutive samples are to be compared afterward, and violent shaking should be avoided.

Filtration

The filter paper used during extraction can contain significant amounts of NH_4^+ and NO_3^- that may contaminate extracts (Maynard *et al.*, 2007). For example, Wiltshire & Laubscher (1989) analysed duplicate samples that were either filtrated or centrifuged. Results showed

that filtration with paper increased the contents of NH_4^+ in 24 soils with an average of 2.5 ± 3.8 mg N/kg compared to centrifugation. The expected error caused by filter paper becomes important when the contents are converted to kg N/ha.

Mulvaney (1996) recommends that filter paper should be washed before use. If KCl is used as an extractant, 20 ml of 2.0 M KCl and 20 ml deionized water should be filtered in a Buchner funnel followed by oven or air drying at 40 to 70°C. However, Wiltshire & Laubscher (1989) found that the error caused by filter paper could not be easily avoided by prewashing. Moreover, this error could also not be corrected by subtracting filtered blanks, due to differences between individual filter paper discs (Wiltshire & Laubscher, 1989).

An alternative to cellulose- and paper filters could be to use more expensive glass fibre filters, containing sufficiently low quantities of NH_4^+ and NO_3^- or to make use of the more economic centrifugation (Wiltshire & Laubscher, 1989; Mulvaney, 1996).

2.3.2 Determination of ammonium and nitrate

2.3.2.1 Colorimetric methods

Colorimetry is extensively used for inorganic N determination in soil extracts. Automated colorimetric techniques that use continuous flow analysers is a preferred method for routine analysis (Maynard *et al.*, 2007). The Berthelot reaction is used for NH_4^+ -N, and the Griess-Ilosvay method for NO_3^- . An advantage of both methods is that 2.0 M KCl does not interfere with the reactions involved (Mulvaney, 1996).

Manual ammonium determination

In the past, the Nessler method was used which involves the reaction of potassium, mercury and iodine with NH_4^+ present in a sample to produce a yellowish-brown colour (Jeong *et al.*, 2013). The sensitivity of this method is however limited and measurements are vulnerable to interference from mainly Mg, Ca, Fe and S. This interference can be avoided with steam distillation, and the NH_4^+ in the distilled sample is then determined easier with acidimetric titration than with colorimetry. These limitations have reduced the use of the Nessler method and led to the development of the now commonly used Berthelot reaction (Mulvaney, 1996).

The Berthelot reaction is based on the indophenol blue method for the determination of NH_4^+ . Ammonia reacts with phenol under alkaline conditions in the presence of an oxidizing agent such as sodium hypochlorite and a catalyst such as sodium nitroprusside to form an intense blue colour. Phenol is used more often than other phenolic compounds. However,

sodium salicylate is also used sometimes instead of phenol since it is less toxic. Colour development is strongly influenced by pH and a buffer is used to ensure uniform pH for analysis. Gentle heating is normally applied to increase sensitivity and reduce analysis time. The colour is stable for at least an hour after its development and then slowly begins to fade (Mulvaney, 1996).

Manual nitrate determination

Many methods for the colorimetric determination of NO_3^- exist. Nitrate can be determined manually by using the nitrophenoldisulfonic yellow colour method. However, this procedure is complicated by interferences caused by organic matter, Cl^- and NO_2^- . Therefore, using KCl as an extractant will cause interference (Mulvaney, 1996).

An alternative is the reaction of brucine and NO_3^- that produces a blue colour. This method is more convenient and simpler than the phenoldisulphonic acid method, but is vulnerable to interference caused by organic matter, NO_2^- and strong reducing or oxidizing agents. Brucine also needs to be prepared frequently due to its instability which is very inconvenient since brucine is extremely toxic (Mulvaney, 1996).

An easier way of determining NO_3^- uses the reaction of chromotropic acid in concentrated H_2SO_4 . Determination of NO_3^- with this method is convenient and rapid, with less interference than with the phenoldisulphonic acid method. However, the method is less sensitive when using 1.0 M KCl as an extractant. It also underestimates NO_3^- in an $\text{Ca}(\text{OH})_2$ extract when soluble organic matter is present, because organic matter causes interference with colour development (Mulvaney, 1996).

Another method used is the transnitration of salicylic acid, also in concentrated H_2SO_4 , to produce nitrosalicylic acid that can be determined after adding NaOH. However, interference is again caused by Cl^- , rendering KCl unsuitable as an extractant (Mulvaney, 1996).

As a result, NO_3^- is usually determined by means of the Griess-Ilosvay method. In this method the NO_3^- is reduced to NO_2^- using copperized cadmium (Mulvaney, 1996; Maynard *et al.*, 2007; Gelderman & Beegle, 2012). The NO_2^- is then determined by using a modified Griess-Ilosvay method based on the principle that NO_2^- reacts with diazotizing agents (aromatic amines) in acidic solutions to produce diazo salts (Gelderman & Beegle, 2012). These salts bind with aromatic agents to form reddish purple azo compounds or azo dyes. The intensity of the reddish purple colour that develops is proportional to the NO_3^- concentration in the soil extract (Mulvaney, 1996).

Automated analysis of ammonium and nitrate

When it comes to routine analysis, the preferred method is automated colorimetry that makes use of continuous flow analysis. Continuous flow injection systems such as segmented flow analysis and flow injection analysis are rapid, sensitive and free from most interference. The most commonly used method for determination of NO_3^- and NH_4^+ is segmented flow analysis after extraction of 2.0 M KCl. Flow injection methods are generally based on the same chemical reactions as the manual determinations, just with different instruments (Mulvaney, 1996; Maynard *et al.*, 2007)

The indophenol blue procedure for NH_4^+ determination and the Griess-Ilosvay procedure for NO_3^- determination are sensitive, simple, convenient and fast and therefore widely used for automated analyses (Mulvaney, 1996). The Griess-Ilosvay procedure for NO_3^- is very sensitive and allows for sufficient dilution to effectively eliminate interferences by any coloured extract (Gelderman & Beegle, 2012). However, the instrumentation is quite expensive (Gelderman & Beegle, 2012) and suspended matter in the reduction column can restrict sample flow at high concentrations of Cu, Fe and other heavy metals, which can result in low readings (Nathan *et al.*, 2012).

Ultraviolet adsorption difference

Nitrate absorbs UV radiation, making it possible to determine the NO_3^- concentration in a soil extract. Serious interferences are however caused by soil constituents such as organic matter that absorbs UV radiation at the same wavelength as NO_3^- , which is roughly at 0.21 μm . An alternative is the UV difference or dual wavelength method (Mulvaney, 1996).

With this method, the UV absorbance is measured before and after NO_3^- reduction to non-absorbing species. Before reduction, UV absorbance of NO_3^- plus species without NO_3^- is measured at 0.21 μm . After reduction the UV absorbance of only non-absorbing species is measured at 0.27 μm . The difference in absorbance is then used to estimate the NO_3^- concentration. In the presence of NO_2^- this difference represents both NO_3^- and NO_2^- , but these two ions can also be determined separately (Mulvaney, 1996).

The UV difference method is precise, sensitive and NO_3^- analysis results compares well to results of steam distillation. Usage of the dual-wavelength method reduces sample analysis time and eliminates any need for chemical treatments to remove NO_3^- . However, serious error can be caused by the variability of other elements in the extract (Mulvaney, 1996).

2.3.2.2 Ion chromatography

Ion chromatography is a common method for determining anions and cations in water samples (Michalski & Kurzyca, 2006). Ion chromatography is one sub-method in a large field of chromatographic methods. In traditional analysis, chromatography is the separation of substances according to their colour and their determination through visual observation (Eith *et al.*, 2001). However, not all ions can be characterized by visible colours and other determination methods are used today. Different methods used for detection of substances include conductometric analysis (electrochemical) as well as UV and mass spectrometry (spectroscopic detection) (Eith *et al.*, 2001; Michalski & Kurzyca, 2006). Selecting a suitable detector should be made according to the analytical question (Eith *et al.*, 2001).

With ion chromatography a few anions and cations can be determined simultaneously in a short time (Mulvaney, 1996; Michalski & Kurzyca, 2006). These include inorganic and organic ions. Only a small sample volume is needed and results have a high sensitivity and good reproducibility (Michalski & Kurzyca, 2006). Analysis is vulnerable to interference caused by concentrated salt solutions and extractions are therefore usually done with water or dilute salt solutions, preventing the determination of exchangeable NH_4^+ (Mulvaney, 1996). When sulfate interference is a problem, CaCl_2 is recommended for ion chromatography extracts (Griffin *et al.*, 2009). Although equipment for ion chromatography is still high (Mulvaney, 1996), it is more affordable today than it used to be (Eith *et al.*, 2001).

2.3.2.3 Ion specific electrode

Specific ion electrodes offer advantages over colorimetry and steam distillation since they are simpler to use, less expensive and rapid (Griffin *et al.*, 2009). A brief description of the principles of the NH_4^+ - and NO_3^- electrodes follow.

Electrodes for ammonium

An NH_4^+ electrode makes use of a cation sensitive liquid membrane. Unfortunately, it is sensitive to K^+ interference and extraction with KCl or K_2SO_4 is not available. An alternative is the NH_3 gas sensing electrode with an internal reference electrode. For this electrode, the solution to be analysed is alkalinized to convert NH_4^+ to NH_3 . The NH_3 activity is determined by measuring the pH of the internal filling solution into which the NH_3 diffuses. Analysis with the NH_3 electrode is unaffected by soil constituents in extracts (Mulvaney, 1996).

Electrodes for nitrate

The functioning of a NO_3^- -specific ion electrode is similar to that of a conventional pH electrode (Myers & Paul, 1968; Gelderman & Beegle, 2012). In a pH electrode, the potential develops across a glass membrane, but in a NO_3^- electrode, the potential develops across a thin layer of gel or liquid. This gel does not mix in water and is the ion exchanger, specifically selective for NO_3^- ions (Gelderman & Beegle, 2012). The ion exchanger is dissolved in an organic solvent and infused with a thermos-setting plastic membrane, separating the internal reference solution from the analysis solution (Mulvaney, 1996). This porous membrane holds the ion exchanger layer in place. The liquid internal filling contains fixed concentrations of NO_3^- and provides a stable potential between the internal Ag/AgCl reference element and the inside surface of the membrane (Gelderman & Beegle, 2012). The electrode is immersed in a NO_3^- containing solution, where the NO_3^- binds with the ion exchanger, and is transported over the membrane. An electrical potential develops between the two sides of the membrane (Mulvaney, 1996).

The electrode responds to the activity of unassociated ions and not to the NO_3^- ions bound to the complexing agent. If NO_3^- ion activity in the sample solution is higher than that inside the internal filling solution, NO_3^- ions will diffuse into the electrode and the opposite occurs if the activity in the sample solution is lower than that of the internal filling. Diffusion of NO_3^- ions continue until equilibrium is reached and then the electrical potential developed over the membrane will prevent further net diffusion (Gelderman & Beegle, 2012). The difference between the NO_3^- content of the reference solution and that of the sample thus determines the magnitude of the developed potential and this potential is measured relative to a constant generated potential of an external reference electrode. The response time of the NO_3^- electrode varies from several minutes at low concentrations to a few seconds at high NO_3^- concentrations (Mulvaney, 1996). The instrument is also less sensitive at high levels of NO_3^- (Myers & Paul, 1968).

Anions such as Cl^- and HCO_3^- interfere with NO_3^- determination (Myers & Paul, 1968). Interference of Cl^- makes the use of KCl as an extractant unsuitable (Mulvaney, 1996; Griffin *et al.*, 2009). If KCl is used, electrodes can underestimate NO_3^- in such a concentrated salt solution (Mulvaney, 1996). As an alternative, Mulvaney (1996) recommends that distilled water or dilute salt solutions can be used in soils with a high anion exchange capacity. Such solutions include 0.025 M $\text{Al}_2(\text{SO}_4)_3$; 0.01 M CuSO_4 ; a mixture of 0.01 M $\text{Al}_2(\text{SO}_4)_3$, 0.01 M Ag_2SO_4 , 0.02 M H_3BO_3 and 0.02 M H_3NSO_3 (sulfamic acid); 0.02 M $\text{Na}_3\text{C}_6\text{H}_5\text{O}_7$; 0.01 M or saturated CaSO_4 ; 0.04 M $\text{KAl}(\text{SO}_4)_2$; and 0.12 or 0.04 M $(\text{NH}_4)_2\text{SO}_4$.

Yet, the NO_3^- electrode has several shortcomings. The NO_3^- electrode is subject to interference by other anions and lacks sensitivity which makes the use of a small soil to extractant ration necessary. It is also subject to subtle variations in sample handling and possibly even differences among electrodes supplied by a manufacturer. The NO_3^- electrode needs constant re-standardization, preparation and reference electrodes are necessary. The interchangeable sensor membrane also has a limited operational lifespan (Mulvaney, 1996; Griffin *et al.*, 2009). Electrodes for determination of NO_3^- and NH_4^+ are therefore not widely accepted as a routine method for the determination of inorganic N (Mulvaney, 1996).

2.3.2.4 Steam distillation

According to Mulvaney (1996), procedures for steam distillation are reliable, precise and accurate. Analysis is also unaffected by inorganic and organic constituents present in soil extracts and determinations can be carried out on coloured or murky extracts. Besides for inorganic N, the apparatus required can be used to determine total N, nonexchangeable NH_4^+ and organic N as well. Steam distillation also allows for isotope-ratio analysis of collected exchangeable N in the distillate.

Methods for determining inorganic N by steam distillation are shown in Table 2.3. Determination of NH_4^+ , NO_3^- and NO_2^- can be done simultaneously or NH_4^+ and NO_3^- can be determined individually (Mulvaney, 1996).

Table 2.3 Steam distillation methods for determining different forms of inorganic N (Mulvaney, 1996)

Form of N determined	Method
NH_4^+	Steam distillation with MgO
NO_3^-	Steam distillation with MgO and Devarda's alloy after NO_2^- is destroyed with sulfamic acid and after NH_4^+ removed with MgO steam distillation
$\text{NH}_4^+ + \text{NO}_3^-$	After NO_2^- is destroyed with sulfamic acid, steam distillation commences with MgO. Devarda's alloy is added immediately after adding MgO.
$\text{NO}_3^- + \text{NO}_2^-$	Steam distillation with MgO and Devarda's alloy after NH_4^+ is removed with MgO steam distillation
$\text{NH}_4^+ + \text{NO}_3^- + \text{NO}_2^-$	Steam distillation with MgO and adding Devarda's alloy before distillation

After extraction of inorganic N with 2.0 M KCl, steam distillation is performed for 3 to 4 minutes with a mild base such as MgO to convert NH_4^+ -N to NH_3 -N with or without a reducing agent such as Devarda's alloy. The reducing agent converts NO_3^- -N or NO_3^- plus NO_2^- -N to NH_3 -N. Determining NH_4^+ and NO_3^- in the presence of NO_2^- is possible, because sulfamic acid decomposes NO_2^- fast and quantitatively at room temperature and does not react with NH_4^+ or NO_3^- nor does it interfere with their determination (Mulvaney, 1996).

The $\text{NH}_3\text{-N}$ is thereafter released and collected in a boric acid (H_3BO_3) indicator solution. Subsequent quantitative determination of $\text{NH}_4^+\text{-N}$ from the $\text{NH}_3\text{-N}$ released through steam distillation is possible with titration using a standardized acid (Mulvaney, 1996). The standard titration reagent used is H_2SO_4 (Mulvaney, 1996) or HCl (Berg & Gardner, 1978). The change in colour indicating the endpoint of titration is from green/blue to a permanent faint pink (Berg & Gardner, 1978).

2.3.2.5 Micro diffusion

Methods for micro diffusion are related to those of steam distillation, because NH_4^+ , NO_3^- and NO_2^- are determined by conversion to NH_3 . The difference is that the NH_3 released by this conversion is separated at room temperature by micro diffusion instead of distillation with steam. If NO_2^- is absent, $\text{NH}_4^+\text{-N}$ is determined from the released NH_3 by treating the sample with MgO , while $\text{NO}_3^-\text{-N}$ is determined after the addition of Devarda's alloy. When NO_2^- is present, NO_3^- is determined with the same procedure after treatment of the extract with sulfamic acid that decomposes NO_2^- . In either case, the NH_3 released is absorbed in a H_3BO_3 indicator solution and then determined by titration as described in the previous section. The choice of reagent used in micro diffusion is limited by the design of the diffusion unit (Mulvaney, 1996).

Micro diffusion is less laborious than steam distillation and equipment needed is cheaper than those of steam distillation, resulting in lower analysis cost. However, a diffusion period of 1 to 2 days is needed and results cannot be retrieved immediately. The volume of soil extract that can be used also limits the sensitivity of this method (Mulvaney, 1996).

Advanced diffusion methods were developed by Mulvaney *et al.* (1997) to improve simplicity, reliability and to increase dynamic range and the scope of applications. The method developed involved treating the soil extract with MgO or MgO plus Devarda's alloy to convert $\text{NH}_4^+\text{-N}$, $\text{NO}_3^-\text{-N}$, and $\text{NO}_2^-\text{-N}$ to $\text{NH}_3\text{-N}$. The NH_3 is collected in a H_3BO_3 -indicator solution in a petri dish suspended from a Mason-jar lid and determined quantitatively through acidimetric titration. The Mason-jar diffusion method is not only simpler, but also more convenient, precise and accurate than conventional steam distillation. Soil extractants that can be used for this determination method include distilled water, 0.5 M K_2SO_4 , 1.0 M, 2.0 or 4.0 M KCl , 2.0 M KCl (Mulvaney *et al.*, 1997).

2.4 EMI sensor and EC_a measurements

2.4.1 EMI sensor function

An EMI sensor consists of a transmitting coil at one end of the instrument that induces a circular eddy-current into the soil. Each current loop generates a secondary EM field proportional in value to the current flowing in the loop. The receiver coil on the other end of the EM instrument intercepts a fraction of the secondary field from every loop and the sum of the signals heightens and forms an output voltage related to EC_a . Differences in soil properties, coil spacing, coil orientation, frequency and sensor distance from the soil surface influences the amplitude and phase differences between the secondary and primary fields (Corwin & Lesch, 2005). A visual representation of the EC sensor based on the principle of EMI can be seen in Figure 2.6.

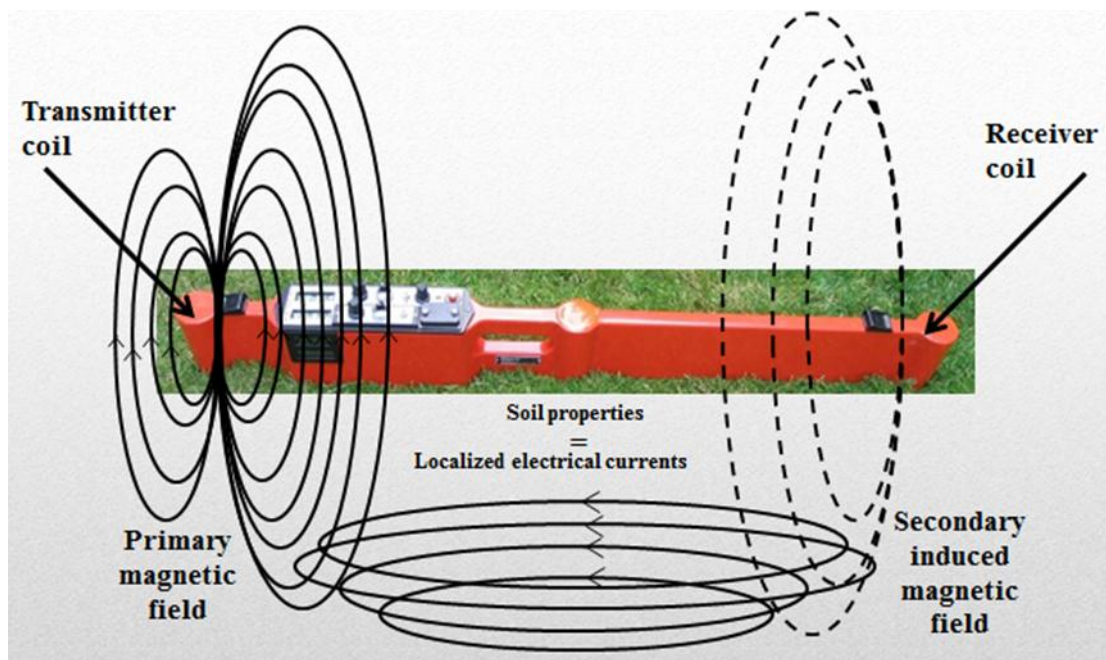


Figure 2.6 The operating principle of the EMI sensor (Grisso *et al.*, 2009).

The most common EMI instruments currently used include the Geonics EM31 and EM38 (Corwin & Lesch, 2005). The EM38 sensor is portable and designed to measure salinity in the root zone. This area is typically from the surface to a depth of 750 mm (Amezqueta, 2007) to 1000 mm (Corwin *et al.*, 2003a) when held in the horizontal (EM_H) operation mode. When placed in the vertical (EM_V) position the EM38 takes readings from the surface to a depth of 1500 mm (Corwin & Lesch, 2005; Amezqueta, 2007). These two operating modes can be seen in Figure 2.7. The EM31 sensor measures up to a depth of about 6 m (Corwin & Lesch, 2005).

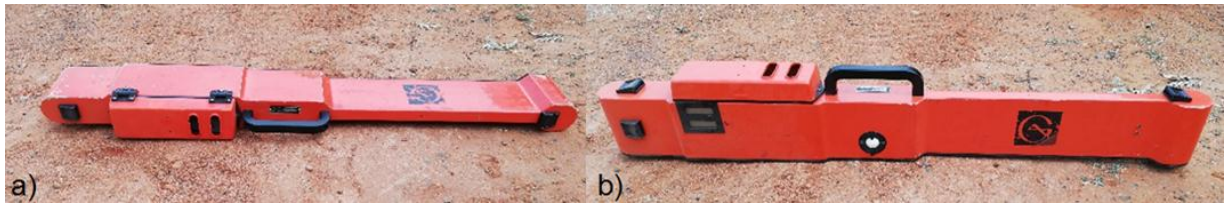


Figure 2.7 The EM38 in the a) horizontal mode with the coils parallel to the soil surface and b) vertical orientation with the coils perpendicular to the soil surface.

The intensity of an EM survey depends on how much detail is desired, any number of spatial EC_a measurements can be taken with a mobile unit in regularly spaced transects over a field (Corwin & Lesch, 2003). Figure 2.8 shows such a specially designed on-the-go unit. The EM38 sensor is mounted in trailer away from metallic objects that cause interference with EM readings. A global positioning system (GPS) is mounted on the vehicle to record sensor reading locations and a Trimble high resolution GPS base station enhances locational information. As mentioned earlier, advantages of EMI include rapid measurement, ease, relatively low costs and large volumes of reliable data collected (Corwin *et al.*, 2010; Doolittle & Brevik, 2014). The measured soil volume is large, up to 2 to 3 m³ (Amezketta, 2007).

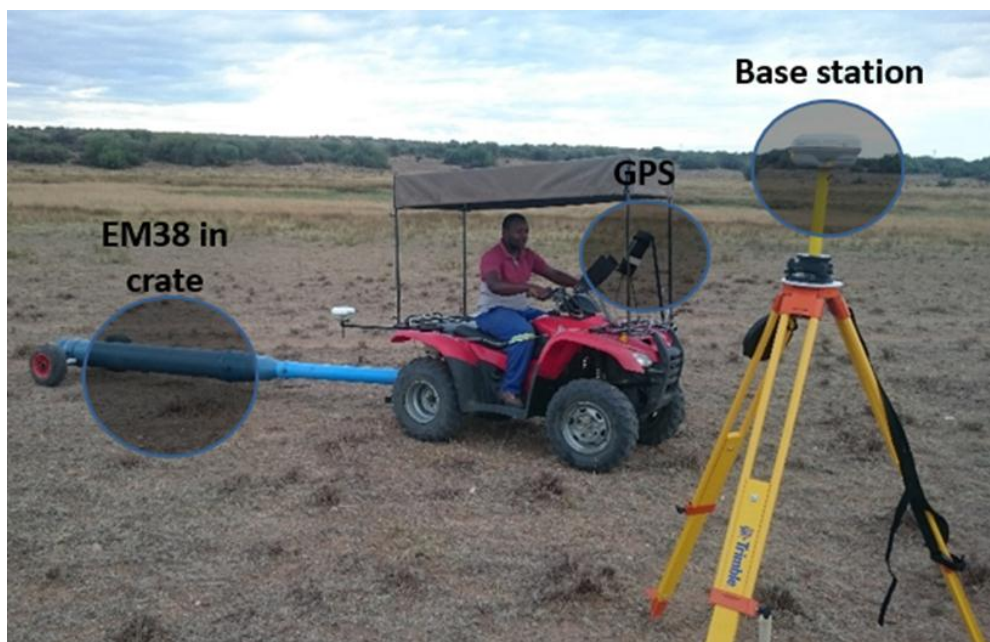


Figure 2.8 A mobile EMI soil survey unit for continuous soil measurement (photo courtesy of Van's Lab Limited).

Additional to the EC_a measurement, with both EM_v and EM_H measurements at the same georeferenced location, profile ratios and geometric means can be calculated. The profile ratios are defined as EM_v/EM_H and provide an indication of the EC_a profile shape and correspond to the leaching fraction. Profile ratios of one indicate a uniform profile, ratios less than one indicate an increase in conductivity with depth, and ratios more than one indicate an inverted profile where conductivity decreases with depth. The geometric means of the EM

levels are defined as $\sqrt{(EM_V \times EM_H)}$ and gives an approximate indication of the cumulative salinity level in the root zone (Corwin *et al.*, 2003a).

2.4.2 Principles of the EC_a measurements

An EMI sensor measures the changes in EC_a which is a depth weighted average conductivity measurement for a column of soil to a specific depth (Doolittle & Brevik, 2014). There are three pathways of current flow that contributes to EC_a , namely i) solid-liquid phase via the exchangeable cations related to the clay minerals, ii) the liquid phase through dissolved solids in the soil solution in large pores and iii) the solid phase path of soil particles that are in continuous contact (Corwin & Lesch, 2005).

The three pathways can be described by the following electrical conductivity model (Rhoades *et al.*, 1989):

$$EC_a = \left[\frac{(\theta_{ss} + \theta_{ws})^2 EC_{ws} EC_{ss}}{(\theta_{ss} EC_{ws}) + (\theta_{ws} EC_{ss})} \right] + (\theta_w - \theta_{ws}) EC_{wc} \quad 2.1$$

where, θ_{ss} ($cm^3 cm^{-3}$) = Volumetric water content of the surface conductance
 θ_{ws} ($cm^3 cm^{-3}$) = Volumetric water content in the soil – water path
 θ_{wc} ($cm^3 cm^{-3}$) = Volumetric water content in the continuous liquid path
 θ_w ($cm^3 cm^{-3}$) = Total volumetric water content ($\theta_{ws} + \theta_{wc}$)
 θ_{sc} ($cm^3 cm^{-3}$) = Volumetric water content of the hardened solid soil phase
 EC_{ws} ($dS m^{-1}$) = Electrical conductivity of the soil – water path
 EC_{wc} ($dS m^{-1}$) = Electrical conductivity of the continuous liquid phase
 EC_{ss} ($dS m^{-1}$) = Electrical conductivity of the surface conductance
 EC_{sc} ($dS m^{-1}$) = Electrical conductivity of the hardened solid soil phase
 $\theta_{sc} EC_{sc}$ = Negligible

Because of the three conductance pathways, the conductivity of the soil is influenced by various soil properties. Therefore, the EMI sensor does not measure just one soil variable but responds to many (Adamchuk, 2010). Variations in EC_a are thus due to the influence of the combined conductance of numerous dynamic and static physical and chemical soil properties that can cause changes in the conductivity of the soil (Corwin & Lesch, 2005; Grisso *et al.*, 2009; Doolittle & Brevik, 2014).

The main physical and chemical soil properties that influence EC_a include salinity, bulk density, water content and saturation percentage. Bulk density and saturation percentage are influenced directly by organic matter and clay content. The exchange surfaces found on organic matter and clay surfaces provide the solid-liquid phase path through exchangeable cations. Clay content and clay type, CEC and organic matter are thus additional factors that

influence EC_a (Corwin & Lesch, 2005). Indirect factors that influence the properties that determine EC_a include ionic composition, soil structure, pH, CEC, soil organic carbon content, $CaCO_3$ content and nutrient levels. EMI has been used to evaluate these soil properties, as well as exchangeable Ca and Mg, lithology and mineralogy, soil compaction, field scale solute leaching rates, herbicide partition coefficients, groundwater recharge, soil map unit boundaries, soil drainage classes and available N (Corwin & Lesch, 2005; Doolittle & Brevik, 2014).

Another important factor that influences EC_a is temperature. If air temperature increases with $1^\circ C$, EC_a increases at a rate of roughly 1.9%. Generally, values of EC_a are expressed at a $25^\circ C$ reference temperature for purposes of comparison (Corwin & Lesch, 2005).

The spatial variability and magnitude of EC_a in a field is generally dominated by one or two of the above mentioned factors and differs from one field to the next. This makes the interpretation and use of EC_a measurements very site-specific and soil-specific (Corwin & Lesch, 2005; Heil & Schmidhalter, 2017).

2.4.3 EC_a data application

2.4.3.1 Geostatistics

Geostatistics offer many techniques suitable for studies where mapping is involved. These techniques include combinations of nonlinear or linear estimation with one or more spatial properties using the methods of kriging, inverse distance weighing, nearest neighbours, pooling, and others. A geostatistical analysis can also be used to determine whether a spatial correlation exists between two soil properties, for example between EC_a and salinity. This can be accomplished by using a function to describe spatial correlation. Functions include the covariance function, autocorrelation function, or the variogram. Results determine if further geostatistical analysis is justified or if classical statistical methods can be used (Yates & Warrick, 2002).

To increase the efficiency of soil EC_a data collection and interpretation, the U.S. Salinity Laboratory Staff developed geostatistical software for conductivity modelling, namely “Electrical conductivity Sampling Assessment and Prediction” or “ESAP”. This software is user-friendly and allows firstly, the generation of conductivity survey maps and directed soil sampling designs according to these maps (Amezketta, 2007). Secondly, the software allows the calibration of conductivity signal data to soil salinity data, and lastly the interpretation of the predicted spatial soil salinity data (Amezketta, 2007).

2.4.3.2 Software directed soil sampling

The ESAP software package uses EC_a survey data to identify optimal locations for soil sampling. Soil samples are needed to calibrate soil sample laboratory measurements to EC_a data and to understand the dominant soil properties that influence EC_a (Corwin & Lesch, 2003). Two EC_a -directed soil sampling approaches are used, namely design-based sampling and model-based sampling. The first consists mainly of the use of simple random, stratified random, cluster and unsupervised classification sampling, while the latter and preferred method makes use of optimized spatial response surface sampling designs (RSSD) (Corwin *et al.*, 2006; Corwin *et al.*, 2010).

The goal of the RSSD statistical methodology is to firstly select sampling site locations for the purpose of optimizing the fitting of a spatial regression model by examining the input EC_a survey data and selecting those EC_a survey sites that represent statistically optimal sample sites (Lesch *et al.*, 2000). Secondly the RSSD program selects a set of sampling locations that best covers all of the spatial variability in the field (Corwin & Lesch, 2003; Corwin *et al.*, 2006; Wienhold & Doran, 2008). The identified sampling sites represent $\pm 95\%$ of the observed range in the geometric mean EM data, $\pm 95\%$ of the observed range in the EM profile ratio data, and are spatially distributed in a uniform manner (Corwin *et al.*, 2003a).

The number of sampling locations can be defined within the ESAP program (Corwin *et al.*, 2003b). Usually 6, 12 or 20 sites are selected, depending on the level of EC_a variability on a site (Corwin & Lesch, 2003). This process of automatically selecting calibration sites saves the researcher time and effort (Amezketta, 2007). The number of samples needed for calibration can be much lower than those needed during systematic grid sampling because many soil properties follow patterns that are easily reflected with on-the-go soil sensing (Adamchuk, 2010). Thus, the workload in the field and laboratory is much less than for traditional methods (Amezketta, 2007).

2.4.3.3 Salinity modelling and assessment

Apparent electrical conductivity needs to be converted to salinity of the saturated paste extract (EC_e) for the efficient use of conductivity signal data. There are two cases of conversion techniques, namely deterministic and stochastic.

With the deterministic approach empirical or theoretical models are used to convert EC_a to EC_e . Deterministic models are static and parameters are considered to be known and no values of EC_e need to be determined. Deterministic models, however, require additional soil properties such as texture, soil water content and temperature to be known (Lesch *et al.*,

2000; Corwin & Lesch, 2003). The deterministic approach used in the ESAP-calibrate program employs the dual pathway parallel conductance (DPPC) equation developed by Rhoades *et al.* (1989). This model uses measured values of soil texture, electrical conductivity, water content, bulk density and temperature to estimate EC_e (Lesch *et al.*, 2000).

With a stochastic approach, laboratory measured soil variables are calibrated to EC_a survey data to facilitate the soil property estimation process. The stochastic approach uses statistical modelling techniques, for example co-kriging or spatial regression, to directly predict EC_e from EC_a data (Corwin & Lesch, 2003). Stochastic models are dynamic, in other words, the model parameters are estimated using laboratory measured soil sample data collected during the survey (Lesch *et al.*, 2000). The stochastic approach used in the ESAP-calibrate program employs direct multiple linear regression estimation (Lesch *et al.*, 2000). The remaining EC_a measurements at each unsampled location throughout the entire survey area are then transformed into predicted values of calibrated soil properties by using the established model (Corwin & Lesch, 2003). Stochastic models are typically more accurate than deterministic models when secondary soil properties across a survey site are not known. However, stochastic models are dependent on location and time (Lesch *et al.*, 2000).

2.4.3.4 Inferring soil properties from EC_a

As mentioned, the ESAP-calibrate program can be used to convert EC_a survey data to EC_e using either a deterministic or stochastic approach. Another application is to use stochastic calibration models to predict secondary soil properties that influence EC_a (Lesch *et al.*, 2000). The spatial distribution of EC_a in a field can therefore be used to estimate and map the variability of one or more of the soil properties that directly or indirectly influences EC_a (Corwin & Lesch, 2003; Corwin *et al.*, 2006).

The correlation analysis between EC_a and measured soil variables i) serve in determining the main soil property that influences the EC_a measurement within the study area, ii) helps to interpret the spatial distribution of soil salinity and iii) allows prediction of the expected correlation structure between EC_a data and different soil properties (Amezqueta, 2007).

Many field studies on EC_e have been performed and have revealed how site-specific and complex EC_a is (Corwin & Lesch, 2005). It appears that regression constants for the relationships between EC_a and other soil properties can not necessarily be transferred from one site to another, since there are many factors that affect the strength of the EC_a signal

data and therefore the relationships. Also, the regression quality is often determined by the sufficient range of the dependent and independent variables (Heil & Schmidhalter, 2017).

2.4.4 EC_a data to predict inorganic N

2.4.4.1 Relationship between soil electrical conductivity and inorganic N

In research by Patriquin *et al.* (1993), the relationship between EC and NO₃⁻ in 1:1 water extracted soils were investigated using Merckoquant test strips, a field NO₃⁻ analysis method. Beforehand, Patriquin *et al.* (1993) stated that there appears to be no reports on the relationship between EC and NO₃⁻, even though i) EC is closely related to the total concentration of cations in soil and ii) positive relationships have been reported between cations and NO₃⁻. In this study the NO₃⁻ content of 1:1 soil extracts varied between vegetation and soil types and between sampling times in a manner similar to that of EC. The two variables were highly correlated as seen in Figure 2.9. An R² of 0.71 for the regression of NO₃⁻ on EC was found (Patriquin *et al.*, 1993).

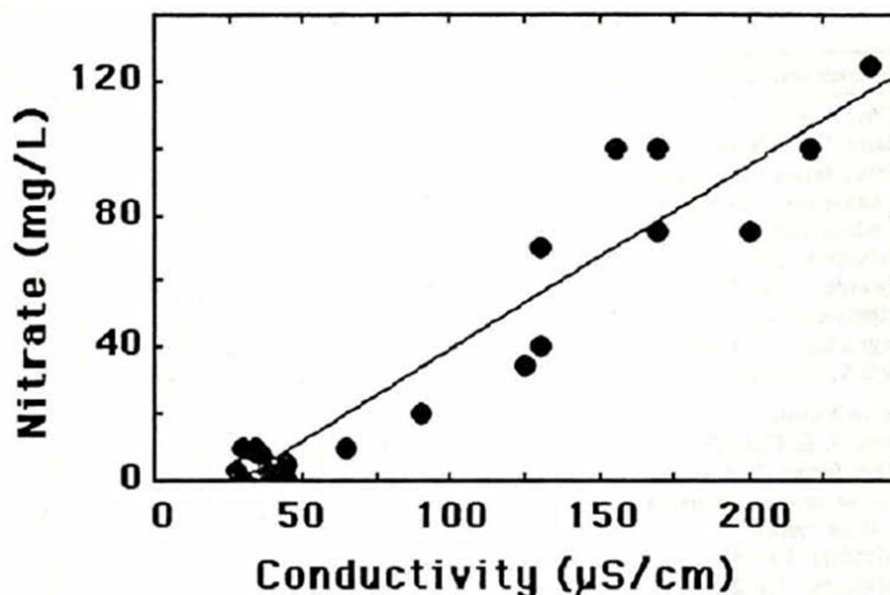


Figure 2.9 Relationship between soil extract NO₃⁻ and EC (Patriquin *et al.*, 1993).

Results showed a negative Y intercept for the relationship between NO₃⁻ and EC. Rather than being linear over the entire range, the relationship appeared to be zero at low values of EC, and above a certain value, NO₃⁻ increased linearly with an increase in EC. Considering that the NO₃⁻ extracted in water is not electrically held on soil colloids, and that there must also be equal quantities of cations in the soil solution to sustain electrical neutrality, the linear relationships found suggest that measurements of EC can give valid relative estimates of the total amounts in the soil solution and consequently of the relative potential for leaching losses (Patriquin *et al.*, 1993).

In research by Zhang & Wienhold (2002), one objective was to assess the potential of using changes in EC as a measure of changes in soil inorganic N. Soils were sampled and incubated for 32 days where after EC was measured *in situ* with a portable EC meter (not an EMI sensor) and incubated soils were air dried and analysed for NO_3^- , NH_4^+ , pH and EC. Results showed a strong linear relationship between *in situ* measured EC and NO_3^- -N, suggesting that EC could be used as an estimate of the NO_3^- -N dynamics. Zhang & Wienhold (2002) also remarked that using EC as an estimate of NO_3^- -N will only be possible in soils with low salt contents and free carbonates.

2.4.4.2 EC_a to predict inorganic N in literature

The EM sensor is sensitive to various factors that influence soil conductivity, one amongst others being high nutrient concentrations. Electrical conductivity measurements can be used to determine soluble nutrients, cations and anions and to monitor soil organic matter mineralization. It is therefore logical to assume that the determination of the soluble NO_3^- anion as well as the NH_4^+ cation by means of EC_a measurements could be possible (Eigenberg *et al.*, 2002).

Corwin *et al.* (2003a) conducted a soil quality survey on clay loam soils at a 32.4 ha saline-sodic site divided into eight paddocks. The site was located on Westlake Farms, which resides in Kings County on the west side of California's arid San Joaquin Valley. The methodology used gave a practical way of assessing soil quality in an arid-zone when soil properties are correlated with EC_a. An initial mobile EMI survey was conducted in 1999, followed by a mobile fixed-array survey. The EC_a readings were then used to calculate the geometric mean and profile ratio. The EC_a data and the ESAP v2.0 program were used to identify 40 sampling sites that reflected the spatial heterogeneity of the EC_a measurements. At each identified site two sets of soil samples were taken at 300 mm intervals to a depth of 1200 mm. One soil sample set was used for physical soil property analysis and the other for chemical properties, one of which was the concentration of NO_3^- in the saturated extract. By using the commercial GIS software ArcView 3.1, maps were prepared by interpolation of the measurements at the 40 sampling sites using inverse-distance weighting (IDW) interpolation. Results showed that the concentration of NO_3^- , amongst others, had the highest coefficients of variation. Correlations between both the EM_V and EM_H EC_a measurements and NO_3^- in the saturated extract showed significant correlations.

In another case, Wienhold & Doran (2008) attempted to determine the relationship between EC_a and inherent soil properties. A study was conducted on a 20 ha field in central Nebraska with silt loam soils. An EC_a survey was conducted with an EM38 and data analysed with the

ESAP-95 software to determine soil sampling locations. Soil samples from the identified sampling locations were analysed for NO_3^- -N in 2.0 M KCl extracts. Soil NO_3^- -N values had a wide range from 0.7 to 24.7 g kg^{-1} and correlated well with EC_a having an R^2 of 0.86. The correlation between predicted NO_3^- -N and EC_a was found to be negative. Areas in the field with low NO_3^- -N values were found in some areas with high EC_a values and these areas would require additional N fertilization. On the other hand, areas with low EC_a values and high NO_3^- -N concentrations, additional application of N will most likely cause volatilization of NO_3^- -N and pose a high risk to be leached. In such cases, nitrogen application will have little effect on yields (Wienhold & Doran, 2008).

In research done by Korsæth (2005), the objective was to test if EC_a measurements can be used as an efficient method of monitoring changes in soil inorganic N after fertilizer N application at two different study sites in Norway over two cropping seasons for spring barley. The first study site, Apelsvoll research station, is dominated by gleyed, melanic loam and silty sand textures with an average annual precipitation of 600 mm. The second site, Kise research station, is characterized by 585 mm annual precipitation and the same soil type. At both sites the area studied covered 0.168 ha. For each of the two field trials the three most contrasting replicate blocks regarding soil texture and ignition loss were selected. At each sampling time, EC_a was measured manually with an EM38 in vertical and horizontal mode. The ESAP-RSSD design was not implemented. During the experiment, soil samples were taken before fertilizing/sowing and thereafter at fortnightly intervals. Samples were taken at ten sites where time domain reflectometry soil probes were located. The sampling depth was 0 to 150 mm and 0.4 m from the edge of the plots, between the barley rows. Soil samples were extracted with 1 N KCl for the determination of NH_4^+ -N and NO_3^- -N. The measurements of electrical conductivity were log-transformed and the statistical software package MINITAB was used for correlation analyses. Linear regression models were tested with respect to their ability to predict inorganic N in topsoil during the growing season.

Results showed that the concentrations of inorganic N were strongly correlated with EC_a at both locations studied and in both years (Korsæth, 2005). Positive correlations were found between EM_H and log-transformed concentrations of inorganic N at both locations for all fertilizer treatments. Correlation strength was roughly the same for NO_3^- and NH_4^- at Apelsvoll, but in most cases at Kise, EM_H correlated stronger with NO_3^- than with NH_4^- . Korsæth (2005) reported on work done by Eigenberg & Nienaber (1998) who also found a significant correlation between EM_H and NO_3^- , but not for NH_4^+ . Korsæth (2005) concluded that EC_a appears to hold promise for the monitoring of inorganic N concentrations during crop growth, even on highly variable soils.

EC_a has great potential in monitoring NO₃⁻-N dynamics during the growing season (Eigenberg *et al.*, 2002). The authors conducted a study on a centre-pivot irrigated field at the US Meat Animal Research Centre in the central USA to determine the usefulness of EC_a maps in determining the agronomic effectiveness and environmental consequences of N fertilization. Soils at this site were characterized as silt loam soils. Five plot treatments of manure and compost and an N fertilizer control were replicated four times. The field (5.95 ha) was arranged in a complete randomized block design with a split plot for winter cover crop against no cover crop. Two samples were taken throughout the growing season within one day of an EC_a survey. Samples were taken at randomly selected sites with a hand probe at depths of 0 to 230 mm and 230 to 460 mm and used to determine KCl extractable NH₄⁺-N and NO₃⁻-N. Georeferenced EC_a measurements were taken with an EM38 in horizontal orientation. The EM38 sensor was transported through the field mounted on a trailer pulled behind an all-terrain vehicle. When the maize became too high the sensor was pulled on a plastic sled by hand. At a speed of 6 m/s, approximately 40 measurements were collected across the length of each plot for each pass (Eigenberg *et al.*, 2002).

Maps were generated using inverse distance interpolation and correlations of EC_a with NO₃⁻ were determined. Results revealed that the profile weighted EC_a values (0 to 750 mm) were highly correlated with soil NO₃⁻-N in the surface 0 to 230 mm and 230 to 460 mm soil layers throughout the growing season. Consecutive EC_a measurements were effective in identifying the dynamic changes in inorganic N during the maize-growing season. Further, EC_a maps of different consecutive survey times provided insights into temporal soil dynamics revealing changes in soil conductivity and plant available N. EC_a could also serve as a measure of N sufficiency for maize early in the growing season, as well as an indicator of surplus N after harvest when N losses due to leaching or denitrification is likely (Eigenberg *et al.*, 2002).

Compared to the above discussed research, contradicting results were found by Corwin *et al.* (2003b) who conducted an extensive EC_a survey on the silty clay soils of a 32.4 ha site located in the Broadview Water District also on the west side of the San Joaquin Valley in central California. The research objective was to identify soil properties that influence cotton yield. Instead of an EM38 sensor, mobile fixed array EC equipment was used to conduct an intensive EC_a survey of roughly 4000 georeferenced EC_a measurements. The equipment measured EC_a to a depth of about 1200 to 1500 mm. The ESAP 95 v2.01 software was used to identify 60 sampling locations through a model based sampling design. Two sets of soil samples were taken at each location in 300 mm depth increments up to 1800 mm. Nitrate-N analysis was done using 1:1 water extracts. For all statistical correlation and regression analyses, the average NO₃⁻-N over the 0 to 1500 mm depth was used. Results

showed that NO_3^- -N had the highest coefficient of variation, indicating high spatial variability. However, the study found no significant correlation between NO_3^- -N and EC_a or between NO_3^- -N and cotton yield.

2.5 Statistics for method-comparison studies

Comparison of any two different measurement or sampling methods for the same variable is often executed by using inappropriate statistical methods. A favourite statistical method often used is correlation analysis. Calculating the product-moment correlation coefficient (R) is an indication of the strength of the linear relationship between pairs of data (Giavarina, 2015).

Correlation analysis only provides information on the association between variables (Altman & Bland, 1983) and not on the difference between the variables or their agreement (Giavarina, 2015). This analysis is sensitive to the range of values and cannot differentiate between random or systematic differences between two variables (Chhapola *et al.*, 2015). So, even in the case of significant systematic bias between two measurements, there can be high correlation between two variables (Bland & Altman, 1986; Chhapola *et al.*, 2015; Giavarina, 2015). Thus, it is wrong to conclude from a high correlation that two methods agree and can be used interchangeably (Altman & Bland, 1983).

Another popular approach when analysing two methods is to plot the data and draw a regression line (Altman & Bland, 1983). Linear regression finds the best line that predicts one variable from another and quantifies goodness of fit with the coefficient of determination, R^2 (Giavarina, 2015). Yet, for the purpose of comparing methods (assessing their agreement), deviation of the scatterplot from the line of equality (where $y=x$) is more informative (Altman & Bland, 1983). Plotting the data and drawing a line of equality on which all points would lie if the two measurement methods gave exactly the same reading each time helps to visually assess the degree of agreement between measurements (Bland & Altman, 1986).

According to Altman & Bland (1983), a reason for using poor methodology is that researchers tend to imitate what they read in other published papers and many papers are published where the same incorrect methods are repeatedly used. It is possibly understandable that those who follow such examples in published papers assume that they are using the suitable statistical methods. A further reason for using unsuitable statistical techniques are that textbooks are scanned in search of the most similar-looking research problem and correlation analysis is then most frequently used. Altman & Bland (1983) further

recommends that journals should become enlightened and return papers that use unsuitable statistical analysis techniques.

When attempting to conduct a method comparison study, the right question that should be asked is if methods are comparable to the point where one can be replaced by the other with enough accuracy for the intended analysis, in other words, if the methods agree (Altman & Bland, 1983). It is therefore essential to assess agreement when comparing two methods. Agreement is not something that is simply absent or present, but should be quantified (Chhapola *et al.*, 2015).

Therefore, as an alternative approach to correlation and regression analysis, Altman & Bland (1983) proposed an analysis based on quantifying agreement between two quantitative measurements by using the mean difference and limits of agreement. In this method the difference between the two methods (A-B) is plotted on the y-axis against the mean (A+B)/2 on the x-axis. The degree of agreement can be summarized by calculating the mean difference (d) and the standard deviation of the differences (s). The statistical limits of agreement can be calculated by using the mean and standard deviation of the differences between the two methods. According to the authors 95% of differences between one measurement and the other should lie within ± 2 standard deviations of the mean difference (Bland & Altman, 1986; Giavarina, 2015).

The estimates of bias and limits of agreement are subject to sampling error which makes calculating their precision necessary, i.e. confidence intervals (CI) (Altman & Bland, 1983; Bland & Altman, 1986; Chhapola *et al.*, 2015; Giavarina, 2015). The 95% CI of the mean difference shows the magnitude of the difference. Significant systematic difference is present if the line of zero difference or equality ($y=0$) does not fall in this interval (Giavarina, 2015). The 95% CI is calculated based in the t-distribution which is also used when doing a paired t-test. Therefore, if the line of zero difference falls within the 95% CI of the bias, the P-value from a paired t-test will also be higher than 0.05 and show no significant difference (Schall; Personal communication³). The 95% CI of the limits of agreement give an estimation of the possible size of the sampling error (Giavarina, 2015). The abbreviations of variables and equations used in the calculations discussed above are given in Table 2.4.

In Figure 2.10 an example of a Bland-Altman plot where the mean difference (d) is represented by a central horizontal line is displayed. The mean difference here is -27.2 units,

³ Prof R. Schall, Department Mathematical Statistics and Actuarial Sciences, University of the Free State, South Africa.

meaning that on average, method B gives readings of 27.2 units higher than method A (Giavarina, 2015). From the mean difference line, three additional horizontal lines are constructed, two representing the 95% limits of agreement and one showing the line of equality or zero difference (Chhapola *et al.*, 2015).

Table 2.4 Abbreviations of variables and equations related to Bland-Altman analysis (Bland & Altman, 1986)

Parameter	Abbreviation	Equation
Mean difference or Bias	d	-
Standard deviation of differences	s	-
Sample size	n	-
Degrees of freedom	$n - 1$	-
t -Distribution	t	-
Upper limit of agreement	$ULOA$	$d + 2s$
Lower limit of agreement	$LLOA$	$d - 2s$
Standard error of mean difference	$SE d$	$\sqrt{s^2/n}$
Standard error of agreement limits	$SEd \pm 2s$	$\sqrt{3s^2/n}$
95% Confidence interval of the bias	$CI bias$	$d \pm (t \times (SE d))$
95% Confidence interval of the upper limit of agreement	$CI ULOA$	$ULA \pm (t \times (SEd \pm 2s))$
95% Confidence interval of the lower limit of agreement	$CI LLOA$	$LLA \pm (t \times (SEd \pm 2s))$

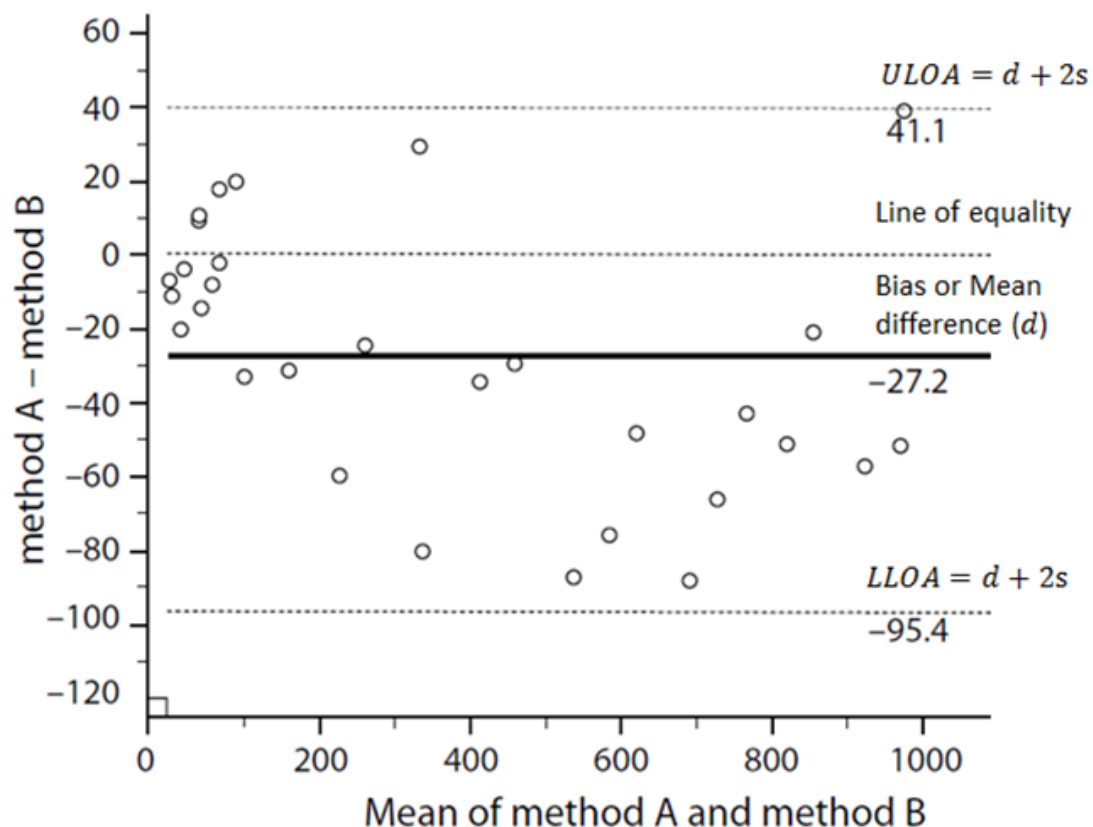


Figure 2.10 The Bland-Altman plot with the mean difference, limits of agreement and line of equality (Giavarina, 2015).

On a Bland-Altman plot heteroscedastic distribution is often observed, implicating that the size of the differences increases with the size of the measurement. In such a case,

logarithmic transformation of original data may be needed. Back transformation (anti-log) of logarithmic transformed data is also proposed for meaningful understanding of the limits of agreement. An alternative for simple interpretation is to plot the percentage difference between the two methods against the mean (Chhapola *et al.*, 2015).

The Bland-Altman plot offers many advantages. It allows easy visual assessment of the bias, i.e. the degree of agreement. Moreover, it helps evaluate the scatter of data, to spot outliers and to identify any trend or relationship between the degree of the differences and size of measurement (Altman & Bland, 1983; Chhapola *et al.*, 2015). Since being proposed in 1983, this method has been widely used and the 1986 paper by Bland and Altman “Statistical methods for assessing agreement between two methods of clinical measurement” have been cited over 30 000 times by various scientific papers (Giavarina, 2015).

The Bland-Altman method does, however, not indicate if the agreement between two methods is sufficient or if one method can be interchanged with the other. This method only quantifies the bias and range of agreement (Giavarina, 2015). Conclusions regarding the agreement and interchangeability of methods should be made considering the limits of agreement and the width of the limits compared to prior defined scientific criteria. If acceptable scientific limits of laboratory measured variables are not available, a Delphi survey can be carried out which is a multistage process of group facilitation designed to transform expert opinion into a group consensus (Chhapola *et al.*, 2015).

2.6 Conclusion

The selection of a suitable site-specific soil sampling method depends on the research topic and its objectives, resources available as well as personal judgement. Site-specific soil sampling can be conducted according to grid-, management zone- or geostatistical methods, each with a number of different designs that can be used. It is obvious that there is no single optimal sampling strategy due to field variability and management differences.

Regarding the advised sampling depth for N for the intention of making fertilizer recommendations, soils should be sampled to a minimum depth of 600 mm. Soils are also often sampled from 600 to 1200 mm. As for the drying temperatures of soils intended for N analysis, it can be concluded that, generally, concentrations of NO_3^- in air dried samples are higher than that in samples dried at high temperatures. Conversely, NH_4^+ can be expected to increase with high drying temperatures. It is advised that temperatures remain below 30°C to avoid chemical transformations.

A vast volume of literature is available on the methods for extraction and determination of soil inorganic N. The most commonly used extraction method for both NH_4^+ and NO_3^- is a neutral K salt solution of 2.0 M KCl. Further, it is well established that water can be used as an extractant for NO_3^- . However, the use of the soil's saturated paste extract is not mentioned in literature for NO_3^- and NH_4^+ extraction and determination against a standard such as 2.0 M KCl.

Regarding extraction times and the ratio of soil to extractant, many possibilities exist as alternatives to the standard practices. However, deviating from the recommendations for these variables could result in less nutrients being extracted. Another very important laboratory factor to consider is the presence of N in the filter paper used during extraction.

Determination methods are extensive and include specific ion electrodes, ion chromatography, steam distillation, micro diffusion and manual colorimetric techniques, to only name a few. However, for routine analysis the preferred method is automated colorimetric techniques that use continuous flow analysers.

After the conduction of a georeferenced EC_a survey, EC_a measurements and ESAP software can be used for the establishment of soil sampling sites which reflect 95% of the spatial variability in the EC_a measurements over a specific field. EMI soil sensors and the ESAP software package thus have the potential to reduce sampling intensity and cost necessary to characterize spatial patterns in a field. The use of EMI sensors have been demonstrated to be very useful in assessing, predicting and mapping spatial patterns of primary and secondary soil properties that influences EC_a . The EC_a measurements have also proven capable of estimating NO_3^- and NH_4^+ . Improved understanding of N dynamics by means of EMI sensors allows the development of management practices that better match inputs with crop needs and reduce the potential for environmental contamination.

CHAPTER 3. MATERIALS AND METHODS

3.1 Study site description

Four sites were selected for the current study. The sites are situated near Douglas in the Northern Cape, Luckhoff in the Free State, Hofmeyr in the Eastern Cape, and Empangeni in KwaZulu-Natal (Figure 3.1). The sites form part of a research project on salt management funded by the Water Research Commission (Project K5/2499//4).

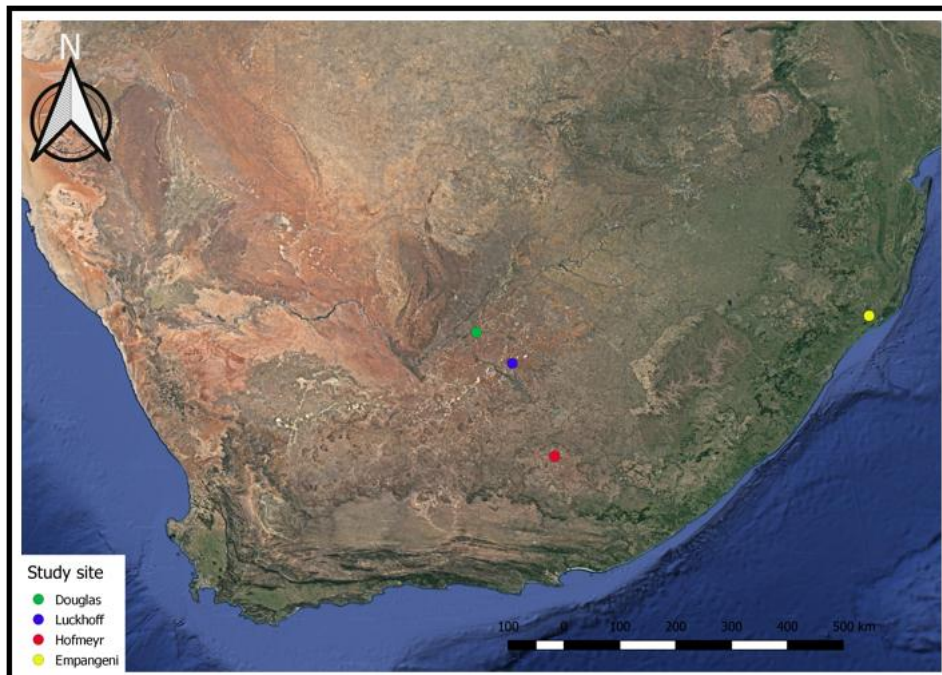


Figure 3.1 Location of the four study sites in South Africa.

3.1.1 Study site locations

All fields selected for the study are irrigated with centre pivot irrigation systems. The first study site (Figure 3.2a) is a 30 ha field situated on Zoutpansdrift farm, about 20 km northwest of Douglas. This field is irrigated by water abstracted from the Lower Riet River. For the second study site (Figure 3.2b), the De Kroon farm is situated about 40 km south west of Luckhoff. The farm is located along the Settlement section of the Orange-Riet Irrigation Scheme and irrigated with water from the Orange River. Of the four centre pivot irrigated fields on De Kroon, only the 40 ha field was selected for this study. The third study site is situated on Juriesbaken farm, located along the Fish River between Steynsburg and Middelburg. One of the four 55 ha fields (Figure 3.2c top left) was selected. The fields are irrigated with water from the Gariiep Dam, via the Orange-Fish Tunnel, which stretches from the Gariiep Dam to Teebus a few kilometres from the fields. The last study site consists of two fields (Figure 3.2d) located in the Heatonville district on a farm named Celina under the

business name Vriendschap Boerdery, Melmoth. The fields are irrigated with water from the Goedertroudam. Approximately 20 ha of the northern field and 55 ha of the southern field were used, adding up to 75 ha.

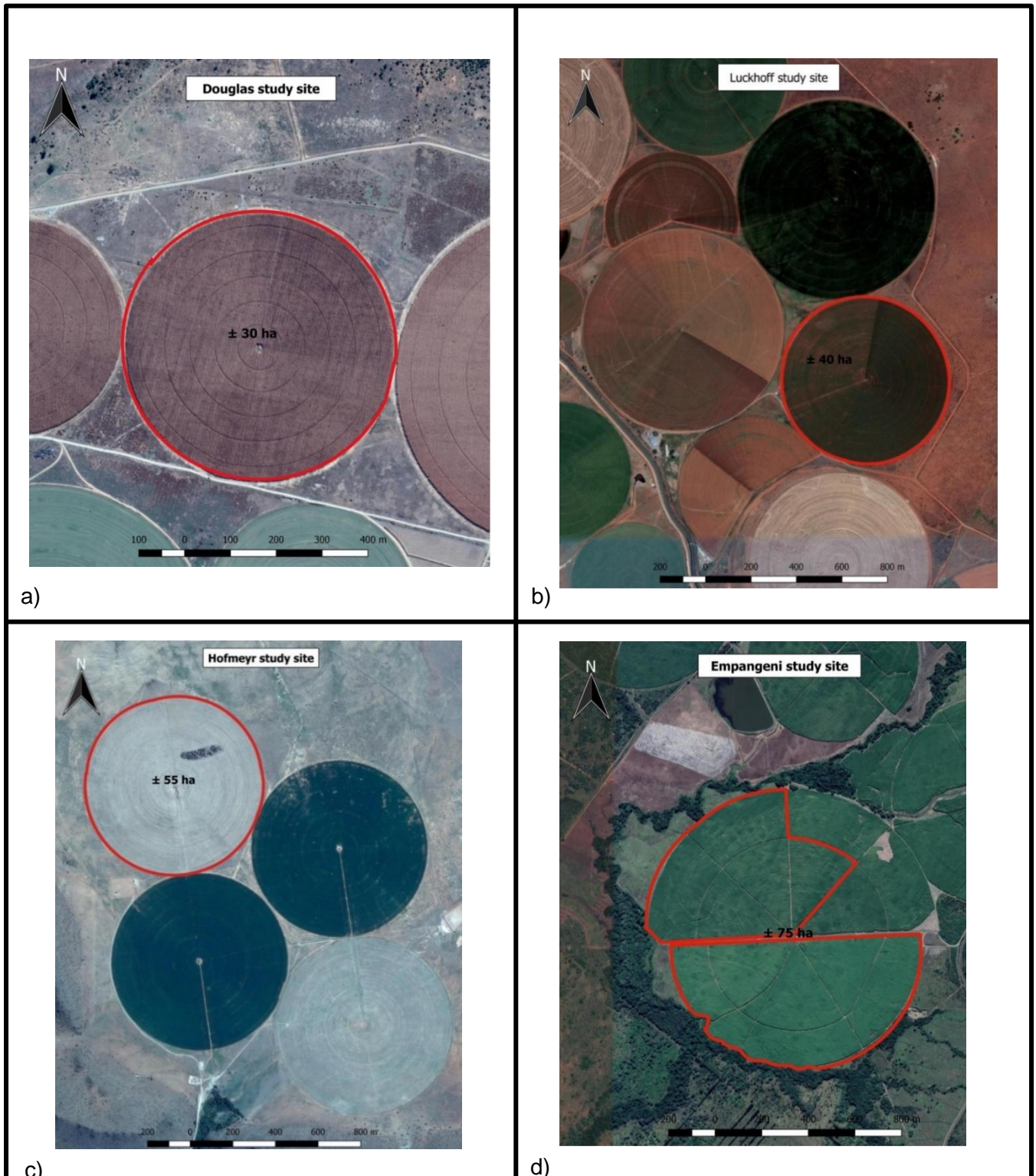


Figure 3.2 Study sites, outlined in red, situated near a) Douglas, b) Luckhoff, c) Hofmeyr and d) Empangeni.

3.1.2 Weather

The climate at Douglas is classified as hot semi-arid (BSh) according to the Köppen-Geiger classification system and receives little rainfall throughout the year. The climate in the Luckhoff area is classified as cold semi-arid (BSk) and like Douglas does not receive much rainfall. The climate near Hofmeyr can again be classified as cold semi-arid (BSk) with little rainfall throughout the year. The climate at Empangeni differs from the rest and is classified as humid subtropical (Cfa) with significant amounts of rainfall during the year (climate-data.org, 2019).

Different weather stations were used to gather data to describe the weather conditions for the year 2016 when soil samples were taken. The DeHoek weather station was used for Douglas and is located roughly 34 km west of the study site. Data from the Rust station was used for Luckhoff and is located 33 km south of the study site. The Grootfontein station was used for the Hofmeyr study site, however this station is about 49 km west of the site and closer to Middelburg than to Hofmeyr. For the Empangeni site, data from two stations were combined to obtain a complete dataset for 2016. For January and April to October the Heatonville station, 2.25 km east of the site, was used and for February and March data of the Mbonambi station, roughly 28 km east of the site, was used.

The weather data from these weather stations are compiled in Appendix 1. In Table 3.1 the data for each site for the year 2016 are summarized. The highest average maximum (29.04°C) as well as the lowest average minimum (7.89°C) temperatures was recorded at Douglas. The Douglas site also had the lowest total rainfall for the year at 206 mm, while Empangeni had the highest amount of rainfall at 555 mm.

Table 3.1 Summary of weather data for 2016 at each study site (ARC-ISCW, 2017)

	Mean Max T (°C)	Mean Min T (°C)	Mean Max RH (%)	Mean Min RH (%)	Mean Total Radiation (MJ/m ²)	Mean Wind Speed (m/s)	Total Rainfall (mm)	Total Relative ETo (mm)
Douglas	29.0	7.9	84.6	19.5	19.2	1.9	205.8	1613.8
Luckhoff	27.8	8.5	85.4	20.6	19.9	2.0	131.1	1939.0
Hofmeyr	26.6	8.9	20.5	*	18.8	1.2	274.8	1409.3
Empangeni	27.6	16.6	89.5	44.2	14.6	2.4	554.9	1009.8

*No data

3.1.3 Topography

For the Water Research Commission (WRC) project, geographical elevation data was gathered for all study sites with the Trimble® TSC3 controller with Trimble Access™ software along with the Trimble® R4 GNSS System. This data was processed using the Quantum GIS version 2.18 program, an open source geographical information system, to produce elevation maps for all the study sites (Figures 3.3a, b, c and d). For interpolation the deterministic natural neighbour method was used with a pixel cell size of 1 m². It is a weighted average method that works well with clustered scattered points and can handle large datasets.

The satellite image for the Douglas site was not included in the map, because coordinates of the map and those of the satellite image could not be aligned. Map coordinates are in easting and northing format and the border between UTM zone 34S and 35S falls exactly on this field.

Elevation for the Douglas site (Figure 3.3a) was found to be relatively constant with a maximum of 1040.98 m and minimum 1040.02 m above mean sea level and total relief of 0.96 m.

The map for the Luckhoff site (Figure 3.3b) shows that the maximum elevation relative to mean sea level is 1241.1 m and decreases to a minimum of 1227.2 m. The decrease in elevation is generally in a west-southwestern direction with a total relief of 13.9 m. The contour interval is 0.25 m and contour lines are evenly spaced, indicating a uniform slope.

For the Hofmeyr site (Figure 3.3c), a maximum elevation relative to mean sea level is 1247.3 m and decreases in a south-eastern direction to a minimum of 1225.9 m with the total relief being 21.4. The interval between contour lines are 1 m, contour lines are evenly spaced, indicating a uniform slope, but in the area of highest elevation, the distance between contour lines decrease, indicating an increase in slope percentage.

At the Empangeni site (Figure 3.3d), the maximum elevation relative to mean sea level is 123.1 m and decreases to a minimum of 95.7 m with a total relief of 27.7 m. The decrease in elevation is generally in a south-western direction and elevation increases to both the east and to the north. The variability of the spacing between contour lines indicate complex variability in the slope. For example, in the northern part of the field, contour lines are spaced closer together indicating steeper slopes and concentric circles indicate small local hills, whereas contour lines in the southern and western part of the field are spaced wide apart, representing a gentle slope.

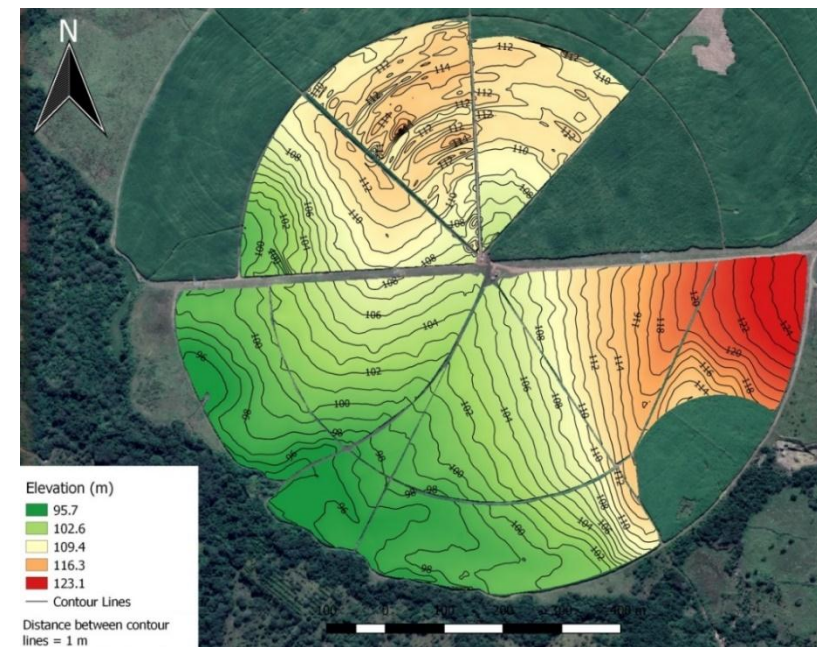
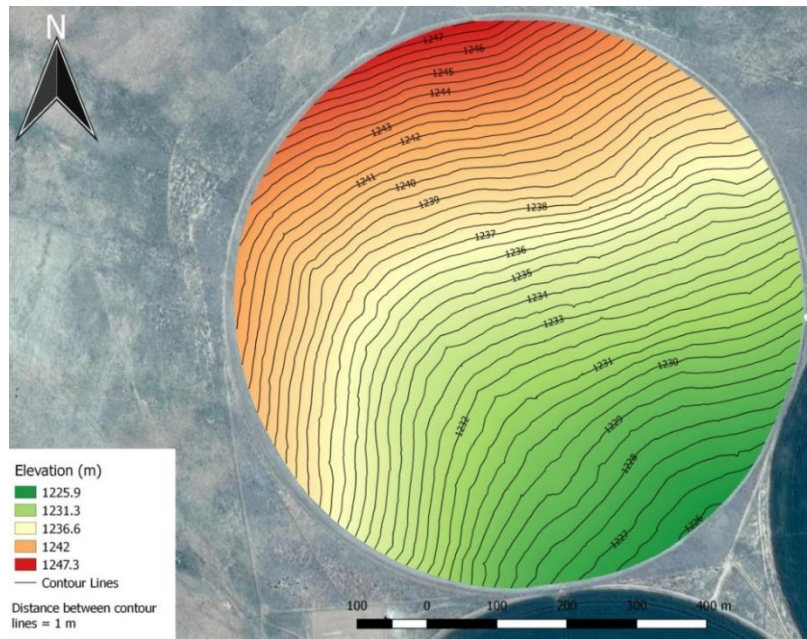
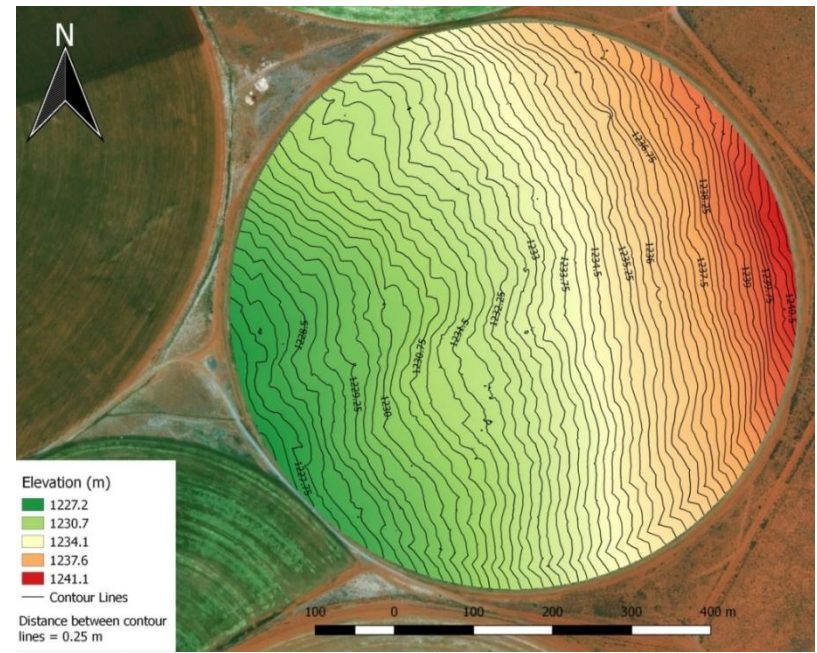
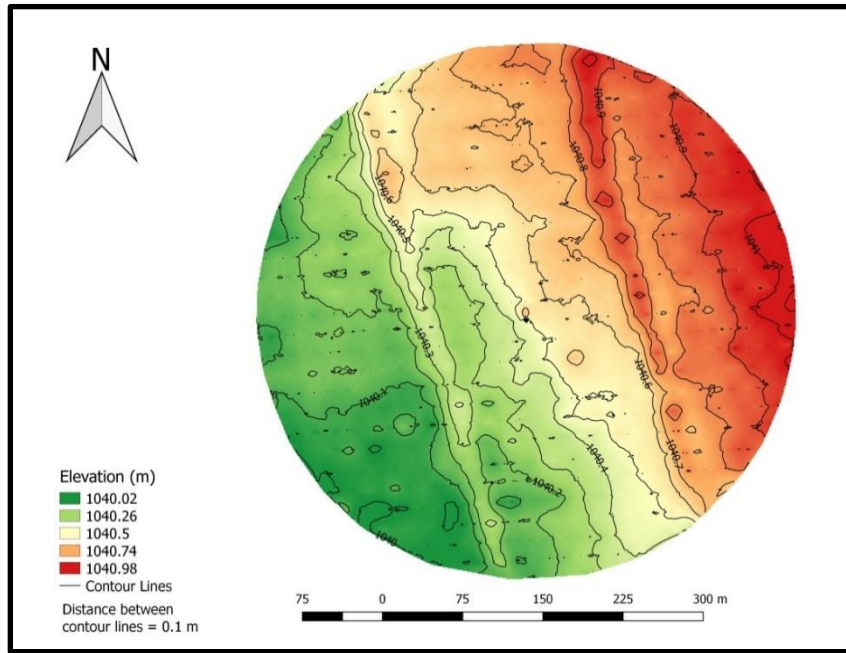


Figure 3.3 Elevation maps of the fields at a) Douglas, b) Luckhoff, c) Hofmeyr and d) Empangeni.

3.1.4 Soils

Soils of the fields used for the WRC project were classified according to the South African Taxonomic Soil Classification System (Soil Classification Working Group, 1991). Soil forms identified at the Douglas, Luckhoff, Hofmeyr and Empangeni sites are depicted in Figure 3.4a to d, respectively and summarized in Table 3.2.

Table 3.2 Soil forms and corresponding horizons identified at the four study sites

Study site	Soil form	A-horizon	B-horizon	C-horizon
Douglas	Augrabies	Orthic	Neocarbonate	
	Brandvlei	Orthic	Soft carbonate	
	Montagu	Orthic	Neocarbonate	Unspecified material with signs of wetness
	Addo	Orthic	Neocarbonate	Soft carbonate
	Molopo	Orthic	Yellow apedal	Soft carbonate
	Clovelly	Orthic	Yellow apedal	
Luckhoff	Hutton	Orthic	Red apedal	
Hofmeyr	Glenrosa	Orthic	Lithocutanic	
	Mispah	Orthic	Hard rock	
	Oakleaf	Orthic	Neocutanic	
	Valsrivier	Orthic	Pedocutanic	Unconsolidated material without signs of wetness
Empangeni	Tukulu	Orthic	Neocutanic	Unspecified material with signs of wetness
	Swartland	Orthic	Pedocutanic	Saprolite
	Westleigh	Orthic	Soft plinthic	
	Katspruit	Orthic	G	
	Longlands	Orthic	E	Soft plinthic
	Glenrosa	Orthic	Lithocutanic	
	Willowbrook	Melanic	G	

Soils identified at the Douglas site are characterized by Orthic A-horizons followed by mainly calcium carbonate containing subsoils indicating low external drainage rates. The Montagu soil form is described as having unspecified material with signs of wetness in the C horizon which confirms poor drainage. Soils at the Luckhoff site was dominated by the Hutton form, originating from wind-blown sands deposited. The Glenrosa and Mispah soil forms at the 55 ha site of Hofmeyr, indicates that these are shallow and marginal soils. Soil forms identified at the Empangeni site are characterized by E, G and soft plinthic B subsoil horizons which are regarded as hydromorphic soils that develop through leaching and formation of mottles due to periodic or permanent presence of water (Soil Classification Working Group, 1991).

In Figure 3.5 a box-and-whisker plot illustrates the variability in clay content for each sampling depth for the different study sites. The lower line of each box represents the first quartile (25% of data lies below Q1) and the upper line represents the third quartile (75% of data lies below Q3). The middle line is the median and the cross is the mean. The upper and lower whiskers represent the maximum and minimum values excluding any outliers.

It is clear from results depicted that, regarding the particle size distribution, the soils are very different and clay percentage vary from approximately 10 to 45%. Soils from the Luckhoff

site has a very low clay content, varying round 10%. Soils of Hofmeyr and Empangeni sites are shallow and both have high clay contents in the top- and subsoil. Interesting to note that the average clay content of the deep subsoil at Hofmeyr (22%) is considerably lower than that of Empangeni (33%). The clay percentage of the soils at Douglas increase with depth.

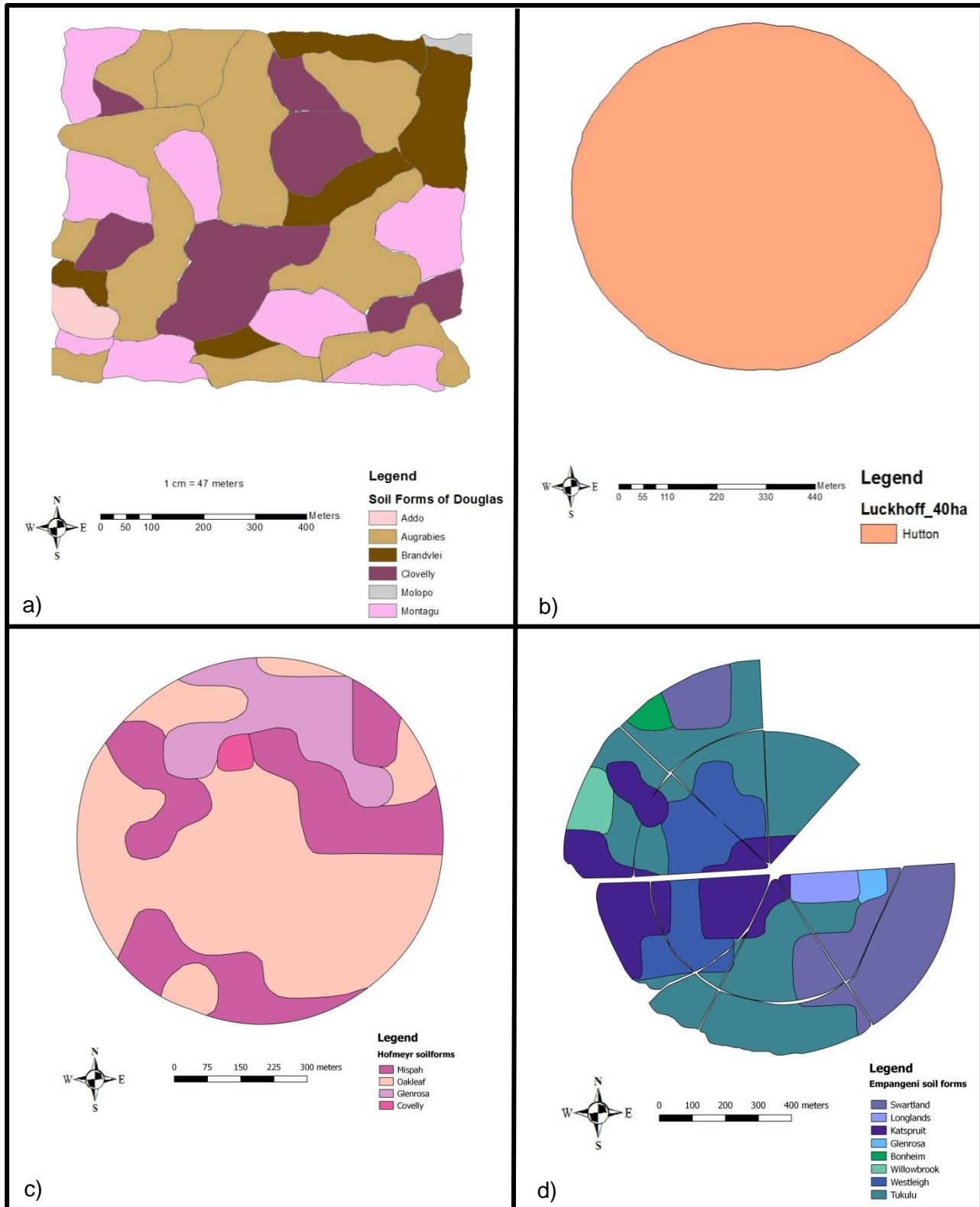


Figure 3.4 Maps of the soil forms identified at a) Douglas, b) Luckhoff, c) Hofmeyr and d) Empangeni.

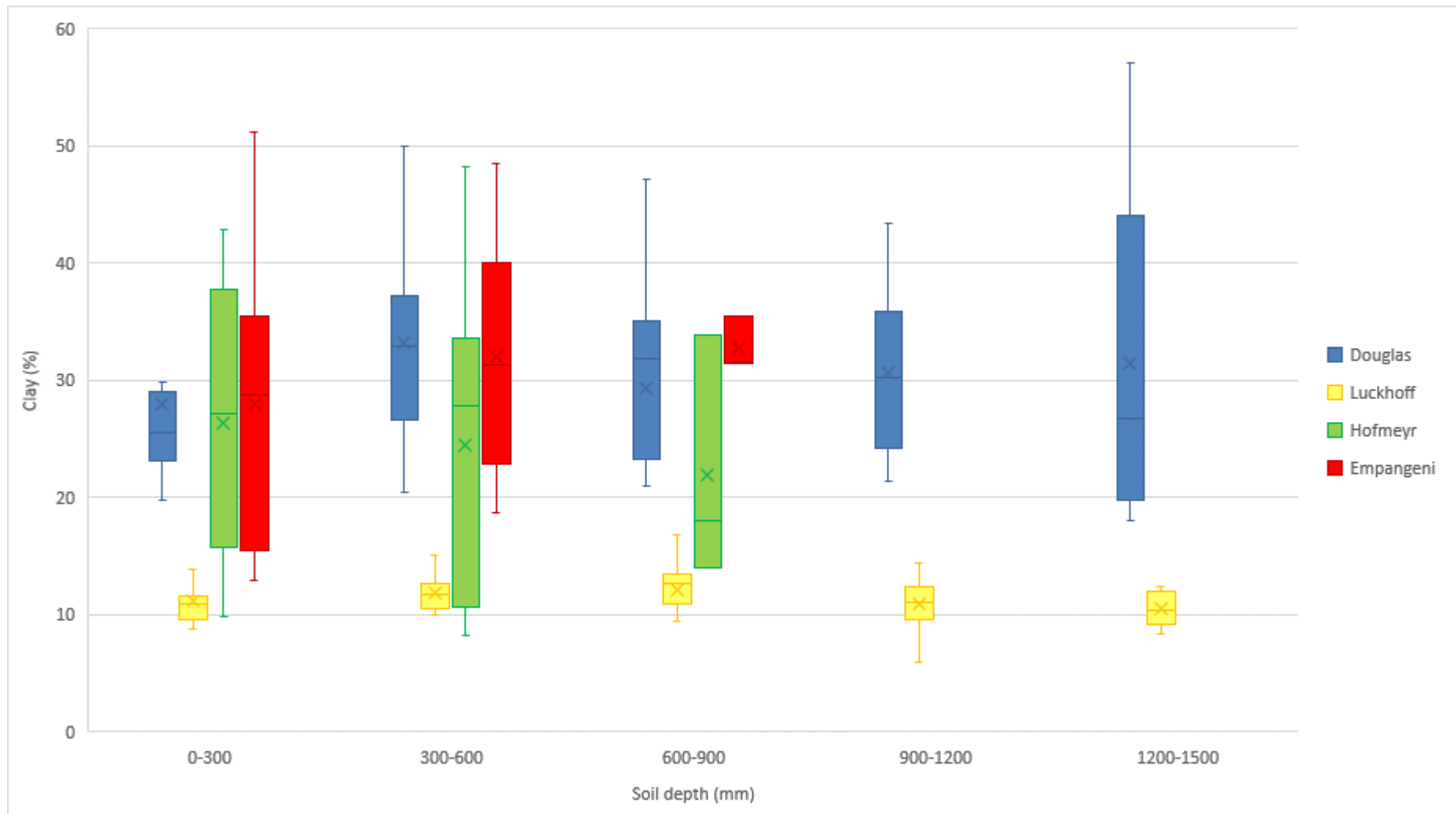


Figure 3.5 Clay percentage for the different soil depth intervals at sites of a) Douglas, b) Luckhoff, d) Hofmeyr and d) Empangeni.

3.1.5 Management practices

Some relevant soil and crop management practices implemented by the farmers during the course of this study are given in Table 3.3. Samples were taken in the winter of 2016. At this time wheat was cultivated on the study sites of Douglas, Luckhoff and Hofmeyr, and sugarcane at Empangeni.

Table 3.3 Agronomic practices applied on the four study sites during 2016 when soil samples were taken

	Douglas (Jun-Dec 2016)	Luckhoff (Jun-Dec 2016)	Hofmeyr (Jun-Dec 2016)	Empangeni (July 2016 - July 2017)	
				Part 1 (54 ha)	Part 2 (68 ha)
Crop	Wheat	Wheat	Wheat	Sugarcane	
Cultivar	PAN 3497	SST 835	SST 884	N53	N41
Planting density	80 kg/ha	100 kg/ha	130 kg/ha	195200 Pls/ha	165000 Pls/ha
Planting dates	07-Jul-16	16-Jun-16	03-Aug-16	Jul-15	
First harvest date	07-Dec-16	29-Nov-16	10-Dec-16	28-Jul-16	
Second harvest date				01-Aug-17	
Post-harvest crop residue management	Burn	Retained	Retain	Burn at harvest; spread remainder of residue (± 7 t/ha)	
Pest management		Spray for lice	*	None	
Weed management	MCPA/Resolve	Spray for weeds before wheat covers soil surface		Chemically	
Cultivation practices	CLG up to 450 mm	Plough to 300 mm depth, followed by tillage to 300 mm depth	Burn and plant	No-till	
Total kg N ha ⁻¹	280	252	*	120	
Total kg P ha ⁻¹	55	42		30	
Total kg K ha ⁻¹	85	52		150	
Method of fertilizer application	Granular fertilizer with plant; Liquid fertilizer the rest of the season	Fertigation through centre pivot	Band application of planter-mixture and fertigation thereafter	Broadcast	
Organic fertilizers	None	None	*	8 t/ha chicken litter in 2015 before planting	
Total irrigation water applied (mm)	540	*	*	740	

*No information available

3.2 Soil sampling and EC_a data collection

A Geonics EM38-MK2 soil sensor in vertical orientation was used to conduct an initial EC_a survey on all study sites for the WRC project. The sensor (Figure 2.8) was enclosed in a plastic trailer to avoid metallic interference while being drawn over the field with a quad bike for the collection of georeferenced EC_a data. With the initial EC_a data collected at the start of the winter cropping season in 2016, 12 soil sampling points were identified for each study site using ESAP-RSSD sampling methodology (Corwin *et al.*, 2006; Wienhold & Doran, 2008). Maps showing the transects of EC_a data collection over the fields, as well as the 12 identified sampling points for the Douglas, Luckhoff, Hofmeyr and Empangeni study sites are shown in Figures 3.6a to d, respectively. Figure 3.7a to d shows the maps of the spatial variability in EC_a for each site. The natural neighbour interpolation method was used and the purpose of the mapping EC_a data were to visualise EC_a-distribution across the fields as a first step in analysing the data.

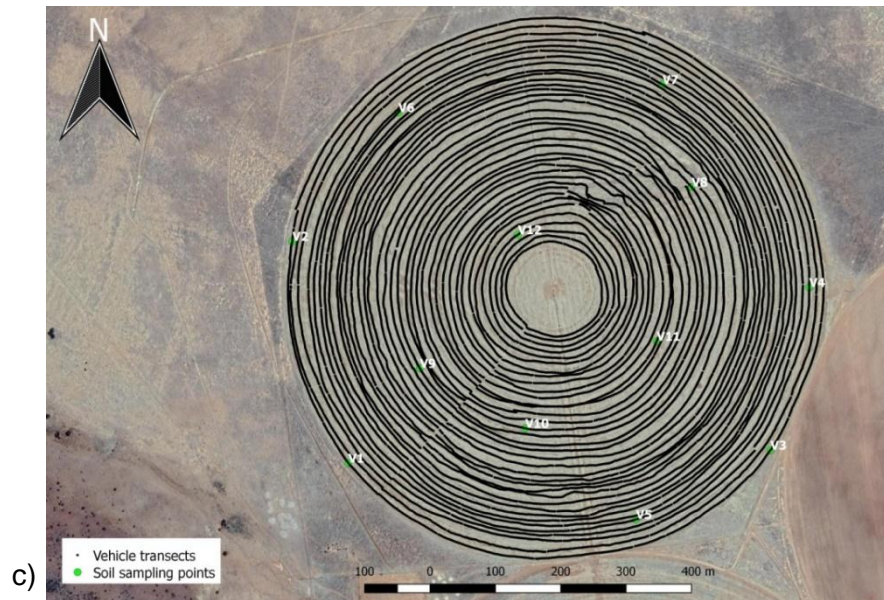
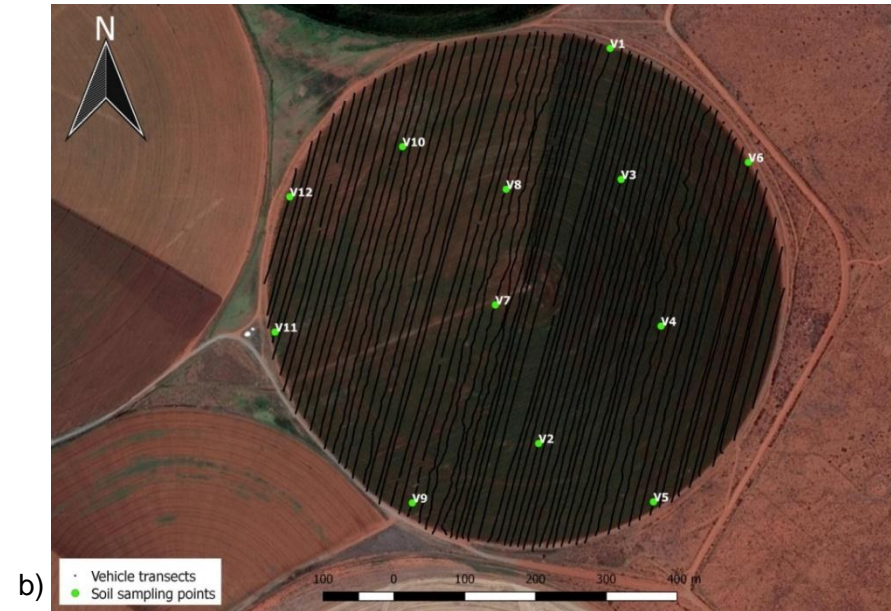
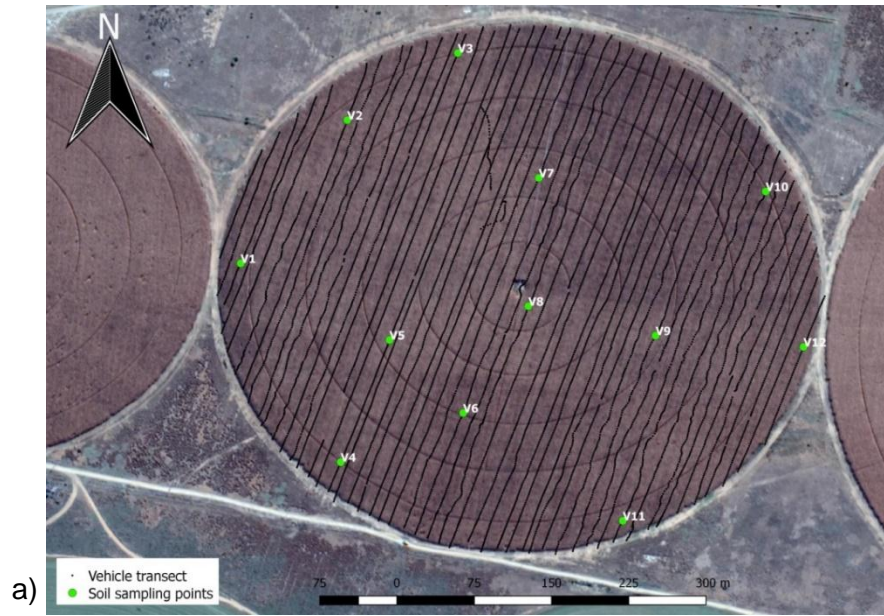


Figure 3.6 Route maps of transects driven by the mobile sensor unit showing EMI measuring points and soil sampling points at the a) Douglas, b) Luckhoff, c) Hofmeyr and d) Empangeni study sites.

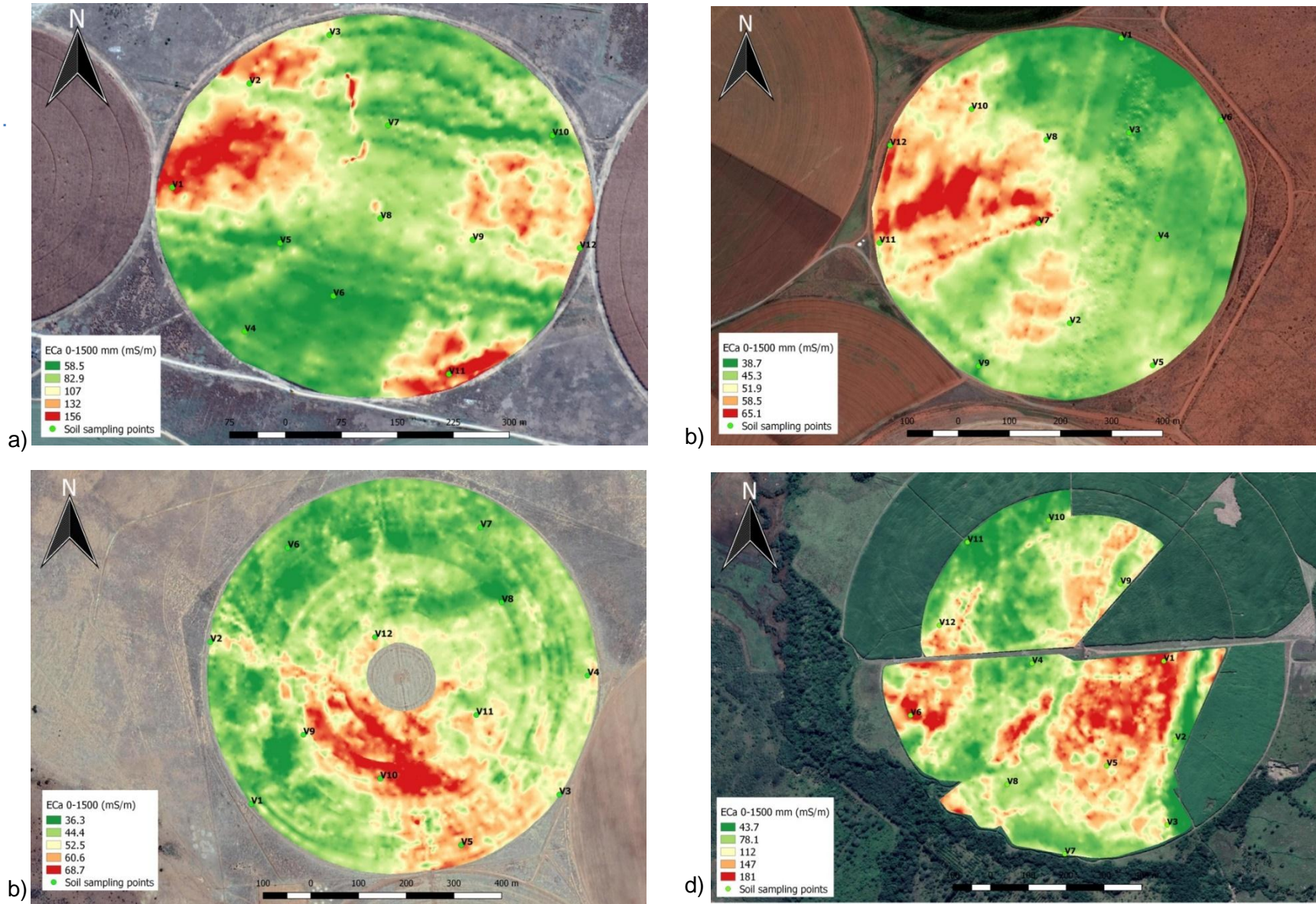


Figure 3.7 Spatial variability of EC_a to a depth of 1500 mm and soil sampling points at a) Douglas, b) Luckhoff, c) Hofmeyr and d) Empangeni study sites.

It is these soil sampling points that were used for the collection of soil samples for the present study. Table 3.4 contains the coordinates of each sampling point at each site. The Luckhoff study site was sampled on 19 September 2016, Douglas on 20 September 2016, Hofmeyr on 20 October 2016 and Empangeni on 25 October 2016.

Table 3.4 GPS coordinates of the sampling points for the different study sites

Point	Douglas		Luckhoff		Hofmeyr		Empangeni	
	Longitude	Latitude	Easting	Northing	Easting	Northing	Easting	Northing
V1	23.99600	-29.02496	277909.5	6719045.8	361887.3	6516397.5	381037.5	6824986.1
V2	23.99707	-29.02353	277808.4	6718487.5	361797.1	6516734.6	381067.9	6824777.5
V3	23.99817	-29.02286	277924.9	6718860.6	362533.0	6516425.8	381046.1	6824552.5
V4	23.99700	-29.02694	277981.4	6718653.3	362588.9	6516674.7	380689.2	6824980.4
V5	23.99749	-29.02573	277970.7	6718405.0	362328.7	6516317.5	380886.5	6824708.8
V6	23.99822	-29.02645	278104.7	6718884.8	361956.8	6516933.1	380367.9	6824842.6
V7	23.99898	-29.02411	277747.3	6718683.2	362360.3	6516981.1	380775.8	6824475.5
V8	23.99887	-29.02539	277762.5	6718846.6	362407.1	6516825.2	380623.4	6824659.9
V9	24.00014	-29.02568	277629.9	6718403.4	361994.8	6516543.5	380923.0	6825190.5
V10	24.00124	-29.02424	277616.1	6718906.9	362157.2	6516454.1	380733.1	6825358.9
V11	23.99981	-29.02753	277435.9	6718644.9	362356.8	6516589.5	380518.4	6825300.8
V12	24.00161	-29.02580	277456.8	6718836.0	362142.2	6516749.1	380443.7	6825080.9

Before samples were collected, five georeferenced EC_a readings were taken at each of the sampling points with an EM38-MK2 sensor in vertical orientation, except for Hofmeyr where soils are shallow (maximum 900 mm) and EC_a readings were taken horizontally. The measurements were taken in the centre and on the four corners of a 1 m² area because the EM38-MK2 sensor has a measurement width of 1 m in the vertical orientation (Geonics Ltd, 2010). Afterwards soil samples were collected also in the centre and four corners of the 1 m² area (Figure 3.8). A soil auger was used and samples were taken in 300 mm depth increments to 1500 mm because the EM38-MK2 sensor measures to this depth in the vertical orientation (Corwin & Lesch, 2005).

The soil samples from position 1 in Figure 3.8 were prepared and analysed as single samples, while those from positions 2, 3, 4 and 5 were composited by mixing equal volumes and hence analysed as composite samples. This sampling procedure is illustrated in Figure 3.9. The single and composite soil samples were promptly transported to the University of the Free State and placed in a drying room at 40°C. After a week, the samples were ground sieved (<2 mm) and stored.

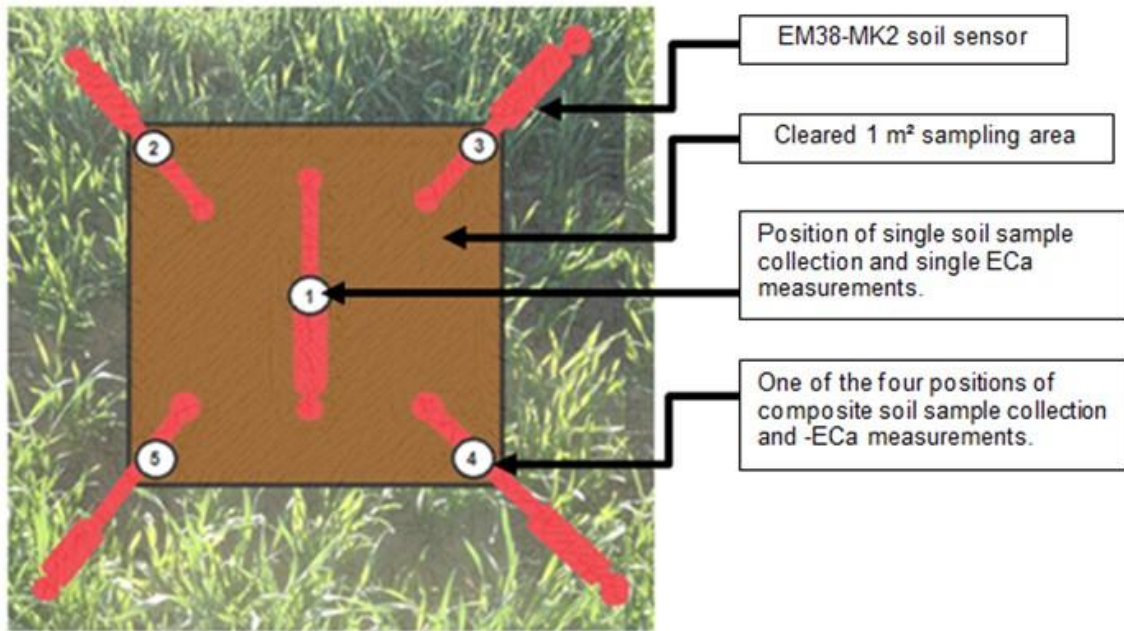


Figure 3.8 Orientation of the EM38-MK2 for EC_a readings and sampling positions at a soil sampling location in a selected field.



Figure 3.9 Soil samples collected from the four corners of the 1 m² cleared area in a selected field to prepare a composite sample.

3.3 Soil property analysis

For analysis of the $\text{NH}_4^+\text{-N}$ and $\text{NO}_3^-\text{-N}$ concentrations in soil samples, two different extractions were done. These included a 2.0 M KCl extraction, which is regarded as the standard accepted method, and a saturated paste extraction, which is normally used for electrical conductivity determination. The saturated paste extract will hereafter be referred to as SATe.

To prepare a 2.0 M KCl solution, 150 g of KCl was dissolved in 1 l of deionized water (Mulvaney, 1996; Griffin *et al.*, 2009). The extraction procedure involved weighing 10 g of soil and adding 100 ml 2.0 M KCl (Maynard *et al.*, 2007). The samples were shaken for an hour at 1620 rpm. Afterwards, samples were allowed to settle for an hour before being filtered through Munktell Ahlstrom fine grade 390 filter paper (Figure 3.10).



Figure 3.10 Filtration of the 2.0 M KCl soil extracts.

For the SATe, a saturated soil paste was prepared for each soil sample by mixing 250 g dry soil with distilled water (United States Salinity Laboratory Staff, 1954). The soil pastes were covered with plastic wrap and left for 24 hours at 25°C for salts to equilibrate. Büchner funnels along with Munktell Ahlstrom grade 3HW filter paper were mounted on Büchner flasks and connected to a suction pressure pipe. Soil pastes were transferred to the funnels and saturated extracts collected at -60 kPa. Thereafter extracts were filtered through Munktell Ahlstrom fine grade 390 filter paper to remove all suspended soil particles.

In order to determine the inorganic nitrogen contribution from the Munktell Ahlstrom filter paper, either 100 ml 2.0 M KCl or 100 ml distilled water was filtered through the filter paper as was the case with soil samples.

The NH_4^+ and NO_3^- concentrations in the soil and filter paper were simultaneously determined colorimetrically with a Skalar SAN plus segmented flow analyser (Model: SA5000). Automated flow analysis combined with spectrophotometry was chosen for its speed, accuracy, convenience and simplicity (Mulvaney, 1996).

Automated segmented flow analysis is a continuous flow method of chemical analysis in which a stream of reagents and samples, segmented with air bubbles, is pumped through a manifold to undergo treatment such as mixing, heating and dialysis. Air segmentation is used to eliminate cross contamination and to provide an aliquot to mix different reagents. There after the product of the reactions enter a flow cell to be detected. This cell operates at a specific wavelength.

The automated determination of NO_3^- is based on the cadmium reduction method (Mulvaney, 1996; Griffin *et al.*, 2009; Gelderman & Beegle, 2012). After dialysis, the sample is buffered at pH 8.2 and passed through a column containing granulated copper-cadmium to reduce the NO_3^- to NO_2^- . The NO_2^- originally present plus the reduced NO_3^- is determined by diazotising with sulfanilamide and coupling with N-(1-naphthyl) ethylenediamine dihydrochloride to form a highly coloured pink azo dye which is measured at 540 nm. The assumption is that NO_2^- occur usually in very low concentrations in soil.

Ammonium is determined through the NH_3 method and is also an automated procedure based on the modified Berthelot reaction (Mulvaney, 1996; Maynard *et al.*, 2007; Nathan *et al.*, 2012). Ammonia is chlorinated to monochloramine which reacts with salicylate to 5-aminosalicylate. After oxidation and oxidative coupling a green coloured complex is formed. The absorption of the formed complex is measured at 660 nm.

Additional soil properties determined included the particle size distribution using the pipette method and the bulk density, determined by the core method (The Non-Affiliated Soil Analysis Work Committee, 1990).

3.4 Data analysis

3.4.1 Inorganic N concentrations

Very low/insignificant concentrations of $\text{NH}_4^+\text{-N}$ and $\text{NO}_3^-\text{-N}$ were detected in the filter papers and it was decided therefore to not correct the $\text{NH}_4^+\text{-N}$ and $\text{NO}_3^-\text{-N}$ concentrations of the soil samples. Concentrations of $\text{NH}_4^+\text{-N}$ and $\text{NO}_3^-\text{-N}$ were added together to get total inorganic N (TIN).

The Shapiro-Wilk test indicated that data were not normality distributed. Using Microsoft Excel Version 14.0.7166.5000 (32-bit), data was log transformed (natural log) to improve normal distribution and log transformed data was used for all statistical analysis.

3.4.2 Comparing single and composite soil samples

The research question was whether $\text{NO}_3^-\text{-N}$, $\text{NH}_4^+\text{-N}$ and TIN concentrations in KCl extracts of single soil samples agreed with those measured in composite soil samples, so that the one sampling procedure can be substituted for the other.

In order to answer this research question, data was pooled to compare single vs. composite sampling irrespective of study site, sampling point and soil depth. Soil samples collected varied extensively in clay percentage (Figure 3.5) and the sampling methods were compared over all sites to obtain a practical answer to the research question, namely whether to take a single sample or a composite sample for routine inorganic N analysis, irrespective of where samples are taken.

In keeping with the research question, the statistical analysis focussed on the assessment of agreement, primarily using the Bland-Altman method which is discussed in depth in the literature review of Chapter 2 Section 2.5 (Bland & Altman, 1983).

\log_e transformed concentrations of $\text{NO}_3^-\text{-N}$, $\text{NH}_4^+\text{-N}$ and TIN in single soil samples were plotted against those of composite soil samples to illustrate the relationship between the two methods (linear regression). Analysis of agreement was accomplished by using the Bland-Altman method, namely plotting the difference between the two methods (Single - Composite) on the y-axis against the average $((\text{Single} + \text{Composite})/2)$ on the x-axis and calculating the bias and limits of agreement (Altman & Bland, 1983). Agreement between methods was evaluated based on if the line of equality fell within the 95% confidence intervals of the bias. Bland-Altman plots were done on Microsoft Excel Version 14.0.7166.5000 (32-bit).

For purposes of this study, the line of equality relative to the confidence intervals of the bias in the Bland-Altman plots were used as an indication whether agreement was sufficient or not. If the line of equality falls within the confidence intervals of the bias, it indicates no systematic difference and satisfactory agreement. However, if this line fell outside the confidence intervals of the bias it indicates significant systematic difference and lack of agreement.

3.4.3 Comparing 2.0 M KCl and the saturated paste extraction methods

The research question was whether or not NH_4^+ -N and NO_3^- -N concentrations determined in the SATe, agreed well with the standard KCl extraction method.

The process of extraction and determination of inorganic N should once again be practical for routine analysis and applicable to any study site or sampling depth. Therefore, for each extraction method data were pooled irrespective of site, sampling point, sampling method and soil depth.

Log_e transformed results of the two extraction methods were plotted against each other to show the relationship between the two methods. Extraction methods were further compared by assessing agreement by creating Bland-Altman plots and calculating the bias, limits of agreement and their confidence intervals.

3.4.4 EM38 correlation

The research question asked was what combination of single or composite EC_a measurements and different sampling depths would result in the most statistically significant prediction model for inorganic N. Unfortunately a technical problem (power failure requiring repairs) occurred during EM38 measurements at Empangeni and EC_a data could not be used. Hence, only the Douglas, Luckhoff and Hofmeyr sites were used.

First, the single and composite EC_a measurements (Figure 3.8) were compared in the same manner as the single and composite soil samples. This was done before model calibration. Measurement of EC_a was determined to be normally distributed according to the Shapiro-Wilk test and data was not transformed for purposes of the agreement analysis between single and composite EC_a measurements.

For model calibration, measured EC_a values was used as well as the geometric means of the EC_a at each sampling point.

The geometric mean was calculated using the square root of the deep sensor reading multiplied by the shallow reading:

$$\sqrt{(EM_{0-1500 \text{ mm}} \times EM_{0-750 \text{ mm}})}$$

This calculation gives a relative indication of the cumulative salinity level in the root zone (Corwin *et al.*, 2003a).

Based on the conclusions from the first two research questions, inorganic N results used for model development were those from composite soil samples extracted using the KCl extraction. For model prediction, the concentrations of NO_3^- -N, NH_4^+ -N and TIN determined in extracts of 2.0 M KCl for the samples taken at Douglas, Luckhoff and Hofmeyr were converted to kg/ha by using the measured bulk density at each sampling point and depth. Values of inorganic N in kg/ha for each sampling depth (0 to 300 mm, 300 to 600 mm, 600 to 900 mm, 900 to 1200 mm and 1200 to 1500 mm) were also used to calculate values for cumulative soil depths (0 to 600 mm, 0 to 900 mm, 0 to 1200 mm and 0 to 1500 mm).

These values of inorganic N were also log transformed (natural log) after determined to be non-normally distributed by using the Shapiro-Wilk test. Data of EC_a and elevation was also log transformed for prediction model development. Since topography is an important factor to consider when developing a N fertilizer plan, multiple-linear regression models were developed in MS Excel by using elevation as an x-variable in addition to EC_a to predict inorganic N.

CHAPTER 4. RESULTS AND DISCUSSION: SINGLE VS. COMPOSITE SOIL SAMPLES FOR INORGANIC N DETERMINATION

4.1 Results

4.1.1 Inorganic N concentrations in single and composite samples

Results of inorganic N concentrations in 2.0 M KCl extracts, viz. NO_3^- -N, NH_4^+ -N and TIN, in the single and composite soil samples from the Douglas, Luckhoff, Hofmeyr and Empangeni study sites are given in Appendix 2 (Tables 2a-d), respectively. For each site the average, minimum, maximum and standard deviations were calculated for the sets of single and composite samples.

A graphical depiction of these inorganic N concentrations for the different sampling depths and sites can be seen in the block-and-whisker diagrams of Figure 4.1, 4.2 and 4.3 for NH_4^+ -N, NO_3^- -N, and TIN, respectively.

NH_4^+ -N concentrations: In all of the study sites the average NH_4^+ -N concentrations of both the single and composite soil samples seemed to decrease generally from the topsoil to the subsoil (300-600 mm), where after it stabilize in deeper horizons. Interesting to note that there was a slight built-up of ammonium in the deep subsoil (1200-1500 mm) of the Empangeni site.

NO_3^- -N concentrations: As in the case of NH_4^+ -N, the average NO_3^- -N in both the single and composite soil samples show also a slight decrease from the topsoil to the subsoil (300-600 mm) in all sites. In the deeper soil depths of the Douglas and Luckhoff sites, the nitrate levels increase with depth, while at Hofmeyr it decreases. The nitrate concentrations of the Empangeni site is generally stable over depth. The soils at the Hofmeyr site clearly contained lower NO_3^- -N levels than the other sites.

TIN concentrations: The average total inorganic nitrogen concentrations for both the single and composite soil samples found in different depths vary for the different sites. Just as with NO_3^- -N levels, TIN decreased slightly from top soil to subsoil, then increased further down the soil profile. Soils at the Hofmeyr site showed a definite decrease in TIN with depth. Also at Empangeni there seemed to be a slight decrease in TIN with soil depth, but not as pronounced as at the Hofmeyr site. Concentrations of TIN seemed, to decrease with depth at Hofmeyr and Empangeni, but increased at Douglas and Luckhoff.

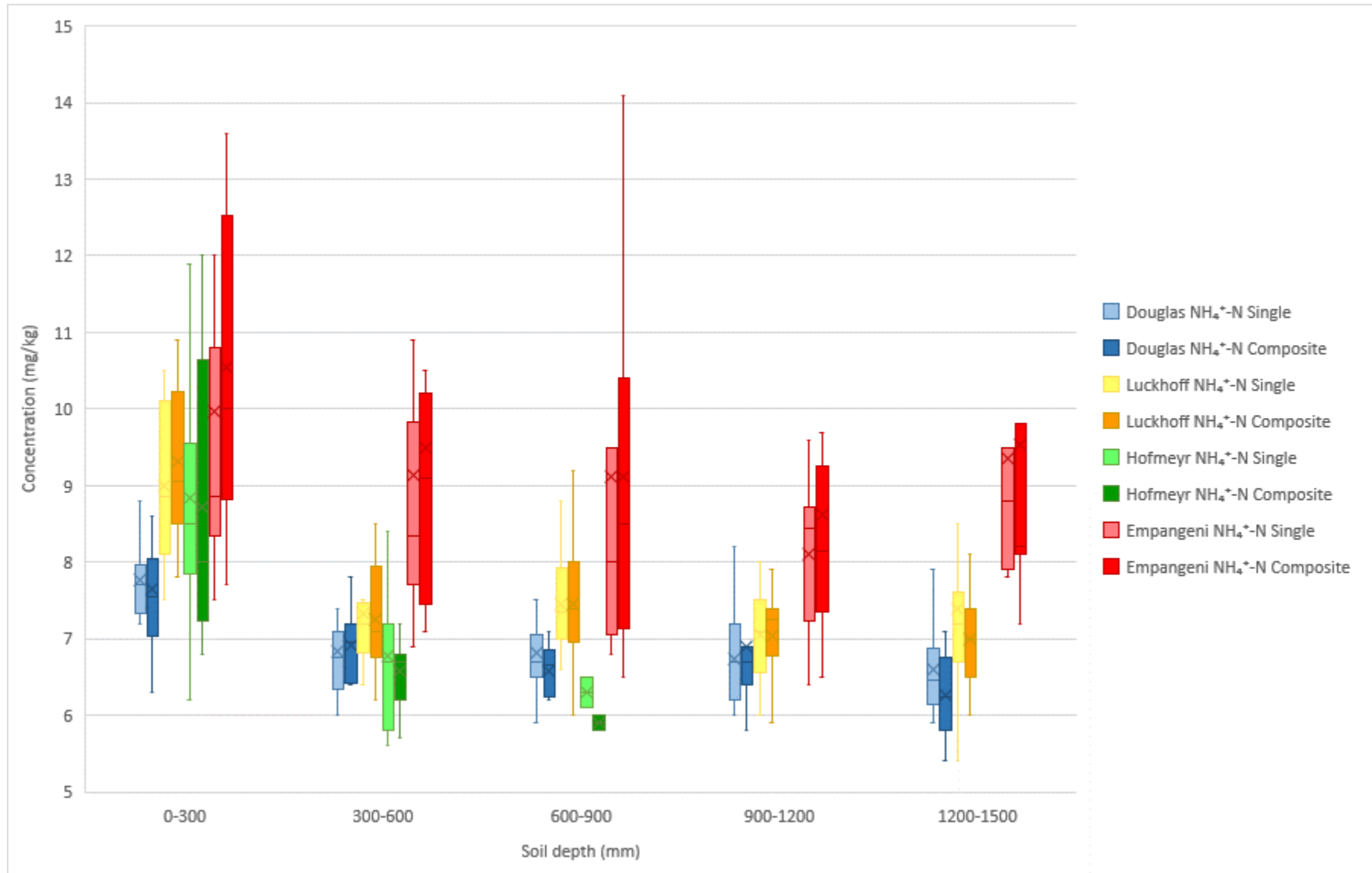


Figure 4.1 2.0 M KCl extracted $\text{NH}_4^+\text{-N}$ concentrations in single and composite soil samples of the depth intervals for the study sites.

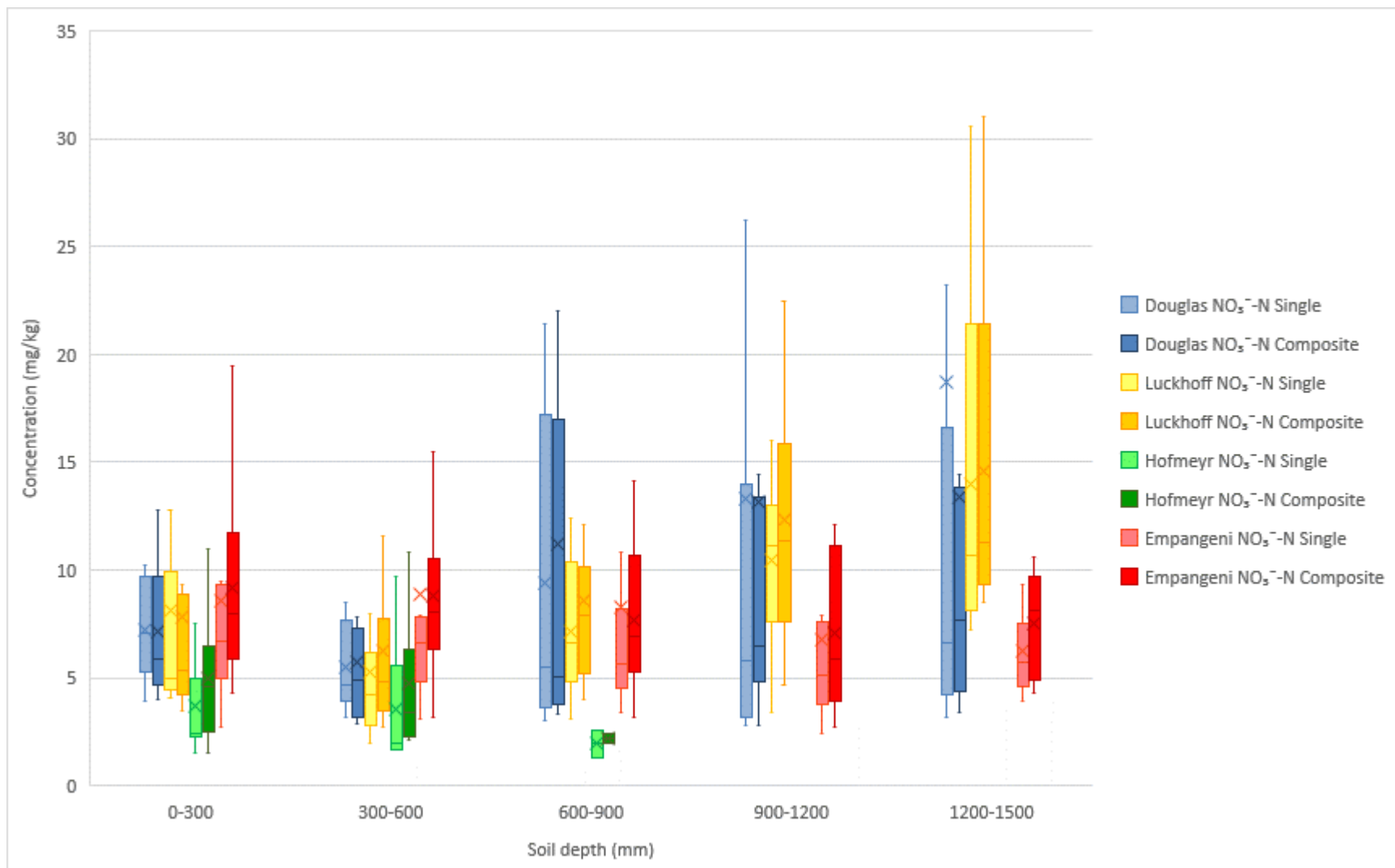


Figure 4.2 A 2.0 M KCl extracted NO₃⁻-N concentrations in single and composite soil samples of the depth intervals for the study sites.

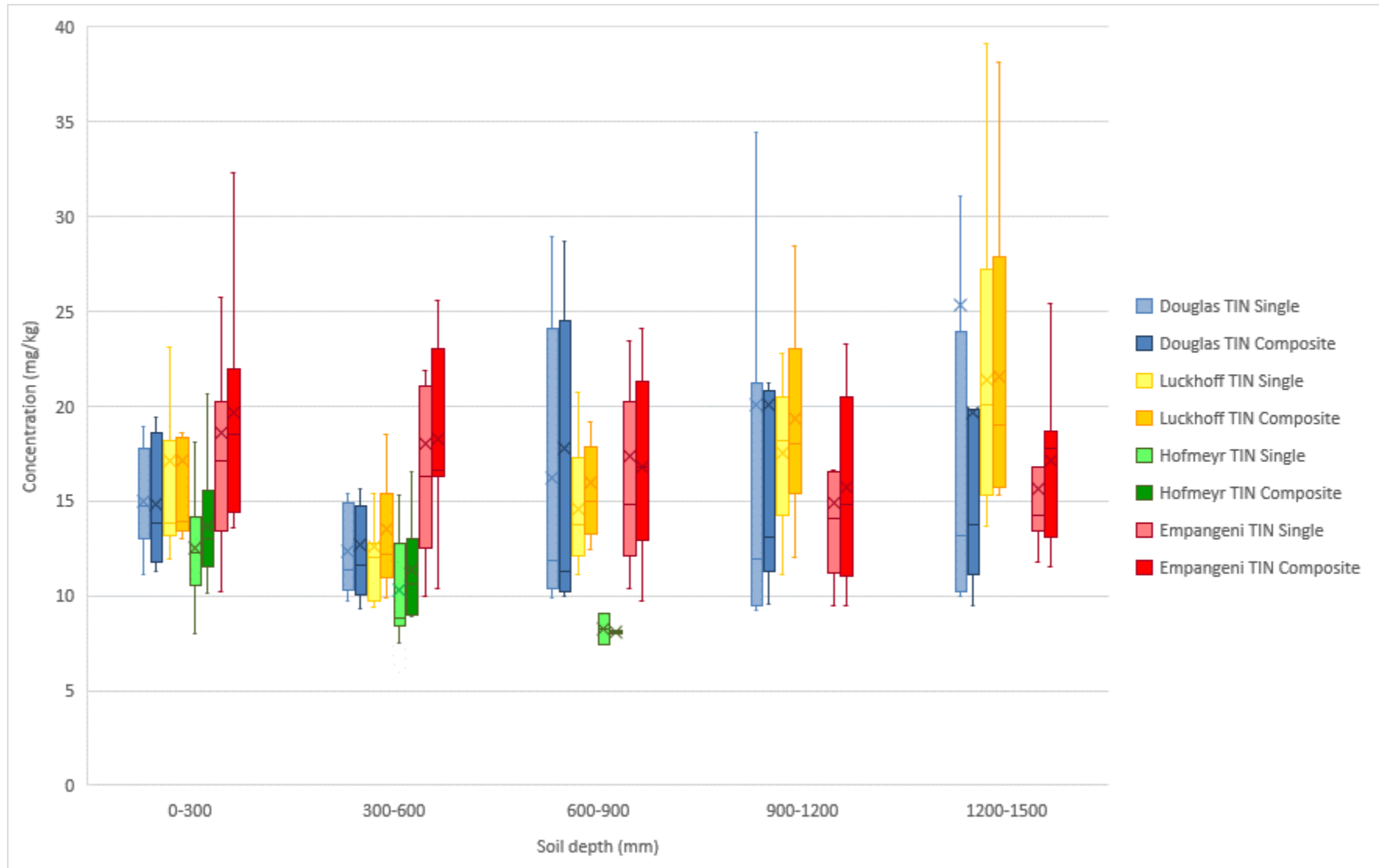


Figure 4.3 Calculated TIN concentrations in single and composite soil samples of the depth intervals for the study sites.

4.1.2 Comparing single and composite samples

4.1.2.1 NH_4^+ -N concentration

For NH_4^+ -N all the data from the four sites were pooled. The single and composite samples were regressed against each other and the results are depicted in Figure 4.4. In addition, a Bland-Altman plot for log transformed ammonium in single and composite samples is presented in Figure 4.5. The shaded areas represent the confidence intervals for the mean difference and the limits of agreement. Coinciding statistics are summarised in Table 4.1.

Table 4.1 Bland-Altman statistics for log and anti-log transformed NH_4^+ -N data

Parameter	Abbreviation	Log	Anti-log
Mean difference or Bias	<i>d</i>	-0.002	0.998
Standard deviation of differences	<i>s</i>	0.158	1.171
Sample size	<i>n</i>	190	-
Degrees of freedom	<i>n - 1</i>	189	-
<i>t</i> -Distribution	<i>t</i>	1.96	-
Upper limit of agreement	<i>ULO</i> A	0.313	1.368
Lower limit of agreement	<i>LLO</i> A	-0.317	0.728
Standard error of mean difference	<i>SE d</i>	0.011	1.011
Standard error of agreement limits	<i>SEd ± 2s</i>	0.02	1.02
95% Confidence interval of the bias	<i>CI bias</i>	-0.024 to 0.021	0.976 to 1.021
95% Confidence interval of the upper limit of agreement	<i>CI ULO</i> A	0.274 to 0.352	1.316 to 1.422
95% Confidence interval of the lower limit of agreement	<i>CI LLO</i> A	-0.356 to -0.278	0.701 to 0.757

As for the different sites, it was observed that data of mainly Empangeni stood out to the side of higher ammonium content on both the regression- and Bland-Altman plots. Further, the regression results show a low coefficient of determination ($R^2=0.48$) between single and composite samples for ammonium. The point of equality for ammonium is ± 2.1 units on the log scale (8.17 mg/kg). Below this value on the regression line, concentrations of ammonium are overestimated by the composite samples compared to the single samples and above this value the reverse is true.

The Bland-Altman plot show good agreement between ammonium concentrations in the single soil sample set and in the composite soil samples set (Figure 4.5). The line of equality falls within the boundaries of the confidence intervals of the bias, indicating no statistically significant systematic difference. When reverting to anti-log values, differences become ratios. Therefore, the anti-log of the bias gives a value of 0.998, implicating that on average the single samples gave ammonium concentrations of 0.2% lower than those of composite samples. Agreement seems to be better for lower concentrations and the bias increases with an increase in concentration. Anti-log values for the confidence intervals of the upper and lower limits of agreement indicate that the concentration of ammonium in single samples is either 31.5 to 42.2% higher or 24.3 to 30% lower than those in composite samples.

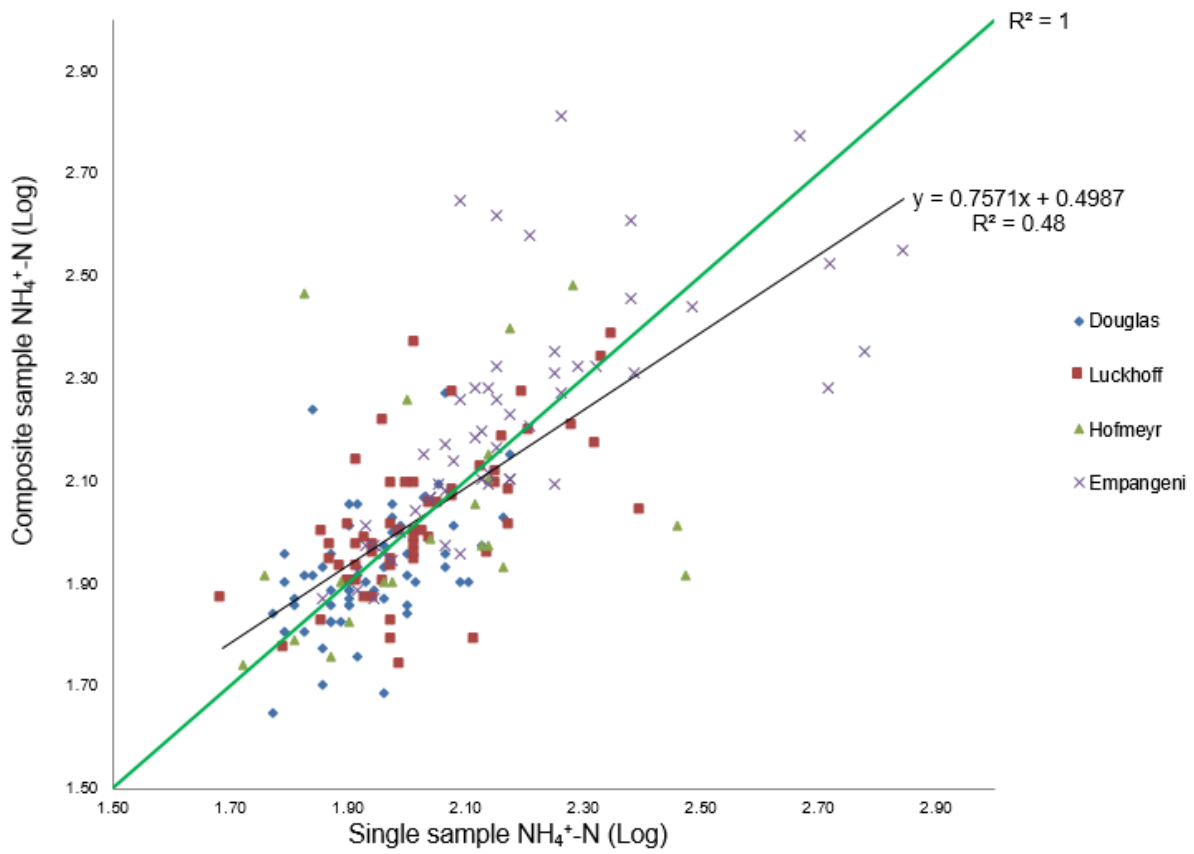


Figure 4.4 Regression plot for comparison of single vs. composite soil sampling in determining $\text{NH}_4^+\text{-N}$ concentrations in soil samples.

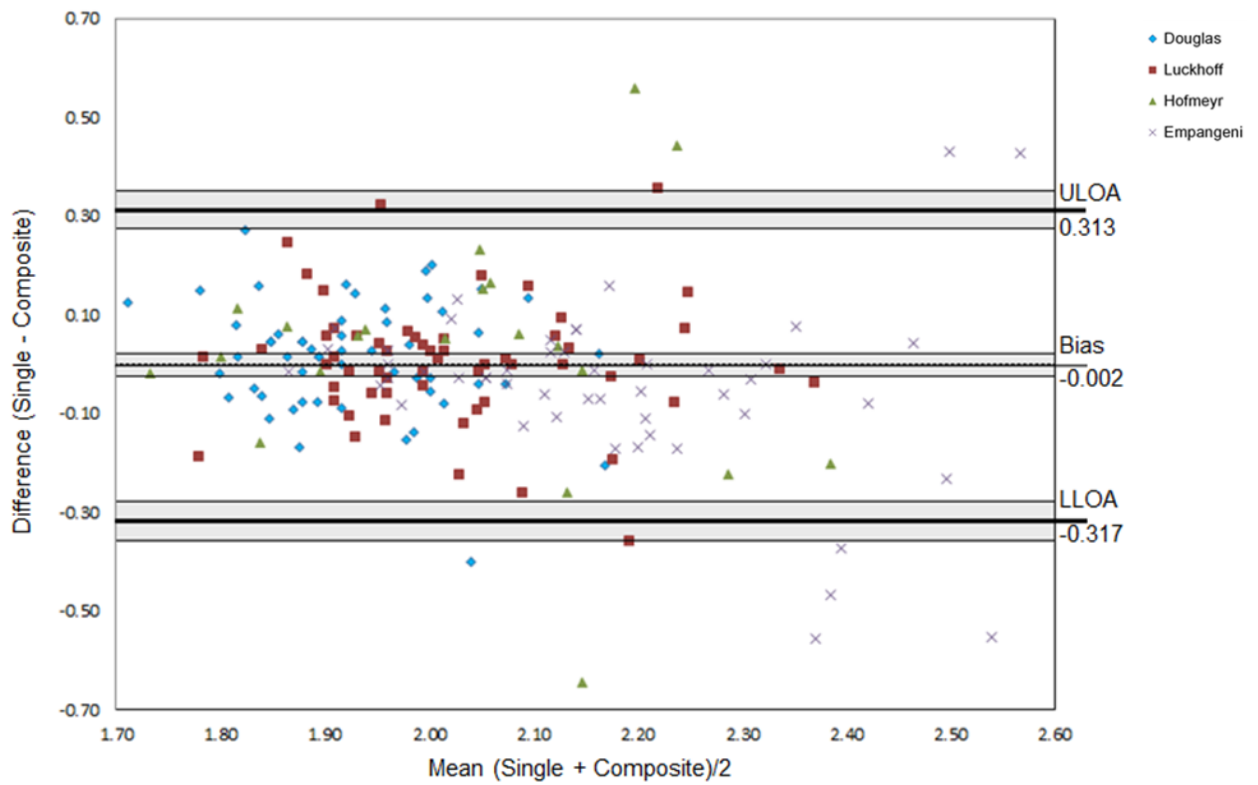


Figure 4.5 A Bland-Altman plot of $\text{NH}_4^+\text{-N}$ concentrations in single and composite soil samples.

4.1.2.2 NO_3^- -N concentration

For agreement analysis of NO_3^- -N in single and composite soil samples, like with NH_4^+ -N concentrations, all four study sites' NO_3^- -N concentrations were used after log transformations and the data of the single samples set was regressed against the composite samples set (Figure 4.6). A Bland-Altman plot for the concentration of NO_3^- -N in single and composite samples is displayed in Figure 4.7. The Bland-Altman statistics for log and anti-log transformed NO_3^- -N data is presented in Table 4.2.

Table 4.2 Bland-Altman statistics for log and anti-log transformed NO_3^- -N data

Parameter	Abbreviation	Log	Anti-log
Mean difference or Bias	<i>d</i>	-0.099	0.906
Standard deviation of differences	<i>s</i>	0.380	1.462
Sample size	<i>n</i>	190	-
Degrees of freedom	<i>n - 1</i>	189	-
<i>t</i> -Distribution	<i>t</i>	1.96	-
Upper limit of agreement	<i>ULO A</i>	0.661	1.937
Lower limit of agreement	<i>LLO A</i>	-0.859	0.424
Standard error of mean difference	<i>SE d</i>	0.028	1.028
Standard error of agreement limits	<i>SEd ± 2s</i>	0.048	1.049
95% Confidence interval of the bias	<i>CI bias</i>	-0.153 to -0.045	0.858 to 0.956
95% Confidence interval of the upper limit of agreement	<i>CI ULO A</i>	0.567 to 0.754	1.763 to 2.126
95% Confidence interval of the lower limit of agreement	<i>CI LLO A</i>	-0.953 to -0.765	0.386 to 0.465

Concerning the different sites, data of Hofmeyr on both plots can be seen having the lowest concentration and the rest of the data is spread out fairly even. The coefficient of determination ($R^2=0.71$), indicates a good relationship between the concentrations of NO_3^- -N in single and composite samples. Compared to the line of equality, NO_3^- -N values in the composite and single samples seem to be equal (point of equality) at a concentration of ± 2 units on the log scale (7.39 mg/kg). However, in composite samples, NO_3^- -N below this point is overestimated and above this concentration is underestimated.

The Bland-Altman plot for NO_3^- -N concentrations in the single vs. composite samples show reasonably good agreement. Yet, the line of equality falls just outside the confidence interval of the bias, indicating presence of a statistically significant systematic difference. The mean difference (bias) is -0.099 on the log scale. An anti-log of the bias gives a value of 0.906, and on average, single samples gave readings 9.4% lower than composite samples. In Table 4.2 the anti-log values of the 95% confidence intervals of the bias have a range of 4.4 to 14.2% lower as indicated by the shaded area on the plot. Anti-log for the confidence intervals of the upper and lower limits of agreement indicates that original NO_3^- -N values for single samples can be up to 53.5 to 51.4% lower or 76.3 to 112.6% higher than those in composite samples. There are a few data points of each site that falls outside the limits of agreement.

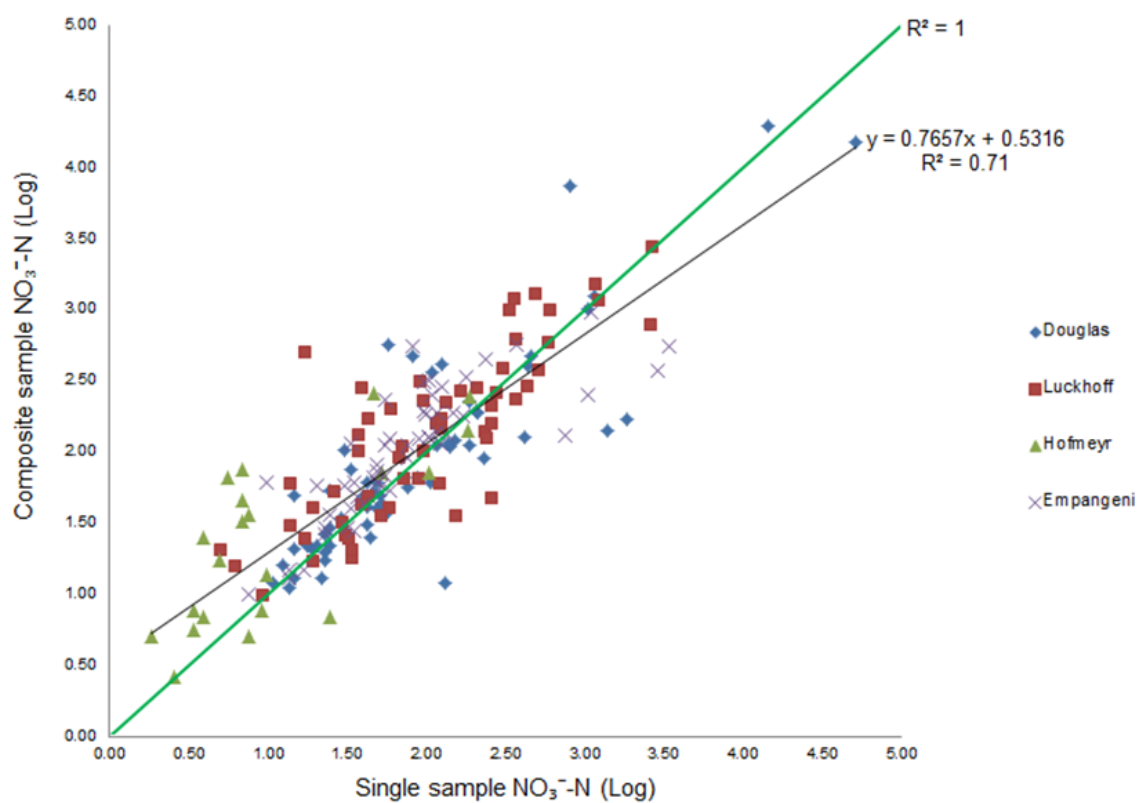


Figure 4.6 Regression of NO_3^- -N concentrations in single soil samples and composite soil samples with a line of equality.

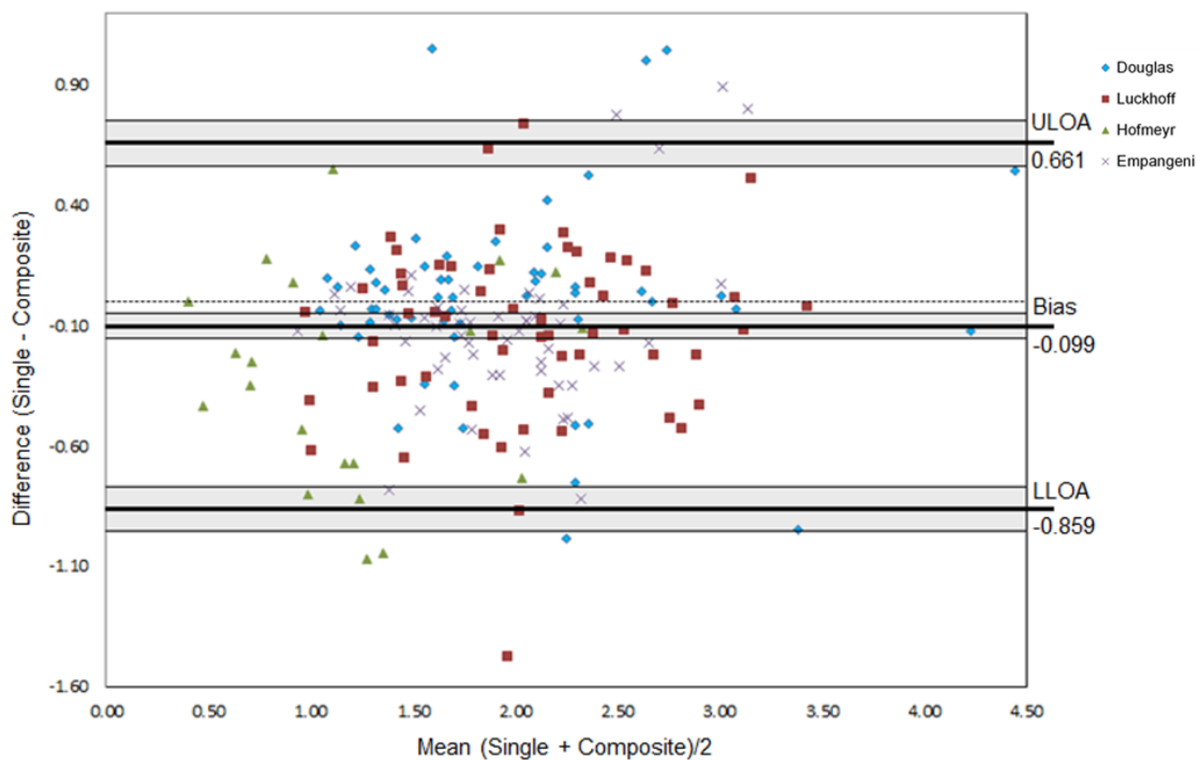


Figure 4.7 A Bland-Altman plot of NO_3^- -N concentrations in single and composite soil samples.

4.1.2.3 TIN concentration

The TIN concentrations in the single samples set was regressed against those in the composite samples set after log transformation (Figure 4.8). The Bland-Altman plot for log transformed (natural logarithm) TIN concentrations in single and composite samples is presented in Figure 4.9. Measures of agreement and precision of estimated limits of agreement are given in Table 4.3.

Table 4.3 Bland-Altman statistics for log and anti-log transformed TIN data

Parameter	Abbreviation	Log	Anti-log
Mean difference or Bias	<i>d</i>	-0.040	0.961
Standard deviation of differences	<i>s</i>	0.216	1.241
Sample size	<i>n</i>	190	-
Degrees of freedom	<i>n - 1</i>	189	-
<i>t</i> -Distribution	<i>t</i>	1.96	-
Upper limit of agreement	<i>ULO A</i>	0.392	1.480
Lower limit of agreement	<i>LLO A</i>	-0.472	0.624
Standard error of mean difference	<i>SE d</i>	0.016	1.016
Standard error of agreement limits	<i>SEd ± 2s</i>	0.027	1.028
95% Confidence interval of the bias	<i>CI bias</i>	-0.070 to -0.009	0.932 to 0.991
95% Confidence interval of the upper limit of agreement	<i>CI ULO A</i>	0.339 to 0.445	1.404 to 1.561
95% Confidence interval of the lower limit of agreement	<i>CI LLO A</i>	-0.525 to -0.419	0.592 to 0.658

On the regression plot there are data points of the Douglas site that are outliers. The rest of the data is generally spread out even around the regression line. Overall, regression of TIN concentrations in single and composite soil samples showed a good coefficient of determination ($R^2=0.70$) between the sampling methods. Concentrations of TIN was equal at ± 2.9 units on the log scale (18.17 mg/kg). Below this value TIN concentration in the composite samples are overestimated and above this value the TIN concentrations in the composite samples are underestimated.

The Bland-Altman plot also suggests good agreement between the TIN concentrations of the single and composite samples. On average composite samples gave results of 0.04 units higher than the single samples on the log scale. This translates to single samples giving results 3.9% lower than composite samples. The line of equality does not fall into this range and indicates statistically significant systematic difference. Confidence intervals of the upper and lower limits of agreement indicate that single samples gave TIN results of up to 40.4 to 56.1% higher or 34.2 to 40.8% lower than composite samples. Data points of all sites fall outside of the confidence intervals of the upper and lower limits of agreement.

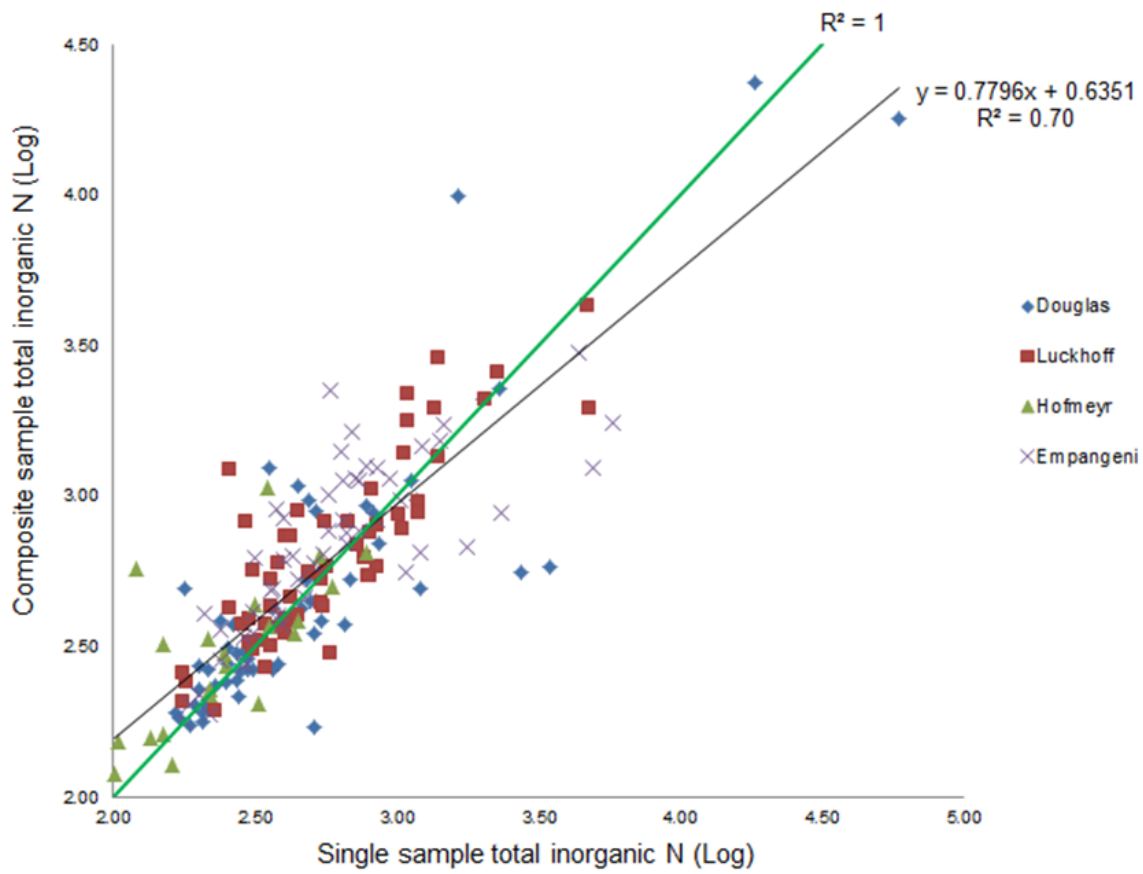


Figure 4.8 Regression line ($R^2=0.70$) and line of equality ($R^2=1$) of log transformed TIN concentrations in single and composite samples.

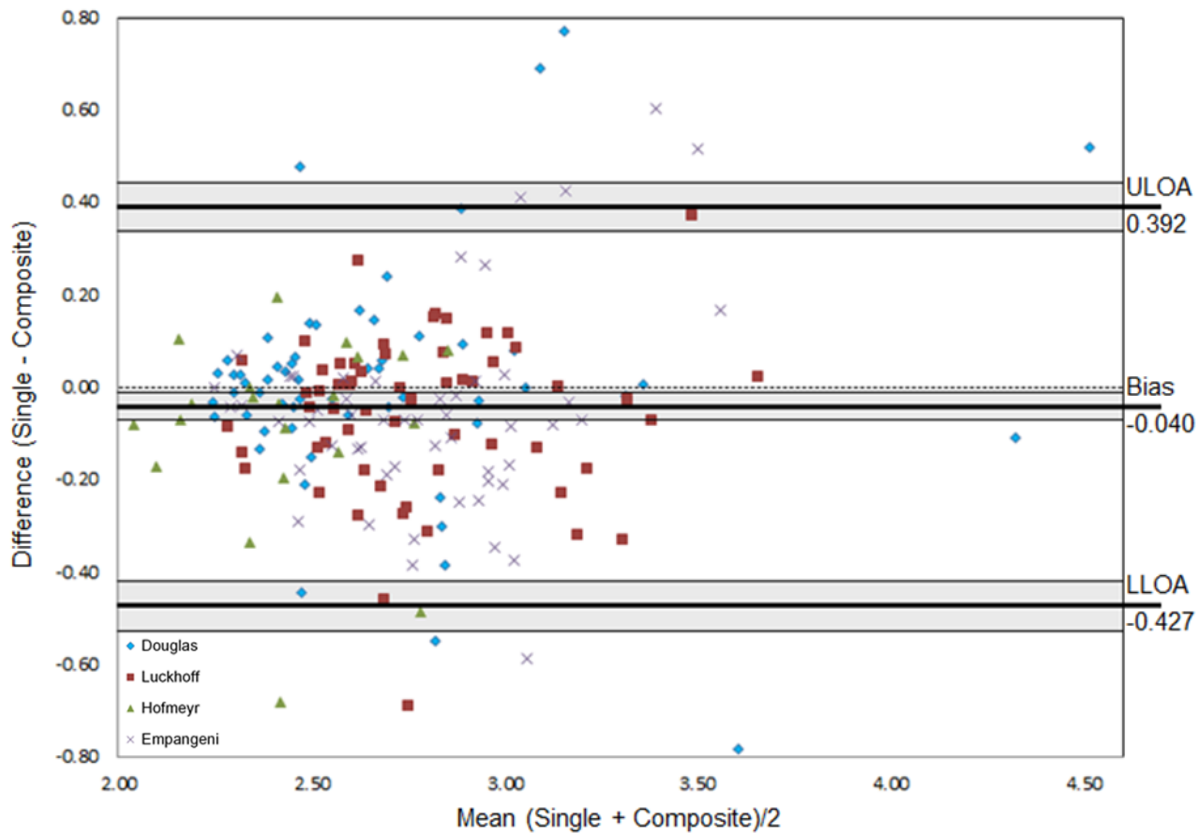


Figure 4.9 A Bland-Altman plot of TIN concentrations in single and composite soil samples.

4.2 Discussion

Considering all the nitrogen species, the difference in agreement between composite and single samples for $\text{NH}_4^+\text{-N}$ and $\text{NO}_3^-\text{-N}$ can be explained probably by the chemical reactions of these two forms of inorganic N and the dynamics between them.

Ammonium carries a positive charge and is adsorbed by either organic or clay colloids in soil which has a negative charge. After being adsorbed the NH_4^+ becomes part of the cation exchange complex and does not move readily through the soil profile. This is where plants take up NH_4^+ , a positively charged ion, by exchanging it with a hydrogen ion (Dorn, 2015). Nitrate, on the other hand, is repelled by the negatively charged organic and clay colloids. Due to the high solubility of $\text{NO}_3^-\text{-N}$ in water it moves easily in soil (Dahnke & Johnson, 1990; Walworth, 2013; Dorn, 2015). Nitrate can be transported downwards in soil when water is added through irrigation or rain, and upwards when water evaporates. Nitrate along with water is taken up by plant roots through the transpiration process (Dorn, 2015).

Unfortunately, its mobility causes NO_3^- to be easily leached and lost if water percolates to below the active part of the root zone. Here the $\text{NO}_3^-\text{-N}$ can be either biologically or chemically reduced through denitrification, especially when a soil is waterlogged (Walworth, 2013; Dorn, 2015). Denitrification is a form of volatilization where NO_3^- is reduced to nitrous oxide or dinitrogen gas (Walworth, 2013) and some studies showed that 4 to 5% of NO_3^- in soil can be lost for every day that the soil stays saturated (Dorn, 2015). In addition, Dahnke & Johnson (1990) states that up to 70% of applied N fertilizer can be lost through denitrification. Nitrate can also be immobilized quickly by micro-organisms in the presence of an energy source, only to reappear after a short period of time as micro-organisms reduce the C:N ratio of the energy source (Dahnke & Johnson, 1990). It can therefore be expected that the concentration of $\text{NO}_3^-\text{-N}$ is more variable than $\text{NH}_4^+\text{-N}$ and composite soil samples are preferable for the determination of $\text{NO}_3^-\text{-N}$.

The dynamics between NO_3^- and NH_4^+ and their concentrations in soil depend on micro-biological activity (Horneck *et al.*, 2011). Under favourable soil water and temperature conditions, that favour crop growth, NH_4^+ is swiftly converted to NO_3^- . Therefore, NH_4^+ does not generally accumulate in soils (Horneck *et al.*, 2011; Flynn, 2015). As a result, NO_3^- is the most common form of inorganic N in arable land and is an indication of the readily available N for plants (Flynn, 2015).

For establishing nutrient levels for fertilizer recommendations, $\text{NO}_3^-\text{-N}$ is generally analysed on its own or along with $\text{NH}_4^+\text{-N}$ for the calculation of TIN. Therefore, the good agreement

found between single and composite samples for NH_4^+ -N are not extremely useful since not many soil-testing programs include the analysis of residual NH_4^+ -N on its own (Dahnke & Johnson, 1990). It can still be recommended that when NH_4^+ -N is analysed alone, a single sample would be sufficient.

The taking of composite samples rather than single samples should still consider the research objectives and the available resources such as time and economic implications. Composite soil sampling is especially laborious if soils are sampled in 300 mm depth increments up to 1500 mm. On the other hand, it can be argued that an advanced site-specific sampling design as modelled by ESAP-RSSD deserves that composite soil samples be taken to so consider micro-variation in soil, thereby implementing a type of “ultra-precision” soil sampling.

CHAPTER 5. RESULTS AND DISCUSSION: KCl EXTRACTION VS. SAT_E FOR INORGANIC N DETERMINATION

5.1 Results

5.1.1 Inorganic N concentrations in different extractions

Concentrations of NH₄⁺-N and NO₃⁻-N in mg/kg determined in extracts of 2.0 M KCl and SAT_E are shown in Appendix 3. These tables also include descriptive statistics (average, minimum, maximum, standard deviation and coefficient of variation) for the different extracts. From the descriptive statistics it is already evident that concentrations of inorganic N determined in the two extracts differ considerably on average. Average concentrations of NO₃⁻-N in the two extracts varied extensively for the different sites. The average NO₃⁻-N in the SAT_E was roughly half that of the KCl extract at Douglas, but at Luckhoff and Hofmeyr NO₃⁻-N was slightly higher while at Empangeni it was slightly lower in the SAT_E. Average concentrations of NH₄⁺-N were much higher in the KCl extract than in the SAT_E for all sites (Appendix 3).

A summary of the inorganic N concentrations extracted with 2.0 M KCl and SAT_E are shown for the different depths and study sites in the form of box and whisker diagrams (Figure 5.1 and 5.2). The results show clearly that the SAT_E extracted markedly less NH₄⁺-N than did the 2.0 M KCl. Concentrations of NO₃⁻-N found in both the SAT_E and 2.0 M KCl differ extensively.

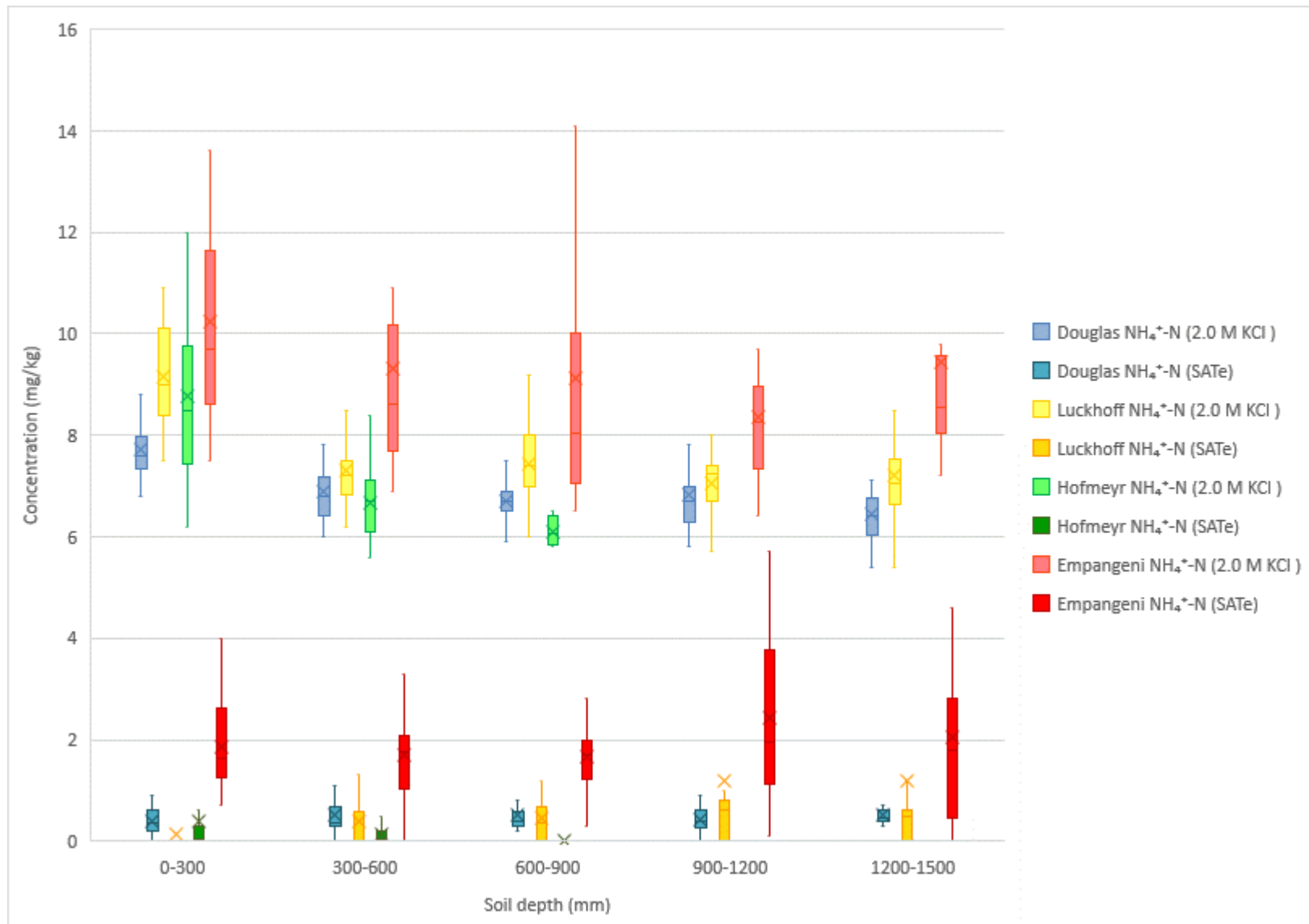


Figure 5.1 NH₄⁺-N concentrations determined in extracts of 2.0 M KCl and SATe in all samples collected at the four study sites.

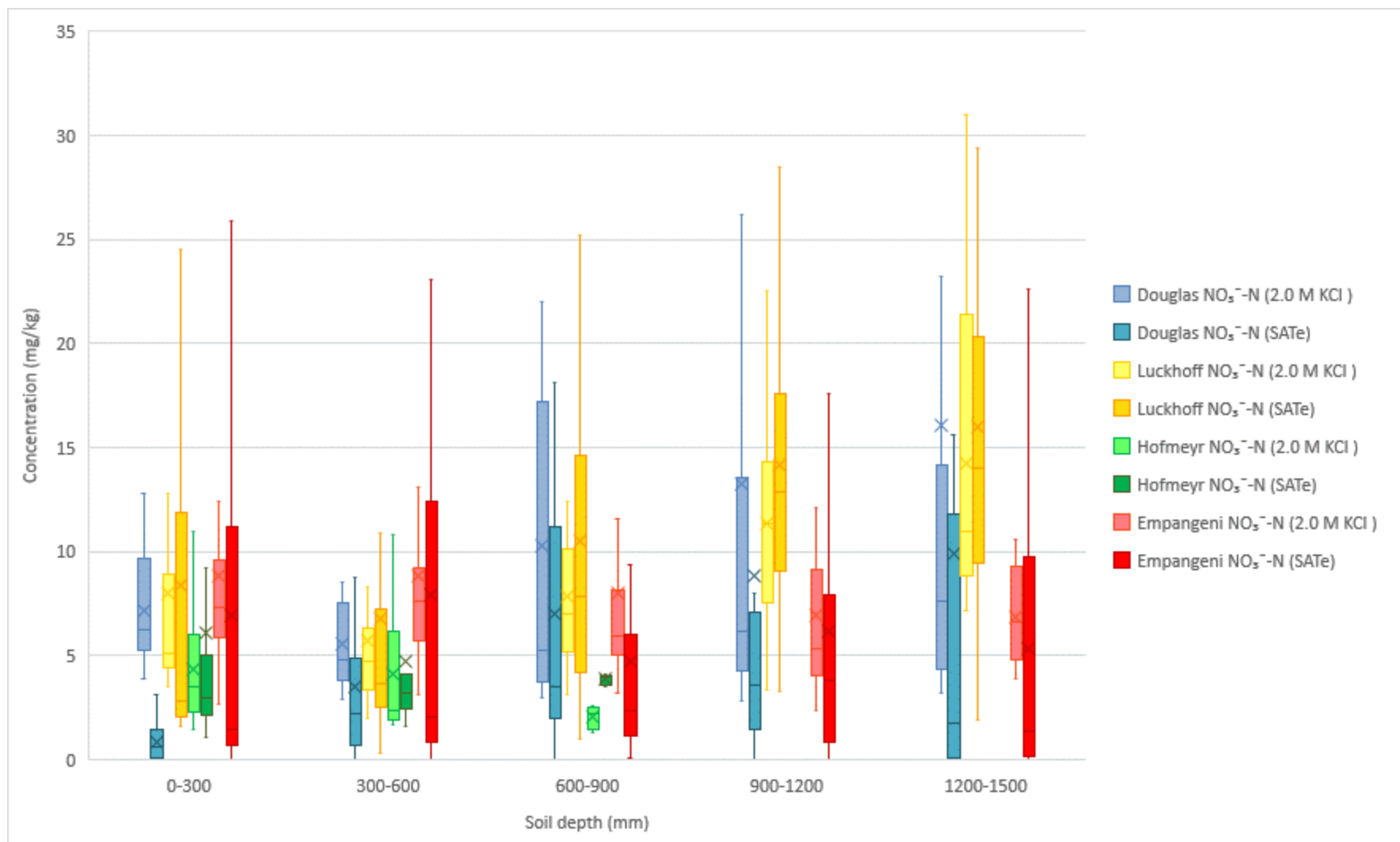


Figure 5.2 NO₃⁻-N concentrations determined in extracts of 2.0 M KCl and SATe in all samples collected at the four study sites.

5.1.2 Comparing SATe and 2.0 M KCl extractions

5.1.2.1 NH_4^+ -N concentrations

Log_e transformed results of the NH_4^+ -N concentrations in extracts of 2.0 M KCl and SATe can be seen regressed against each other in Figure 5.3. The Bland-Altman plot for the difference between NH_4^+ -N in the KCl extract and SATe against the mean can be seen in Figure 5.4. Coinciding statistics are summarised in Table 5.1.

Table 5.1 Bland-Altman statistics for log transformed data of NH_4^+ -N for the two extraction methods as well as back transformation (anti-log) for interpretation purposes

Parameter	Abbreviation	Log	Anti-log
Mean difference or Bias	<i>d</i>	3.166	23.712
Standard deviation of differences	<i>s</i>	1.704	5.495
Sample size	<i>n</i>	380	380
Degrees of freedom	<i>n - 1</i>	379	379
<i>t</i> -Distribution	<i>t</i>	1.96	1.96
Upper limit of agreement	<i>ULO</i> A	6.574	716.054
Lower limit of agreement	<i>LLO</i> A	-0.242	0.785
Standard error of mean difference	<i>SE d</i>	0.087	1.091
Standard error of agreement limits	<i>SEd ± 2s</i>	0.151	1.163
95% Confidence interval of the bias	<i>CI bias</i>	2.995 to 3.337	19.978 to 28.143
95% Confidence interval of the upper limit of agreement	<i>CI ULO</i> A	6.277 to 6.870	532.201 to 963.421
95% Confidence interval of the lower limit of agreement	<i>CI LLO</i> A	-0.539 to 0.055	0.584 to 1.056

On both plots, data from the different sites can be seen clustered in some areas. The correlation between NH_4^+ -N concentrations in extracts of 2.0 M KCl and SATe was extremely poor as indicated by the coefficient of determination ($R^2=0.01$) (Figure 5.3). Generally, NH_4^+ -N values in the KCl extract were effectively constant (± 2 units) on the log scale with a bit of noise. Values in the KCl extract vary from minimum 1.65 to maximum 2.84 units (5.20 to 17.20 mg/kg), while those in the SATe range from minimum -4.16 to maximum 2.85 units (0.02 to 17.23 mg/kg).

The Bland-Altman plot revealed poor agreement between NH_4^+ -N contents in the two extracts. The vast majority of data points are above the line of equality which is also close to the lower limit of agreement. The line of equality does not fall within the confidence intervals of the bias, indicating the presence of a statistically significant systematic difference. Further, a linear regression line through the NH_4^+ -N data in the Bland-Altman plot gave an intercept of ± 4 and a slope of ± -2 . The following relationship between the average $(y_1 + y_2)/2$ and the difference $(y_1 - y_2)$ of the NH_4^+ -N levels in the two extraction methods was calculated:

$$y_1 - y_2 \approx 4 - 2(y_1 + y_2)/2 = 4 - y_1 - y_2 \quad 4.1$$

Therefore, $2y_1 \approx 4$ or $y_1 \approx 2$, so that the shape of the Bland-Altman plot (Figure 5.4) implies that measurement y_1 , i.e. the KCl extract, is approximately constant and equal to 2.

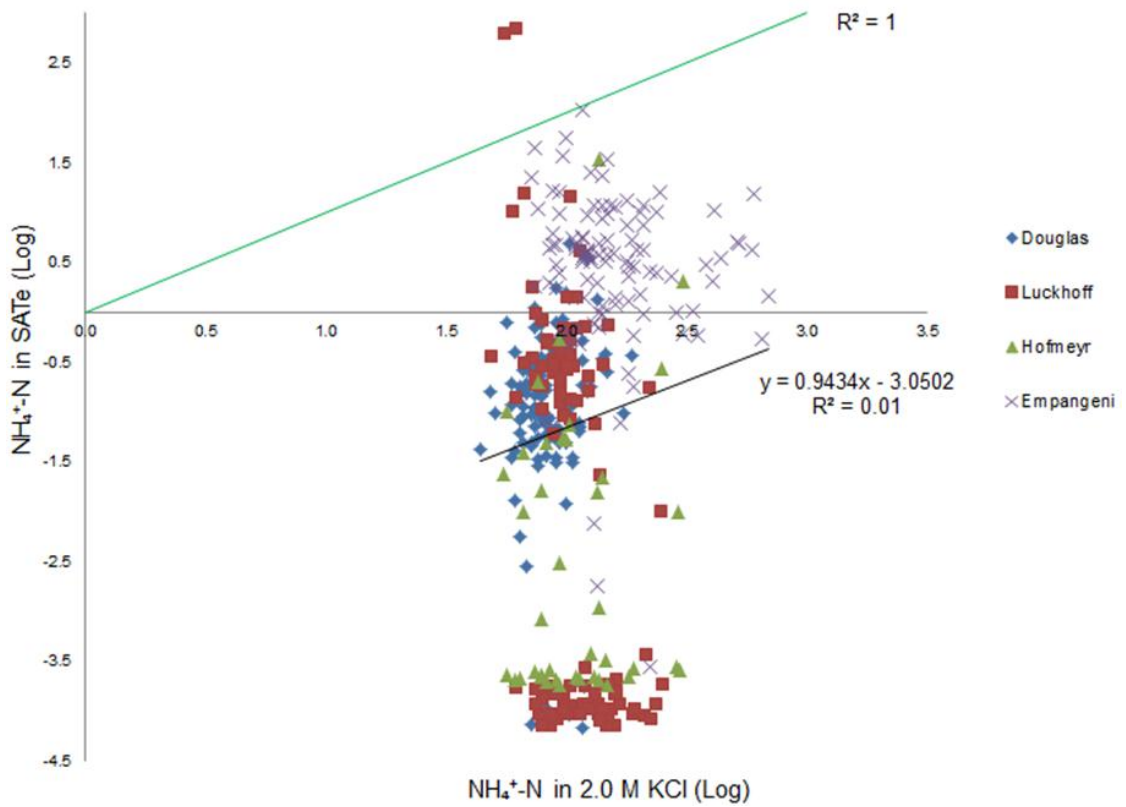


Figure 5.3 Scatterplot for log transformed concentrations of $\text{NH}_4^+\text{-N}$ in 2.0 KCl extracts against the saturated paste extract.

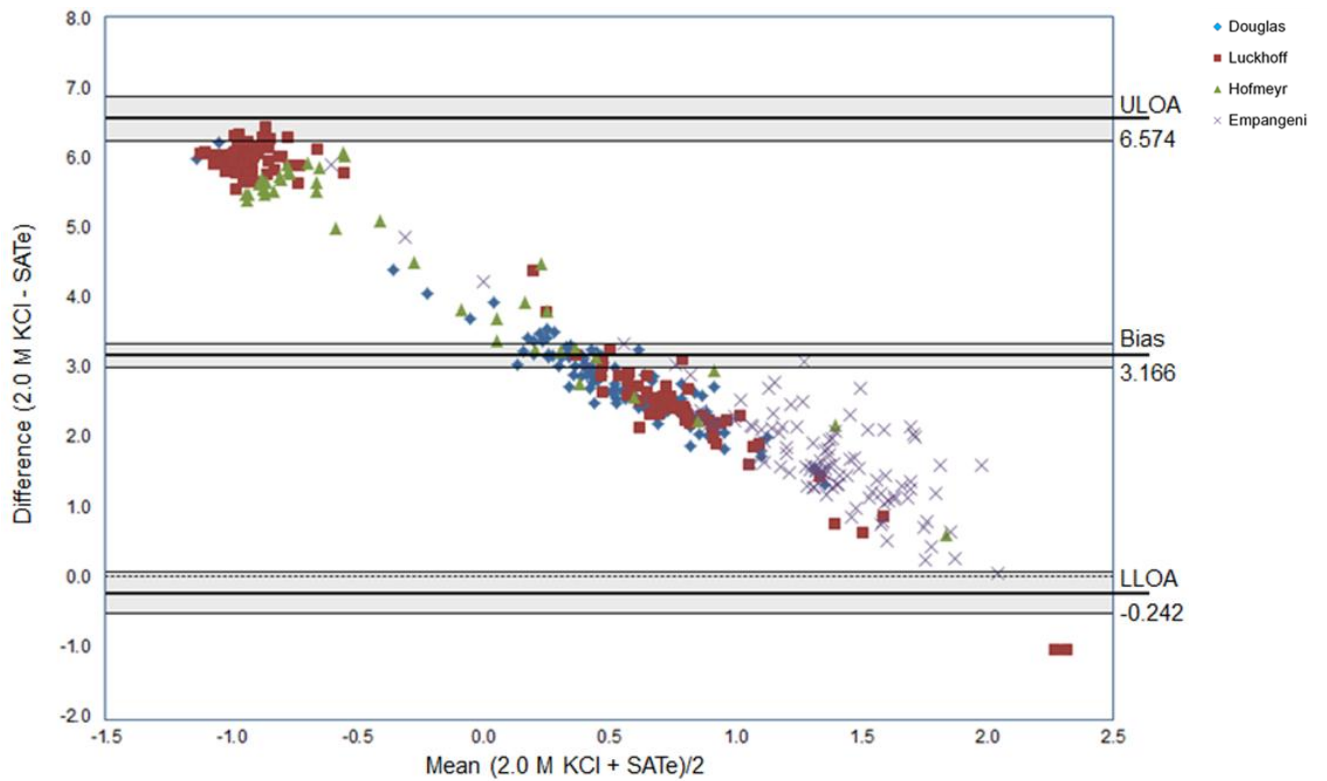


Figure 5.4 Bland-Altman plot for \log_6 transformed values of $\text{NH}_4^+\text{-N}$ extraction methods

5.1.2.2 NO_3^- -N concentrations

A scatterplot for log transformed concentrations of NO_3^- -N in extracts of 2.0 M KCl against that in the SATe, and the line of equality is given in Figure 5.5. The Bland-Altman plot (Figure 5.6) shows the difference between NO_3^- -N in the KCl extract and SATe against the mean of the two extraction methods. In Table 5.2 the measures of agreement, precision of estimated limits of agreement and 95% confidence intervals are given.

Table 5.2 Bland-Altman statistics for log and anti-log transformed NO_3^- -N data

Parameter	Abbreviation	Log	Anti-log
Mean difference or Bias	<i>d</i>	0.733	2.081
Standard deviation of differences	<i>s</i>	1.473	4.360
Sample size	<i>n</i>	380	380
Degrees of freedom	<i>n - 1</i>	379	379
<i>t</i> -distribution	<i>t</i>	1.96	1.96
Upper limit of agreement	<i>ULO</i> A	3.678	39.565
Lower limit of agreement	<i>LLO</i> A	-2.212	0.109
Standard error of mean difference	<i>SE d</i>	0.076	1.078
Standard error of agreement limits	<i>SEd ± 2s</i>	0.131	1.140
95% Confidence interval of the bias	<i>CI bias</i>	0.585 to 0.881	1.795 to 2.413
95% Confidence interval of the upper limit of agreement	<i>CI ULO</i> A	3.421 to 3.934	30.615 to 51.131
95% Confidence interval of the lower limit of agreement	<i>CI LLO</i> A	-2.469 to -1.956	0.085 to 0.141

Once again, data from the different sites can be seen clustered on the two plots. In the case of the regression plot, data from Luckhoff and Homeyr seem to be more in the area of the regression line than that of Douglas and Empangeni. The same case is apparent in the Bland-Altman plot where data from Luckhoff and Hofmeyr are scattered closer to the line of zero difference than the other sites.

Based on the coefficient of determination ($R^2 = 0.16$) for the pooled data, the correlation between NO_3^- -N in the two extracts was very poor. The NO_3^- -N in SATe was mostly underestimated compared to the 2.0 M KCl extract.

In the Bland-Altman plot, the SATe gave lower values than the KCl extract for low concentrations of NO_3^- -N and as concentrations increased so did the agreement. A negative trend for low values of NO_3^- -N is also observed in the scatter of the data. This is similar to the trend observed for, namely values for method y_1 , the KCl extract, is approximately constant. Agreement between the two extraction methods was poor with a bias of 0.733, indicating that on average the SATe gave results 0.733 units lower than KCl extract on the log scale (Table 5.2). When applying the anti-log of the bias it results in a value of 2.081, which means that KCl gave values 108% higher than the SATe values on average. The line of equality does not fall within the confidence intervals of the bias, thereby indicating a statistically significant systematic difference.

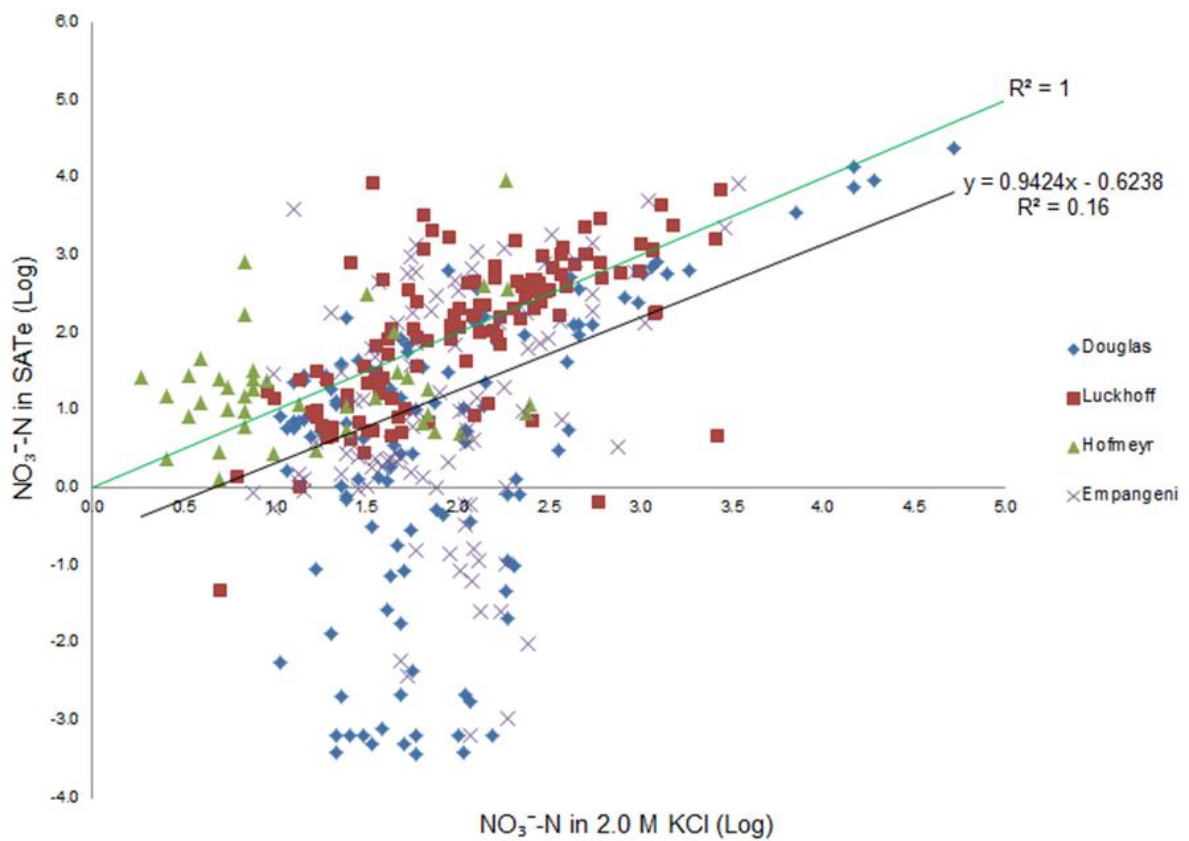


Figure 5.5 Regression of NO_3^- -N concentrations in extracts of 2.0 M KCl and SATe, with a line of equality.

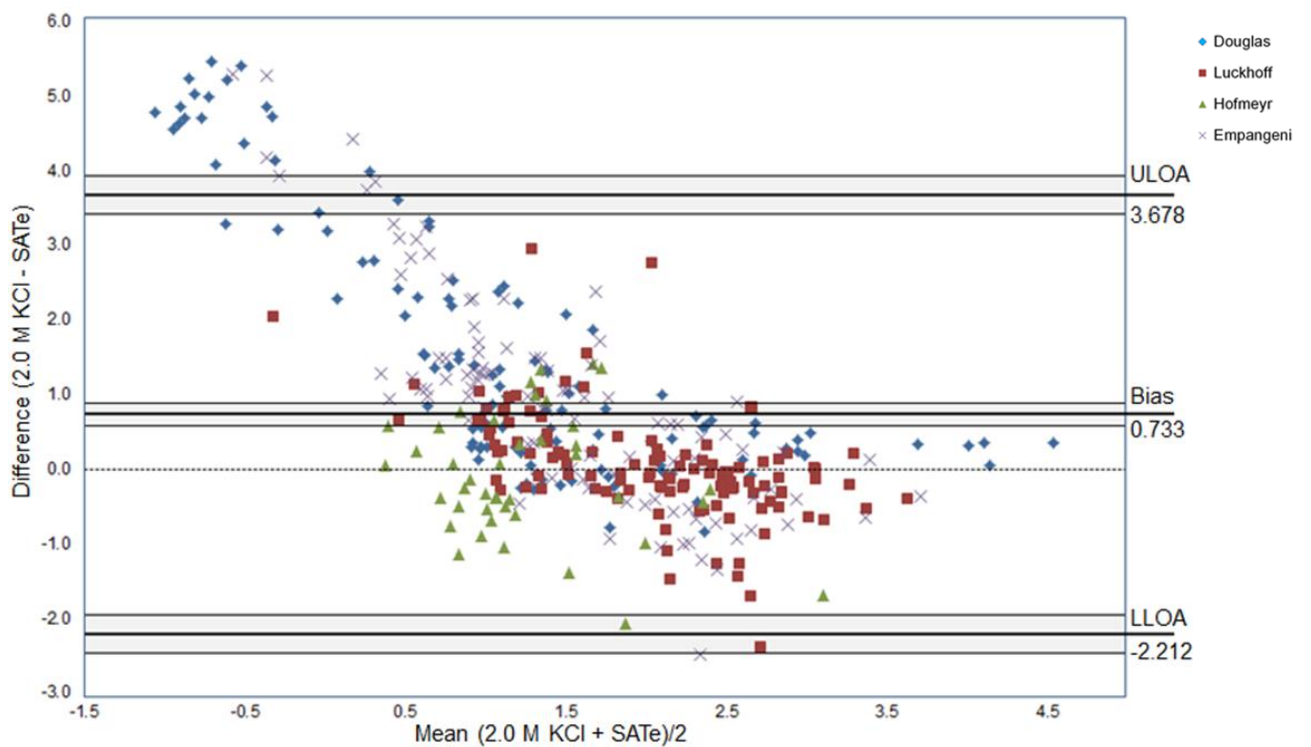


Figure 5.6 Bland-Altman plot for concentrations of NO_3^- -N in 2.0 M KCl and SATe.

5.2 Discussion

Considering the second research question asked, was whether the $\text{NH}_4^+\text{-N}$ and $\text{NO}_3^-\text{-N}$ concentrations in a SATe would agree well with that in a 2.0 M KCl extraction. The SATe is generally used to determine soluble salts by measuring the EC_e , a common soil analysis, especially in EMI surveys. Soluble salts that are most common in soils include Ca^{2+} , Mg^{2+} , Na^+ , Cl^- , SO_4^{2-} , HCO_3^- and to a lesser degree K^+ , CO_3^{2-} , NO_3^- and NH_4^+ (Gartley, 2011).

It could be argued that NH_4^+ is an ion that contributes to the measurement of EC_e (Gartley, 2011) and that collecting the SATe by suction could lead to more NH_4^+ extracted compared to only shaking with water. On the other hand, although NH_4^+ is a soluble cation it is attracted to soil particles and found mainly in exchangeable (adsorbed) and fixed forms. Extraction of exchangeable NH_4^+ therefore requires displacement of NH_4^+ cations from adsorbed positions on clay layers by exchange with another cation such as K^+ in a saline solution (Mulvaney, 1996; Walworth, 2013). It is for this latter characteristic of NH_4^+ that values found in the SATe was lower than that found in the KCl extract.

Further, due to i) NO_3^- being a contributing ion in the magnitude of EC_e (Gartley, 2011), ii) it being well established that water can be used as an extractant for NO_3^- (Berg & Gardner, 1978; Patriquin *et al.*, 1993; Maynard *et al.*, 2007) because of its water solubility (Dahnke & Johnson, 1990), and also iii) because the SATe have been used for the extraction of NO_3^- by Corwin *et al.*, (2003a). It could be hypothesised that a SATe made with water will compare well to a 2.0 M KCl extract. However, results of the present study revealed that the SATe did not agree well with 2.0 M KCl in terms of inorganic nitrogen extraction. A possible explanation could be that extended periods of saturation can cause NO_3^- reduction by denitrification leading to loss through volatilization (Walworth, 2013). Since results in Figure 5.5 revealed that the SATe mostly underestimated values of NO_3^- , leaving soils overnight in saturated conditions at room temperature could favour denitrification and volatilization.

The use of an alternative extractant for inorganic N that could reduce time and cost of chemicals would be advantageous. Unfortunately, the SATe used for EC_e determination during EMI surveys did not prove to be such an alternative in the current study. However, many other water extractions in different soil to water ratios exist for the determination of electrical conductivity (EC) in soils. These soil-water extracts can also be used to measure soluble salts in samples collected after an EMI survey. Therefore, possible further research can be to investigate the use thereof for determination of specifically $\text{NO}_3^-\text{-N}$ by comparing to an accepted standard extraction method such as 2.0 M KCl.

Possible factors influencing the lack of agreement could have been unforeseen laboratory circumstances, for example delayed analysis caused by availability of the instruments for analysis, and it should also be noted that either the 2.0 M KCl or SATe extracts may also contain increasing or decreasing amounts of interfering substances that can effect relationships between the two extracts.

In the event that soil EC does not need to be determined, other less expensive alternatives to KCl for inorganic N extraction exist. For example, Wiltshire & Laubscher (1989) measured NH_4^+ , NO_2^- and NO_3^- in small soil samples of N-poor soils by extracting with NaCl. To validate the extraction method, soils were extracted with 2.0 M KCl and 1.0 M NaCl at a soil to extractant ratio of 1:10. Results showed no significant difference between the extractants and using 1.0 M NaCl reduced the cost of extraction by two thirds at half the molarity of KCl while still conserving the stability of extracts.

CHAPTER 6. RESULTS AND DISCUSSION: APPLYING EC_a DATA FOR INDIRECT MEASUREMENT OF SOIL INORGANIC N

6.1 Results

6.1.1 Single and average EM38 measurements

Appendix 4 shows the single and composite EC_a measurements at different depths at each sampling point for Douglas, Luckhoff and Hofmeyr. This data were regressed against each other (Figure 6.1). A Bland-Altman analysis was done that includes the data from all sites and depths of EC_a readings (Figure 6.2 and Table 6.1).

Table 6.1 Calculated Bland-Altman statistics

Parameter	Abbreviation	EC _a (mS/m)
Mean difference	<i>d</i>	3.961
Standard deviation of differences	<i>s</i>	21.952
Sample size	<i>n</i>	72
Degrees of freedom	<i>n</i> – 1	71
<i>t</i> -distribution	<i>t</i>	1.98
Upper limit of agreement	<i>ULO</i> A	47.865
Lower limit of agreement	<i>LLO</i> A	-39.944
Standard error of mean difference	<i>SE d</i>	2.587
Standard error of agreement limits	<i>SEd</i> ± 2 <i>s</i>	4.481
95% Confidence interval of the bias	<i>CI bias</i>	-1.161 to 9.083
95% Confidence interval of upper limit of agreement	<i>CI ULO</i> A	38.993 to 56.738
95% Confidence interval of lower limit of agreement	<i>CI LLO</i> A	-48.816 to -31.071

The regression plot revealed a very good coefficient of determination ($R^2=0.83$) between measurement techniques. Data from both the 0-750 mm and 0-1500 mm readings at Douglas were higher than the other EC_a measurements.

The Bland-Altman plot (Figure 6.2) showed very good agreement and no statistically significant systematic difference. The line of equality also falls within the confidence intervals of the bias and almost all measurements fall within the limits of agreement. It is also the data from Douglas that fell outside of the upper limit of agreement. It was found that the single and composite EC_a measurements taken in a 1 m² area at the sampling points at Douglas, Luckhoff and Hofmeyr agreed very well.

Agreement results between single and composite EC_a measurements lead to the decision to use the average of the single and composite EC_a readings to develop prediction models. This average will hereafter only be referred to as the EC_a readings or EC_a measurements.

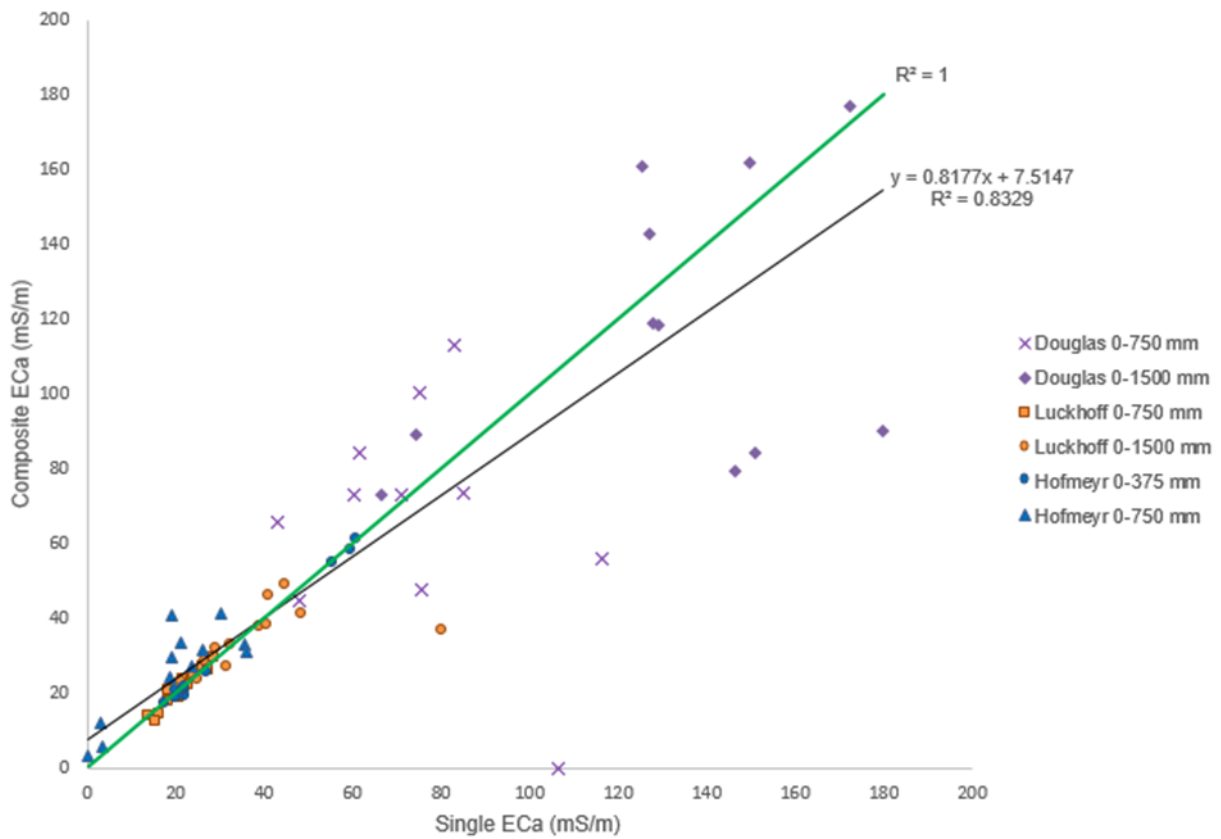


Figure 6.1 Scatterplot of single against composite EC_a measurements.

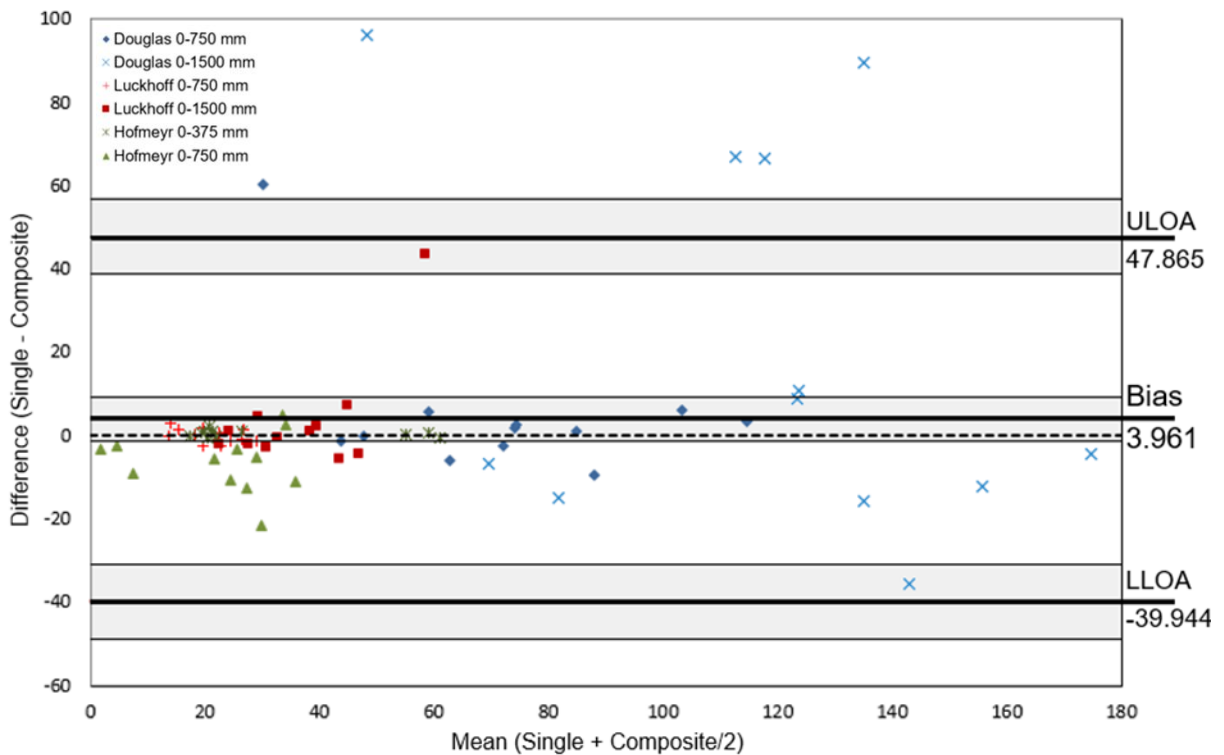


Figure 6.2 Bland-Altman plot for EC_a readings.

6.1.2 Inorganic N prediction models

In Appendix 5 the EC_a measurements as well as the geometric mean for each sampling point are shown for Douglas, Luckhoff and Hofmeyr, respectively. This appendix also includes the elevation data to be used for model development.

The inorganic N in kg/ha for each individual sampling depths in 300 mm increments as well as for cumulative depths (Appendix 6) were used for prediction model development. Model results, i.e. R² and P-values, for Douglas, Luckhoff and Hofmeyr are displayed in Tables 6.2, 6.3, and 6.4, respectively. Since the soils of the Hofmeyr site were very shallow, soil samples were mainly taken at 0 to 300 mm and 300 to 600 mm depths. At only two of the 12 sampling points were soils sampled at 600 to 900 mm depth and therefore no prediction models were developed for this depth.

When using multiple linear regression in MS Excel and incorporating elevation into the prediction models, almost all combinations of EC_a measurements and sampling depths produced models that were not statistically significant. Models were only significant for NH₄⁺-N in the 900 to 1200 mm sampling depth at Douglas for both sensing depths (0 to 750 mm; R²=0.54 and 0 to 1500 mm; R²=0.57).

Table 6.2 Multiple regression model statistics Douglas

EC _a measurement depth		EC _a 0-750		EC _a 0-1500		EC _a Geometric mean	
Statistical variable		R ²	P-Value	R ²	P-Value	R ²	P-Value
NH ₄ ⁺ -N (kg/ha) log	0-300	0.09	0.64	0.16	0.46	0.08	0.69
	300-600	0.04	0.83	0.08	0.69	0.06	0.77
	600-900	0.04	0.85	0.05	0.79	0.01	0.95
	900-1200	0.54	0.05	0.57	0.04	0.48	0.07
	1200-1500	0.11	0.67	0.14	0.6	0.12	0.63
	0-600	0.08	0.69	0.15	0.48	0.08	0.67
	0-900	0.07	0.72	0.12	0.57	0.06	0.77
	0-1200	0.04	0.85	0.15	0.51	0.03	0.9
0-1500	0.41	0.16	0.36	0.21	0.4	0.17	
NO ₃ ⁻ -N (kg/ha) log	0-300	0.29	0.22	0.27	0.24	0.3	0.2
	300-600	0.18	0.41	0.15	0.48	0.17	0.44
	600-900	0.31	0.19	0.24	0.29	0.27	0.24
	900-1200	0.06	0.79	0.06	0.78	0.06	0.78
	1200-1500	0.04	0.88	0.12	0.64	0.07	0.79
	0-600	0.24	0.29	0.21	0.34	0.24	0.29
	0-900	0.27	0.24	0.22	0.32	0.25	0.27
	0-1200	0.17	0.47	0.15	0.52	0.16	0.48
0-1500	0.05	0.84	0.06	0.8	0.06	0.81	
TIN (kg/ha) log	0-300	0.35	0.14	0.27	0.25	0.33	0.17
	300-600	0.16	0.46	0.13	0.54	0.14	0.5
	600-900	0.24	0.3	0.18	0.41	0.21	0.35
	900-1200	0.02	0.92	0.01	0.96	0.02	0.94
	1200-1500	0.03	0.88	0.08	0.74	0.05	0.82
	0-600	0.26	0.27	0.2	0.37	0.23	0.31
	0-900	0.24	0.29	0.19	0.4	0.22	0.33
	0-1200	0.12	0.6	0.09	0.68	0.11	0.64
0-1500	0.04	0.87	0.04	0.87	0.05	0.85	

Table 6.3 Multiple regression model statistics Luckhoff

EC _a measurement depth		EC _a 0-750 mm		EC _a 0-1500 mm		EC _a Geometric mean	
Statistical variable		R ²	P-value	R ²	P-value	R ²	P-value
NH ₄ ⁺ -N (kg/ha) log	0-300	0.02	0.92	0.16	0.45	0.04	0.83
	300-600	0.06	0.76	0.14	0.52	0.10	0.64
	600-900	0.07	0.74	0.07	0.71	0.09	0.66
	900-1200	0.39	0.11	0.29	0.11	0.40	0.10
	1200-1500	0.15	0.52	0.15	0.52	0.15	0.52
	0-600	0.10	0.62	0.05	0.79	0.05	0.79
	0-750	0.09	0.67	0.05	0.80	0.04	0.82
	0-900	0.07	0.71	0.05	0.81	0.04	0.84
	0-1200	0.05	0.80	0.03	0.87	0.02	0.92
	0-1500	0.09	0.68	0.21	0.38	0.17	0.47
NO ₃ ⁻ -N (kg/ha) log	0-300	0.10	0.61	0.09	0.65	0.10	0.63
	300-600	0.03	0.88	0.03	0.87	0.03	0.88
	600-900	0.27	0.24	0.28	0.22	0.31	0.19
	900-1200	0.21	0.34	0.22	0.32	0.23	0.30
	1200-1500	0.28	0.26	0.14	0.54	0.24	0.33
	0-600	0.06	0.76	0.01	0.95	0.03	0.86
	0-750	0.08	0.68	0.01	0.94	0.05	0.79
	0-900	0.10	0.62	0.03	0.88	0.07	0.72
	0-1200	0.17	0.42	0.08	0.69	0.14	0.50
	0-1500	0.18	0.45	0.08	0.71	0.16	0.50
TIN (kg/ha) log	0-300	0.12	0.57	0.12	0.56	0.11	0.59
	300-600	0.05	0.81	0.05	0.80	0.05	0.81
	600-900	0.26	0.26	0.28	0.23	0.30	0.20
	900-1200	0.15	0.47	0.17	0.48	0.18	0.42
	1200-1500	0.31	0.22	0.17	0.48	0.27	0.29
	0-600	0.06	0.75	0.00	0.99	0.01	0.94
	0-750	0.08	0.68	0.00	1.00	0.03	0.89
	0-900	0.10	0.62	0.01	0.97	0.04	0.83
	0-1200	0.18	0.40	0.04	0.82	0.11	0.59
	0-1500	0.21	0.40	0.07	0.75	0.16	0.51

Table 6.4 Multiple regression model statistics Hofmeyr

EC _a measurement depth		EC _a 0-375		EC _a 0-750		EC _a GM	
Statistical variable		R ²	P-Value	R ²	P-Value	R ²	P-Value
NO ₃ ⁻ -N (kg/ha) log	0-300	0.14	0.51	0.12	0.55	0.11	0.59
	300-600	0.32	0.45	0.28	0.52	0.23	0.59
	0-600	0.08	0.85	0.07	0.87	0.05	0.9
NH ₄ ⁺ -N (kg/ha) log	0-300	0.20	0.38	0.28	0.23	0.27	0.25
	300-600	0.22	0.61	0.06	0.88	0.02	0.955
	0-600	0.41	0.35	0.36	0.41	0.27	0.53
TIN (kg/ha) log	0-300	0.16	0.46	0.21	0.35	0.23	0.31
	300-600	0.28	0.51	0.25	0.57	0.21	0.62
	0-600	0.16	0.71	0.17	0.68	0.18	0.67

6.2 Discussion

6.2.1 Single and average EM38 measurements

Good agreement between the single and composite EC_a measurements was probably due to the fact that largely the same soil volume was measured multiple times. The EM38 has two receiver coils with an inter-coil spacing of 0.5 and 1.0 m between the sender and receiver coils and when in the vertical orientation the sensor has a measurement width of 1.0 m (Geonics Ltd, 2010). Therefore, taking an EC_a measurement at one corner of a 1 m²

area would result in an EC_a reading of a soil volume that would also include part of the measured soil volume from adjacent corners as well as the central measurement point.

6.2.2 Inorganic N prediction models

In general, it was found that inorganic N did not correlate well with EC_a measurements for the development of prediction models at Douglas, Luckhoff and Hofmeyr. As discussed in the literature review, finding no correlation between inorganic N and EC_a is not uncommon, since use of EC_a data from EMI surveys is very site-specific (Corwin & Lesch, 2005). It is known that EC_a is a complex physico-chemical soil measurement that is influenced by any soil property that influences pathways of electrical conductance in soil (Corwin *et al.*, 2008b). The magnitude of the EC_a measurement is influenced by physical and chemical soil properties such as texture, bulk density, saturation percentage, drainage, organic matter content, CEC, subsoil parameters and salinity (Grisso *et al.*, 2009). Therefore, EC_a is a function of various soil properties and can be calibrated to any soil property that significantly influences the EC_a reading (Corwin *et al.*, 2008b). Also, if the influence of the in-field changes in one dominating soil property is large enough in comparison to the variation of other soil properties, then EC_a can be calibrated as a direct measurement of it (Sudduth *et al.*, 2001).

Most of the soil properties that dominate the variability in EC_a also show significant co-dependency and provide overlapping and confusing information about EC_a that complicates its interpretation (Corwin *et al.*, 2008b). Consequently, without a good scientific understanding and explanation for what was being measured by EC_a, geospatial EC_a readings and their correlations with soil properties can be easily misinterpreted. Measurements of EC_a is also misused when soil properties that are unrelated or only loosely related to the actual properties being measured are spatially characterized (Corwin *et al.*, 2008b).

As stated by Amezketa (2007), the purpose of correlation analysis between EC_a data and measured soil variables is to identify the main soil property or properties that influence the EC_a measurement within a study area. Therefore, it is likely that inorganic N is not the main soil property influencing EC_a at the sites investigated and that the EC_a dominating soil property remains to be determined.

Under certain conditions, a site-specific N management plan can also be recommended based on EC_a zones, even if inorganic N does not correlate well with EC_a. The EC_a maps can reveal soil type boundaries, ponding areas and eroded areas more clearly than some

conventional survey maps (Franzen & Kitchen, 1999; Adamchuk *et al.*, 2011). Maps of EC_a can also be used along with other data layers such as management history, aerial images, yield maps and the topography maps to reveal variability in plant growth conditions (Adamchuk *et al.*, 2011). The spatial analysis of NO_3^- and site specific crop management based on this variation can maximize production and minimize the impact that N has on the environment (Jurisic *et al.*, 2013).

Additionally, even though Corwin *et al.* (2003b) found no correlation between NO_3^- -N and EC_a , the same authors wrote a chapter in the Handbook of Agricultural Geophysics (Corwin *et al.*, 2008a), where the same research on the cotton fields were used to delineate SSMU's. In cases where yield correlates with EC_a , the spatial distribution of EC_a can be used to direct soil sampling and to determine soil chemical and physical properties that influence yield. This information provides a basis for delineating SSMU's that can also be used for site-specific N management.

The process of identifying SSMU's after Corwin *et al.* (2008a) consists of a few general steps:

- a. Intensive yield monitoring
- b. EC_a survey followed by EC_a -directed soil sampling
- c. Statistical analysis to determine the correlation between EC_a -directed soil sampling and crop yield, thereby identifying the dominant soil properties that influence yield as well as developing a yield response model adjusted for spatial autocorrelation.
- d. Use of GIS to define SSMU's and to make management recommendations based on the crop yield response model and scatter plots.

Using EC_a -directed soil sampling is a viable way of identifying some of the soil properties that causes yield variation. However, crop yield is still influenced by various meteorological, topographic, edaphic, biological and anthropogenic factors that interact complexly. Site-specific management therefore requires considering a broad spectrum of factors that influence crop productivity. It must balance crop productivity with quality, sustainability, optimization of inputs, profitability and minimization of environmental impacts (Corwin *et al.*, 2008a).

CHAPTER 7. CONCLUSIONS AND RECOMMENDATIONS

In short, the research questions of this study were: a) to compare single to composite soil sampling for the determination of inorganic N through Bland-Altman agreement analysis, b) to determine if the SATe could replace the standard 2.0 M KCl extraction for determination of inorganic N in soils, also by using agreement analysis and c) to determine what combination of single or composite EC_a measurements and inorganic N at different sampling depths would produce the most statistically significant model for prediction of inorganic N.

For the first research aim, it was concluded that a composite soil sample taken in a 1 m² area was more suitable when NO_3^- -N or TIN concentrations are to be determined. For NH_4^+ -N concentrations, a single soil sample was sufficient and will reduce the time and cost spent in the field and laboratory. However, for inorganic N fertilizer recommendations, soils are generally analysed for both NH_4^+ -N and NO_3^- -N and not only for NH_4^+ -N. Composite samples are therefore recommended for more accurate determination of both NH_4^+ -N and NO_3^- -N.

From an economic and time efficiency point of view, collecting composite samples are very laborious, but if micro-variation in soils is large, composite samples are essential. By using ESAP-RSSD sample site selection along with composite soil sampling for inorganic N, micro-variability is taken into consideration and soils are sampled in an ultra-precise manner which is important for precision soil and crop management.

Regarding the second research question, it was concluded from scatterplots and Bland-Altman plots that agreement between the two extraction methods were insufficient and 2.0 M KCl cannot be substituted with the SATe for inorganic N determination. A possible explanation for the lack of agreement for NO_3^- -N between the two extracts is NO_3^- loss through volatilization caused by denitrification under saturated conditions. Regarding the lack of agreement for NH_4^+ -N between the two methods, water used in the SATe was insufficient in extracting the adsorbed NH_4^+ cations through suction.

Even though the SATe cannot be used for the determination of inorganic N, other options of soil-water extracts for measuring soluble salts exist. These soil-water extracts can be tested for inorganic N determination specifically NO_3^- -N in further research. It is also recommended that extraction and analysis be done as swiftly as possible to avoid inaccurate results.

For the purpose of developing statistically significant prediction models for inorganic N, the majority of the models were poor and it was concluded that for the sites investigated, inorganic N was not a dominant soil property contributing to the EC_a .

It is known that there are many soil properties that influence EC_a , but that only one or two dominates the EC_a measurement. If the specific soil property in question does not correlate well with EC_a measurements, the collected EC_a data can still be implemented in other ways for site-specific management. A possibility is to divide a field into different classes of EC_a values and manage it accordingly. Another approach is to identify SSMU's through yield monitoring followed by an EC_a survey and RSSD soil sampling, statistical correlation analyses to identify dominant soil properties that influence EC_a and to use GIS to identify SMMU's and make recommendations.

Using EMI sensors, EC_a data and statistical methods to direct soil sampling and to estimate the spatial variability of N is indeed possible in certain fields and can provide information useful for the understanding of crop production and management improvement. But, if N does not correlate with EC_a it is very important to identify the soil properties that do influence EC_a readings the most to so identify those that most influence yield as well. Such properties that could influence the EC_a include, amongst others, EC_e , clay content, water content and bulk density, and the correlation of some of these properties with EC_a will be investigated in the larger WRC project.

REFERENCES

- ADAMCHUK, V.I., 2010. Precision agriculture: Does it make sense? *Better Crops* 94(3):4-6.
- ADAMCHUK, V.I., ROSSEL, R.A.V., SUDDUTH, K.A. & LAMMERS, P.S., 2011. Sensor fusion for precision agriculture. In: *Sensor fusion - Foundation and applications*, C. Thomas (Ed.). InTech publishers. <https://www.intechopen.com/books/sensor-fusion-foundation-and-applications/sensor-fusion-for-precision-agriculture> (Accessed 23/04/2015)
- ADEPETU, J.A., NABHAN, H. & OSINUBI, A., 2000. Simple soil, water and plant testing techniques for soil resource management. Proceedings of a training course held in Ibadan, Nigeria, 16-27 Sept 1996. AGL/MISC/28/2000. FAO, Rome.
- ALTMAN, D.G. & BLAND, J.M., 1983. Measurement in medicine: the analysis of method comparison studies. *The Statistician* 32:307-317.
- AMEZKETA, E., 2007. Soil salinity assessment using directed soil sampling from a geophysical survey with electromagnetic technology: a case study. *Spanish Journal of Agricultural Research* 5(1):91-101.
- ARC-ISCW, 2017. Weather data measured for 2016. Pretoria, South Africa.
- BATES, T.E., 1993. Soil handling and preparation. In: *Soil sampling and methods of analysis*, M.R. Carter (Ed.). Lewis publishers, United States of America.
- BERG, M.G. & GARDNER, E.H., 1978. Methods of soil analysis used in the soil testing laboratory at Oregon State University. Special Report no. 321, Agricultural Experiment Station, Oregon State University, Corvallis, United State of America.
- BLAND, J.M. & ALTMAN, D.G., 1986. Statistical methods for assessing agreement between two methods of clinical measurement. *The Lancet* 327(8476):307-310.
- BOUMA, J., STOOORVOGEL, J., VAN ALPHEN, B.J. & BOOLTINK, H.W.G., 1999. Pedology, precision agriculture, and the changing paradigm of agricultural research. *Soil Science Society of America Journal* 63(6):1763-1768.
- BREMNER, J.M., 1965. Inorganic forms of nitrogen. In: *Methods of soil analysis, Part 2 – Chemical and microbiological properties*, C.A. Black (Ed.). American Society of Agronomy, Madison, United States of America.

- CHHAPOLA, V., KANWAL, S.K. & BRAR, R., 2015. Reporting standards for Bland–Altman agreement analysis in laboratory research: a cross-sectional survey of current practice. *Annals of Clinical Biochemistry* 52(3):382-386.
- CLIMATE-DATA.ORG, 2019. <https://en.climate-data.org/> (Accessed 16/01/2019)
- CORWIN, D.L., KAFFKA, S.R., HOPMANS, J.W., MORI, Y., VAN GROENIGEN, J.W., VAN KESSEL, C., LESCH, S.M. & OSTER, J.D., 2003a. Assessment and field-scale mapping of soil quality properties of a saline-sodic soil. *Geoderma* 114:231-259.
- CORWIN, D.L. & LESCH, S.M., 2003. Application of soil electrical conductivity to precision agriculture: theory, principles, and guidelines. *Agronomy Journal* 95:455-471.
- CORWIN, D.L. & LESCH, S.M., 2005. Apparent soil electrical conductivity measurements in agriculture. *Computers and Electronics in Agriculture* 46:11-43.
- CORWIN, D.L., LESCH, S.M. & FARAHANI, H.J., 2008b. Theoretical insight on the measurement of soil electrical conductivity. In: *Handbook of agricultural geophysics*, B.J. Allred, J.J. Daniels & M.R. Ehsani (Eds). CRC Press (Taylor & Francis Group), USA.
- CORWIN, D.L., LESCH, S.M., OSTER, J.D. & KAFFKA, S.R., 2006. Monitoring management-induced spatio-temporal changes in soil quality through soil sampling directed by apparent electrical conductivity. *Geoderma* 131(3-4):369-387.
- CORWIN, D.L., LESCH, S.M., SEGAL, E., SKAGGS, T.H. & BRADFORD, S.A., 2010. Comparison of sampling strategies for characterizing spatial variability with apparent soil electrical conductivity directed soil sampling. *Journal of Environmental and Engineering Geophysics* 15(3):147-162.
- CORWIN, D.L., LESCH, S.M., SHOUSE, P.J., SOPPE, R. & AYARS, J.E., 2003b. Identifying soil properties that influence cotton yield using soil sampling directed by apparent soil electrical conductivity. *Agronomy Journal* 95(2):352-364.
- CORWIN, D.L., LESCH, S.M., SHOUSE, P.J., SOPPE, R. & AYARS, J.E., 2008a. Delineating site-specific management units using geospatial EC_a measurements. In: *Handbook of Agricultural Geophysics*, B.J. Allred, J.J. Daniels & M.R. Ehsani (Eds). CRC Press (Taylor & Francis Group), USA.

- DAHNIKE, W.C. & JOHNSON, G.V., 1990. Testing soils for available nitrogen. In: Soil testing and plant analysis, 3rd edn, R.L. Westerman (Ed.). Soil Science Society of America, Madison, USA.
- DINKINS, C.P & JONES, C., 2017. Soil sampling strategies. MontGuide MT200803AG. Montana State University Extension, United States of America.
- DOOLITTLE, J.A. & BREVIK, E.C., 2014. The use of electromagnetic induction techniques in soils studies. *Geoderma* 223-225:33-45.
- DORN, T., 2015. Nitrogen sources. University of Nebraska, Lincoln, United States of America. <http://lancaster.unl.edu/ag/factsheets/288.pdf> (Accessed 08/12/2015)
- EIGENBERG, R.A. & NIENABER, J.A., 1998. Electromagnetic survey of cornfield with repeated manure applications. *Journal of Environmental Quality* 27(6):1511-1515.
- EIGENBERG, R.A., DORAN, J.W., NIENABER, J.A., FERGUSON, R.B. & WOODBURY, B.L., 2002. Electrical conductivity monitoring of soil condition and available N with animal manure and a cover crop. *Agriculture, Ecosystems and Environment* 88(2), 183-193.
- EITH, C., KOLB, M. & SEUBERT, A., 2001. Practical ion chromatography: An introduction, K.H. Viehweger (Ed.). Metrohm Ltd, Switzerland.
- EPA, 2005. Composite soil sampling in site contamination assessment and management. EPA Guidelines. Environment Protection Agency, Adelaide, South Australia.
- FERGUSON, R.B. & HERGERT, G.W., 2009. Soil sampling for precision agriculture. Publication EC154, Institute of Agriculture and Natural Resources, University of Nebraska-Lincoln Extension, United States of America.
- FERGUSON, R.B., HERGERT, G.W., SHAPIRO, C.A. & WORTMANN, C.S., 2007. Guidelines for soil sampling. Publication G1740, Institute of Agricultural and Natural Resources, University of Nebraska-Lincoln Extension, United States of America.
- FLYNN, R., 2015. Interpreting soil tests: Unlock the secrets if your soil. NMSU Cooperative Extension Service, Circular 676. College of Agriculture, Consumer and Environmental Sciences, New Mexico State University, USA.

- FRANZEN, D.W. & PECK, T.R., 1995. Field soil sampling density for variable rate fertilization. *Journal of Production Agriculture* 8(4):568-574.
- FRANZEN, D.W. & CIHACEK, L.J., 1998. Soil sampling as a basis for fertilizer application. NDSU Extension Publication SF-990. North Dakota State University, USA.
- FRANZEN, D.W., CIHACEK, L.J., HOFMAN, V.L. & SWENSON, L.J., 1998. Topography-based sampling compared with grid sampling in the Northern Great Plains. *Journal of Production Agriculture* 11(3):364-370.
- FRANZEN, D.W. & KITCHEN, N.R., 1999. Developing management zones to target nitrogen applications. Potash & Phosphate Institute Site-Specific Management Guidelines, SSMG-5. [http://www.ipni.net/publication/ssmg.nsf/0/A5CD47480DAF17D1852579E500765D7B/\\$FILE/SSMG-05.pdf](http://www.ipni.net/publication/ssmg.nsf/0/A5CD47480DAF17D1852579E500765D7B/$FILE/SSMG-05.pdf) (Accessed 06/12/2015)
- GARTLEY, K.L., 2011. Recommended methods for measuring soluble salts in soils. In: Recommended soil testing procedures for the Northeastern United States. Northeastern Regional Publication No. 493:87-94. Cooperative Extension, University of Delaware, USA.
- GELDERMAN, R.H. & BEEGLE, D., 2012. Nitrate-Nitrogen. In: Recommended chemical soil test procedures for the North Central region (pp.5.2-5.4). North Central Regional Research Publication No. 221 (Revised). North Central Agricultural Experiment Stations, USA.
- GELDERMAN, R.H. & MALLARINO, A.P., 2012. Soil sample preparation. In: Recommended chemical soil test procedures for the North Central region (pp.1.1-1.4). North Central Regional Research Publication No. 221 (Revised). North Central Agricultural Experiment Stations, USA.
- GEONICS LTD, 2010. Operating instructions: EM38-MK2 data logging system for field computers Archer and Allegro MX. EM38-MK2 Version 2.02. Mississauga, Ontario, Canada.
- GIAVARINA, D., 2015. Understanding Bland-Altman analysis. *Biochemia Medica* 25(2):141-151.
- GRIFFIN, G., JOKELA, W., ROSS, D., PETTINELLI, D., MORRIS, T., & WOLF, A., 2009. In: Recommended soil nitrate tests. Recommended soil testing procedures for the

Northeastern United States. Northeastern Regional Publication No. 493: Cooperative Extension, University of Delaware, USA.

GRISSE, R., ALLEY, M., HOLSHOUSE, D. & THOMASON, W., 2009. Precision farming tools: Soil electrical conductivity. Virginia Cooperative Extension Publication 422-508. College of Agriculture and Life Sciences, Virginia Polytechnic Institute and State University, USA.

HABERLE, J., KROULÍK, M., SVOBODA, P., LIPAVSKÝ, J., KREJČOVÁ, J. & CERHANOVÁ, D., 2004. The spatial variability of mineral nitrogen content in topsoil and subsoil. *Plant Soil and Environment* 50(10):425-433.

HAFIF, B., 2014. Effect of tillage on soil nitrogen; a review. *International Journal on Advanced Science, Engineering and Information Technology* 3(4):2088-5334.

HANQUET, B., FRANKINET, M., PAREZ, V. & DESTAIN, M.F., 2002. Mapping within-field soil variability for precision agriculture using electromagnetic induction. Proceedings of the European Agricultural Engineering Conference, Budapest 2002. Paper No 02-PA-004.

HARTZ, T.K., 2007. Soil testing for nutrient availability – Procedures and interpretation for California vegetable crop production. Vegetable Research Institute, University of California, United States of America. https://vric.ucdavis.edu/pdf/fertilization_Soiltestingfornutrientavailability2007.pdf (Accessed 13/12/2018).

HEIL, K. & SCHMIDHALTER, U., 2017. The application of EM38: Determination of soil parameters, selection of soil sampling points and use in agriculture and archaeology. *Sensors* 17(11):2540 (44pp).

HENDRIKS, J., 2011. An analysis of precision agriculture in the South African summer grain producing areas. MBA Mini-dissertation, North-West University, South Africa.

HORNECK, D.A., SULLIVAN, D.M., OWEN, J.S. & HART, J.M., 2011. Soil test interpretation guide. Publication EC1478. Oregon State University Extension, United States of America.

JAMES, D.W. & WELLS, K.L., 1990. Soil sample collection and handling: Technique based on source and degree of field variability. In: *Soil testing and plant analysis*, 3rd edn, R.L. Westerman (Ed.). Soil Science Society of America, Madison, USA.

- JEONG, H., PARK, J. & KIM, H., 2013. Determination of NH_4^+ in environmental water with interfering substances using the modified Nessler method. *Journal of Chemistry*, Article ID 359217 (9 pp).
- JONES, C., JACOBSEN, J. & OLSON-RUTZ, K., 2014. Nutrient management: Module 1 – Soil sampling and laboratory selection. Publication 4449-1, Montana State University Extension, United States of America.
- JURISIC, A., MESIC, M., SESTAK, I. & ZGORELEC, Z., 2013. Horizontal and vertical nitrate-nitrogen distribution under different nitrogen fertilizer levels. 12th Alps-Adria
- KNIGHT, S.M., 2006. Soil mineral nitrogen testing: Practice and interpretation. Research Review No. 58. HGCA Project No. 3083. Agriculture and Horticulture Development Board, Kenilworth, United Kingdom.
- KNOWLES, O. & DAWSON, A., 2018. Current soil sampling methods – a review. In: Farm environmental planning – Science, policy and practice, L.D. Currie & C.L. Christensen (eds). Occasional Report No. 31. Fertilizer and Lime Research Centre, Massey University, New Zealand.
- KORSAETH, A., 2005. Soil apparent electrical conductivity (EC_a) as a means of monitoring changes in soil inorganic N on heterogeneous morainic soils in SE Norway during two growing seasons. *Nutrient Cycling in Agroecosystems* 72(3):213-227.
- LESCH, S.M., RHOADES, J.D. & CORWIN, D.L., 2000. ESAP-95 version 2.01R – User manual and tutorial guide. Research report no. 146. United States Department of Agriculture, Agricultural Research Service, George E. Brown, Jr., Salinity Laboratory, Riverside, California, United States of America.
- LESCH, S.M., 2005. Sensor-directed response surface sampling designs for characterizing spatial variation in soil properties. *Computers and Electronics in Agriculture* 46(1-3):153-179.
- MAYNARD, D.G., KALRA, Y.P. & CRUMBAUGH, J.A., 2007. Nitrate and exchangeable ammonium nitrogen. In: Soil sampling and methods of analysis, 2nd edn, M.R. Carter & E.G. Gregorich (Eds). CRC Press (Taylor & Francis Group), Boca Raton, USA.
- MICHALSKI, R. & KURZYCA, I., 2006. Determination of nitrogen species (nitrate, nitrite and ammonia ions) in environmental samples by ion chromatography. *Polish Journal of Environmental Studies* 15(1):5-18.

- MULVANEY, R.L., 1996. Nitrogen – Inorganic forms. In: Methods of soil analysis, Part 3 – Chemical methods, D.L. Sparks (ed.). Soil Science Society of America, Madison, United States of America.
- MULVANEY, R.L., KHAN, S.A., STEVENS, W.B. & MULVANEY, C.S., 1997. Improved diffusion methods for determination of inorganic nitrogen in soil extracts and water. *Biology and Fertility of Soils* 24(4):413-420.
- MUELLER, A., 2015. The effect of drying and drying temperature on soil analytical test values. MSc Thesis, Oklahoma State University, United States of America.
- MYERS, R.J.K. & PAUL, E.A., 1968. Nitrate ion electrode method for soil nitrate nitrogen determination. *Canadian Journal of Soil Science* 48(3):369-371.
- NATHAN, M.V., STECKER, J.A. & SUN, Y., 2012. Soil testing in Missouri – A guide for conducting soil tests in Missouri. Publication EC923, University of Missouri Extension, Division of Plant Sciences, United States of America.
- NINA, D.O. & SIGUNGA, D.O., 2012. Effects of drying method, storage period and carbon: nitrogen ratio on inorganic nitrogen contents of Vertisols. *African Journal of Environmental Science and Technology* 6(12):476-482.
- OLIVER, M.A. & WEBSTER, R., 2014. A tutorial guide to Geostatistics: Computing and modelling variograms and kriging. *Catena* 133:56-69.
- PATRIQUIN, D.G., BLAIKIE, H., PATRIQUIN, M.J. & YANG, C., 1993. On-farm measurements of pH, electrical conductivity and nitrate in soil extracts for monitoring coupling and decoupling of nutrient cycles. *Biological Agriculture and Horticulture* 9(3):231-272.
- PECK, T.R. & SOLTANPOUR, P.N., 1990. The principles of soil testing. In: Soil testing and plant analysis, 3rd edn, R.L. Westerman (ed.). Soil Science Society of America, Madison, USA.
- PERKINS, L.B., BLANK, R.R., FERGUSON, S.D., JOHNSON, D.W., LINDEMANN, W.C. & RAU, B.M., 2013. Quick start guide to soil methods for ecologists. *Perspectives in Plant Ecology, Evolution and Systematics* 15(4):237-244.
- PETERS, J.B. & LABOSKI, C.A.M., 2013. Sampling soils for testing. Publication A2100, University of Wisconsin Extension, United States of America.

- RAINS, G.C., PORTER, W. & PERRY, C.D., 2016. Soil sampling for precision management of crop production. UGA Extension Bulletin 1208. University of Georgia, United States of America.
- RHOADES, J.D., MANTEGHI, N.A., SHOUSE, P.J. & ALVES, W.J., 1989. Estimating soil salinity from saturated soil-paste electrical conductivity. *Soil Science Society of America Journal* 53(2):428-433.
- SHEPPARD, S.C. & ADDISON, J.A., 2007. Soil sample handling and storage. In: *Soil sampling and methods of analysis*, 2nd edn, M.R. Carter & E.G. Gregorich (Eds). CRC Press (Taylor & Francis Group), Boca Raton, USA.
- SOIL CLASSIFICATION WORKING GROUP, 1991. *Soil classification: a taxonomic system for South Africa*. Department of Agricultural Development, South Africa.
- STAFFORD, J.V., 2000. Implementing precision agriculture in the 21st century. *Journal of Agricultural Engineering Research* 76, 267-275.
- SUDDUTH, K.A., DRUMMOND, S.T. & KITCHEN, N.R., 2001. Accuracy issues in electromagnetic induction sensing of soil electrical conductivity for precision agriculture. *Computers and Electronics in Agriculture* 31:239–264.
- TAN, K.H., 2005. *Soil sampling, preparation, and analysis*, 2nd edn. CRC Press (Taylor & Francis Group), Boca Raton, United States of America.
- THE NON-AFFILIATED SOIL ANALYSIS WORK COMMITTEE, 1990. *Handbook of standard soil testing methods for advisory purposes*. Soil Science Society of South Africa, Pretoria, South Africa.
- UNITED STATES SALINITY LABORATORY STAFF, 1954. *Diagnosis and improvement of saline and alkali soils*. L.A. Richards (ed.), Handbook No. 60. United States Department of Agriculture, United States of America.
- USDA-NRCS, 2016. *Sampling soils for nutrient management*. United States Department of Agriculture, Natural Resources Conservation Service 10 East Babcock Street Federal Building Room 443 Bozeman, MT 59715. https://www.nrcs.usda.gov/Internet/FSE_DOCUMENTS/nrcs144p2_051273.pdf (Accessed 05/03/2016).

- VILLAR, N., AIZPURUA, A., CASTELLÓN, A., ORTUZAR, M.A., MORO, M.B.G. & BESGA, G., 2014. Laboratory methods for the estimation of soil apparent N mineralization and wheat N uptake in calcareous soils. *Soil Science* 179(2):84-94.
- WALWORTH, J.L., 2011. *Soil sampling and analysis*. Publication AZ1412, Cooperative Extension, College of Agriculture and Life Sciences, The University of Arizona, United States of America.
- WALWORTH, J.L., 2013. *Nitrogen in soil and the environment*. Publication AZ1591, Cooperative Extension, College of Agriculture and Life Sciences, The University of Arizona, United States of America.
- WHEATLEY, R.E., MACDONALD, R. & SMITH, A.M., 1989. Extraction of nitrogen from soils. *Biology and Fertility of Soils* 8(2):189-190.
- WIENHOLD, B.J. & DORAN, J.W., 2008. Apparent electrical conductivity for delineating spatial variability in soil properties. In: *Handbook of agricultural geophysics*, B.J. Allred, J.J. Daniels & M.R. Ehsani (Eds). CRC Press (Taylor & Francis Group), Boca Raton, United States of America.
- WILTSHIRE, G.H. & LAUBSCHER, D.J., 1989. Economical manual estimation of ammonium, nitrate and total inorganic nitrogen in soils. *South African Journal of Plant and Soil* 6(1):53-58.
- YATES, S.R. & WARRICK, A.W., 2002. Geostatistics. In: *Methods of soil analysis, Part 4 – Physical methods*, H.D. Dane & G.C. Topp (eds). Soil Science Society of America, Madison, United States of America.
- ZHANG, R. & WIENHOLD, B.J., 2002. The effect of soil moisture on mineral nitrogen, soil electrical conductivity, and pH. *Nutrient Cycling in Agroecosystems* 63:251-254.

APPENDICES

Appendix 1. Study site weather data

Table 1.a Douglas study site weather data measured at DeHoek station for 2016 (ARC-ISCW, 2017)

Month	Mean Max T (°C)	Mean Min T (°C)	Mean Max Relative Humidity (%)	Mean Min Relative Humidity (%)	Mean Total Radiation (MJ/m ²)	Mean Wind Speed (m/s)	Total Monthly Rainfall (mm)	Total Monthly Relative ET ₀ (mm)
Jan	34.65	16.57	85.13	25.18	22.47	1.73	69.8	163.67
Feb	35.05	15.11	85.68	17.23	23.02	1.8	26.4	157.87
Mar	31.77	12.34	91.77	21.87	20.15	1.82	44.6	140.14
Apr	28.13	8.08	93.35	26.47	15.25	1.68	10.2	97.21
May	23.32	3.33	94.13	32.2	12.25	1.45	28.2	69.53
Jun	22.47	0.64	92.05	24.98	11.32	1.51	0.4	109.57
Jul	20.12	-0.87	85.38	21.66	13.64	1.85	2	74.55
Aug	24.47	0.79	81.73	15.82	16.82	1.8	3	101.35
Sep	26.75	4.23	80.43	14.86	20.59	2.08	3.8	130.66
Oct	30.3	6.42	78.05	11.47	22.29	1.91	2.6	156.09
Nov	34.87	12.38	74.51	10.42	26.18	2.37	2.2	199.65
Dec	36.59	15.62	72.39	12.24	26.63	2.53	12.6	213.5
Mean	29.04	7.89	84.55	19.53	19.22	1.88	-	-
Total	-	-	-	-	-	-	205.8	1613.79

Table 1.b Luckhoff study site weather data measured at the Rust station for 2016 (ARC-ISCW, 2017)

Month	Mean Max T (°C)	Mean Min T (°C)	Mean Max Relative Humidity (%)	Mean Min Relative Humidity (%)	Mean Total Radiation (MJ/m ²)	Mean Wind Speed (m/s)	Total Monthly Rainfall (mm)	Total Monthly Relative ET ₀ (mm)
Jan	33.91	17.19	85.92	24.14	23.6	2.03	40.89	173.14
Feb	33.79	15.07	87.04	18.11	24.55	1.83	29.46	161.5
Mar	30.33	12.2	92.97	22.76	20.04	1.72	6.35	136.59
Apr	26.2	7.8	96.61	29.52	15.35	1.56	0.25	94.5
May	22.1	3.71	96.93	32.75	11.56	1.48	0	411.61
Jun	20.55	1.1	92.4	26.66	11.35	1.65	1.78	63.71
Jul	18.63	0.21	86.23	24.87	12.95	1.91	25.15	71.11
Aug	22.88	1.39	87.76	17.45	16.22	1.94	4.83	97.93
Sep	25.74	5.22	78.31	15.13	19.5	2.36	8.64	127.84
Oct	29.88	7.85	72.55	10.18	25.63	2.39	0	178.13
Nov	33.77	14.26	71.14	11.45	28.38	2.76	0	205.2
Dec	35.32	16.19	77.4	14.09	29.52	2.58	13.72	217.78
Mean	27.76	8.52	85.44	20.59	19.89	2.02	-	-
Total	-	-	-	-	-	-	131.07	1939.04

Table 1.c Hofmeyr study site weather data measured at the Grooffontein station for 2016 (ARC-ISCW, 2017)

Month	Mean Max T (°C)	Mean Min T (°C)	Mean Min Relative Humidity (%)	Mean Total Radiation (MJ/m ²)	Mean Wind Speed (m/s)	Total Monthly Rainfall (mm)	Total Monthly Relative ET ₀ (mm)
Jan	33.16	16	22.03	22.28	1.09	106.93	152.58
Feb	32.79	13.71	16.63	24.22	1.09	52.83	150.85
Mar	30.18	12.4	20.53	19.42	1.12	31.24	126.77
Apr	26.06	9.28	22.16	14.99	1.12	0	90.91
May	20.56	5.46	32.47	11.26	0.95	17.78	61.73
Jun	18.55	4.71	28.61	10.11	1.21	1.27	54.09
Jul	17.12	1.9	27.31	10.85	1.2	6.86	73.71
Aug	21.46	4.67	19.87	14.29	1.15	9.91	82.94
Sep	24.67	5.78	15.81	19.11	1.27	0	109.74
Oct	27.97	7.44	13.6	22.77	1.14	1.78	135.45
Nov	31.81	11.36	14.17	27.28	1.29	5.84	173.87
Dec	34.77	13.87	13.06	29.5	1.33	40.39	196.67
Mean	26.59	8.88	20.52	18.84	1.16	-	-
Total	-	-	-	-	-	274.83	1409.31

Table 1.d Empangeni site 2016 weather data measured at Heatonville and Mbonambi stations (ARC-ISCW, 2017)

Month	Mean Max T (°C)	Mean Min T (°C)	Mean Max Relative Humidity (%)	Mean Min Relative Humidity (%)	Mean Total Radiation (MJ/m ²)	Mean Wind Speed (m/s)	Total Monthly Rainfall (mm)	Total Monthly Relative ET ₀ (mm)
Jan	31.24	21.08	86.93	44.53	19.86	2.88	45	150.11
Feb	31.59	20.85	92.78	47.01	21.05	2.74	58.67	136.02
Mar	31.02	20.47	94.2	51.82	16.44	2.1	68.07	112.94
Apr	29.99	18.55	89.13	43.17	14.27	2.25	42.4	134.24
May	25.74	15.23	90.55	46.67	11.99	2.01	105.4	74.02
Jun	25.09	13.9	85.57	39.39	10.55	2.09	22.7	66.72
Jul	23.34	12.24	88.43	41.75	10.78	2.17	59.9	68.12
Aug	26.5	13.78	82.95	32.62	14.43	2.76	25.4	117.36
Sep	26.6	15.76	92.19	47.02	13.45	2.78	69	95.14
Oct*	24.35	14.25	92.35	48	12.99	2.55	58.4	55.16
Nov**								
Dec**								
Mean	27.55	16.61	89.51	44.20	14.58	2.43	-	-
Total	-	-	-	-	-	-	554.94	1009.83

*Incomplete data for that month

**No data

Appendix 2. Inorganic N concentrations in single and composite soil samples

Table 2.a Inorganic N concentrations in single and composite soil samples from the Douglas study site. Extraction was done with 2.0 M KCl

Point	Depth (mm)	NO ₃ ⁻ -N (mg/kg)		NH ₄ ⁺ -N (mg/kg)		TIN (mg/kg)	
		Single	Composite	Single	Composite	Single	Composite
V1	0-300	5.1	4.4	7.9	6.9	13	11.3
V1	300-600	3.9	3.6	7.1	7.2	11	10.8
V1	600-900	3.6	3.7	6.7	6.5	10.3	10.2
V1	900-1200	3.2	5.4	6.3	9.4	9.5	14.8
V1	1200-1500	8.2	13.6	6.5	6.2	14.7	19.8
V2	0-300	6.6	5.7	7.8	8.1	14.4	13.8
V2	300-600	3.8	3	6.3	6.8	10.1	9.8
V2	600-900	3	3.3	6.9	6.7	9.9	10
V2	900-1200	2.8	2.9	6.4	6.9	9.2	9.8
V2	1200-1500	3.2	3.7	6.8	6.9	10	10.6
V3	0-300	3.9	4.1	7.2	7.4	11.1	11.5
V3	300-600	3.2	3	6.5	6.4	9.7	9.4
V3	600-900	5.4	4.9	6.7	6.4	12.1	11.3
V4	0-300	5.5	5.4	7.2	7.6	12.7	13
V4	300-600	4	5.6	7.1	6.5	11.1	12.1
V4	600-900	8.6	7.6	6.5	6.6	15.1	14.2
V4	900-1200	5.8	4.8	6.1	6.5	11.9	11.3
V4	1200-1500	3.9	3.4	6.2	6.1	10.1	9.5
V5	0-300	5.4	5.9	7.6	7.9	13	13.8
V5	300-600	4	3.8	7.4	7.1	11.4	10.9
V5	600-900	3.5	3.8	7.1	6.9	10.6	10.7
V5	900-1200	4.6	6.5	6.7	6.6	11.3	13.1
V5	1200-1500	4.4	7.4	6.4	5.9	10.8	13.3
V6	0-300	7.6	5.9	7.4	6.8	15	12.7
V6	300-600	4	4.3	6	7.1	10	11.4
V6	600-900	5.6	5.1	5.9	5.2	11.5	10.3
V6	900-1200	10.7	7	6	6.1	16.7	13.1
V6	1200-1500	8.9	7.9	5.9	6.3	14.8	14.2
V7	0-300	9.7	7.7	7.3	7.5	17	15.2
V7	300-600	5.3	5.5	6.1	6.4	11.4	11.9
V7	600-900	5.1	5	6.5	6.2	11.6	11.2
V7	900-1200	5.1	5.9	6.8	5.8	11.9	11.7
V7	1200-1500	5	5.4	6.7	6.6	11.7	12
V8	0-300	7.7	12.8	7.4	6.3	15.1	19.1
V8	300-600	5.8	15.5	7	6.6	12.8	22.1
V8	600-900	18.4	47.3	6.5	7.1	24.9	54.4
V8	900-1200	64.4	72.6	6.8	6.8	71.2	79.4
V8	1200-1500	111.9	64.9	6.4	5.5	118.3	70.4
V9	0-300	10.2	9.6	8.7	7.6	18.9	17.2
V9	300-600	7.9	7.7	6.7	7.5	14.6	15.2
V9	600-900	21.4	22	7.5	6.7	28.9	28.7
V9	900-1200	6.8	14.4	7.4	6.4	14.2	20.8
V9	1200-1500	14.4	14.4	7.1	5.4	21.5	19.8
V10	0-300	10.1	9.7	7.9	9.7	18	19.4
V10	300-600	8.5	7.8	6.8	7.8	15.3	15.6
V10	600-900	20.5	19.9	6.7	7.8	27.2	27.7
V10	900-1200	14	13.4	7.2	7.8	21.2	21.2
V11	0-300	9.7	10.4	8.8	8.6	18.5	19
V11	300-600	7	6.1	8.4	7.2	15.4	13.3
V11	600-900	13.7	8.1	8.1	6.7	21.8	14.8
V11	900-1200	26.2	9.2	8.2	6.7	34.4	15.9
V11	1200-1500	23.2	8.5	7.9	7.1	31.1	15.6
V12	0-300	5.2	4	8	7.5	13.2	11.5
V12	300-600	8.3	2.9	6.7	6.4	15	9.3
V12	600-900	3.7	3.8	6.6	6.2	10.3	10
V12	900-1200	3.1	2.8	6.2	6.8	9.3	9.6
V12	1200-1500	4.3	4.6	6	6.7	10.3	11.3
Average		10.5	10.0	7.0	6.9	17.5	16.8
Minimum		2.8	2.8	5.9	5.2	9.2	9.3
Maximum		111.9	72.6	8.8	9.7	118.3	79.4
Standard deviation		16.5	13.2	0.7	0.8	16.5	13.1
Coefficient of variation		156.8	132.5	10.3	12.2	94.4	78.0

Table 2.b Inorganic N concentrations in single and composite soil samples from the Luckhoff study site. Extraction was done with 2.0 M KCl

Point	Depth (mm)	NO ₃ ⁻ -N (mg/kg)		NH ₄ ⁺ -N (mg/kg)		TIN (mg/kg)	
		Single	Composite	Single	Composite	Single	Composite
V1	0-300	30.2	18	9.1	9	39.3	27
V1	300-600	4.9	11.6	6.8	6.9	11.7	18.5
V1	600-900	5.9	10	7.2	6.2	13.1	16.2
V1	900-1200	11.9	13.3	6.4	7.4	18.3	20.7
V1	1200-1500	21.4	23.9	7	6.5	28.4	30.4
V2	0-300	5.1	9.3	8.4	8.4	13.5	17.7
V2	300-600	4.8	8.3	7.2	7.5	12	15.8
V2	600-900	7.1	12.1	7	7.1	14.1	19.2
V2	900-1200	11.5	11.2	6.7	6.7	18.2	17.9
V2	1200-1500	7.2	10.5	6.5	7.2	13.7	17.7
V3	0-300	4.6	3.5	8	9.7	12.6	13.2
V3	300-600	2.2	3.3	7.2	6.9	9.4	10.2
V3	600-900	5.8	5	7.7	7.8	13.5	12.8
V3	900-1200	12.9	10.7	7.5	7.4	20.4	18.1
V3	1200-1500	7.8	9	6.8	6.7	14.6	15.7
V4	0-300	4.4	4.1	8.7	8.9	13.1	13
V4	300-600	2	3.7	7.5	7.2	9.5	10.9
V4	600-900	4.5	4	7.1	9.2	11.6	13.2
V4	900-1200	8.9	4.7	6.9	7.3	15.8	12
V4	1200-1500	10.7	8.5	7.5	7	18.2	15.5
V5	0-300	5.1	5.4	10.2	8.8	15.3	14.2
V5	300-600	5.5	4.7	7.1	6.7	12.6	11.4
V5	600-900	6.2	7.1	6.6	6.9	12.8	14
V5	900-1200	13	16.2	7.5	7.1	20.5	23.3
V5	1200-1500	14.9	13.1	6.7	6.7	21.6	19.8
V6	0-300	12.8	21.6	10.3	10.4	23.1	32
V6	300-600	15.9	16	7.2	7	23.1	23
V6	600-900	7	6.1	7	7.2	14	13.3
V6	900-1200	7.2	7.4	6.5	7	13.7	14.4
V6	1200-1500	8.3	10.4	7.2	8.1	15.5	18.5
V7	0-300	4.9	5.1	8.6	8.3	13.5	13.4
V7	300-600	3.6	3.4	6.9	6.5	10.5	9.9
V7	600-900	8.1	8.7	7.5	7.3	15.6	16
V7	900-1200	16	19.9	6.8	7.2	22.8	27.1
V7	1200-1500	30.6	31	8.5	7.1	39.1	38.1
V8	0-300	4.6	3.7	9	9.7	13.6	13.4
V8	300-600	2.6	2.7	6.8	8.5	9.4	11.2
V8	600-900	3.1	4.4	8.8	8	11.9	12.4
V8	900-1200	4.8	7.4	8	7.9	12.8	15.3
V8	1200-1500	9.1	11.3	11	7.7	20.1	19
V9	0-300	4.3	4.5	9.8	9.1	14.1	13.6
V9	300-600	3.4	4	8.6	8.1	12	12.1
V9	600-900	3.1	5.9	8	8	11.1	13.9
V9	900-1200	3.4	14.8	7.7	7.3	11.1	22.1
V9	1200-1500	13.9	11.7	7.6	7.4	21.5	19.1
V10	0-300	11.1	5.3	7.5	10.7	18.6	16
V10	300-600	3.6	5	8.8	7.5	12.4	12.5
V10	600-900	11.1	10.2	7.5	8.1	18.6	18.3
V10	900-1200	10.8	8.1	7.3	7.4	18.1	15.5
V11	0-300	6.3	7.7	10.5	10.9	16.8	18.6
V11	300-600	8	5.9	7.4	8.1	15.4	14
V11	600-900	11.1	9	6.7	7.5	17.8	16.5
V11	900-1200	10.1	11.5	7.3	5.7	17.4	17.2
V11	1200-1500	8.1	9.3	7.2	6	15.3	15.3
V12	0-300	4.1	5.6	7.8	7.8	11.9	13.4
V12	300-600	6.4	6.1	6.4	6.2	12.8	12.3
V12	600-900	12.4	20	8.3	6	20.7	26
V12	900-1200	14.7	22.5	6	5.9	20.7	28.4
V12	1200-1500	21.8	21.4	5.4	6.5	27.2	27.9
Average		8.9	9.8	7.6	7.6	16.5	17.4
Minimum		2.0	2.7	5.4	5.7	9.4	9.9
Maximum		30.6	31.0	11.0	10.9	39.3	38.1
Standard deviation		6.1	6.1	1.1	1.2	6.1	5.9
Coefficient of variation		68.3	62.5	14.8	15.2	36.6	33.8

Table 2.c Inorganic N concentrations in single and composite soil samples from the Hofmeyr study site. Extraction was done with 2.0 M KCl

Point	Depth (mm)	NO ₃ ⁻ -N (mg/kg)		NH ₄ ⁺ -N (mg/kg)		TIN (mg/kg)	
		Single	Composite	Single	Composite	Single	Composite
V1	0-300	9.6	8.5	8.5	8.2	18.1	16.7
V1	300-600	9.7	10.8	5.6	5.7	15.3	16.5
V2	0-300	4	2.3	8.3	7.8	12.3	10.1
V3	0-300	1.5	1.5	8.8	11	10.3	12.5
V3	300-600	2	3.4	8.4	7.2	10.4	10.6
V4	0-300	2.7	3.1	7.7	7.3	10.4	10.4
V5	0-300	2.4	2	9.8	12	12.2	14
V5	300-600	1.7	2.1	5.8	6.8	7.5	8.9
V5	600-900	2.6	2.4	6.5	5.8	9.1	8.2
V6	0-300	2.3	4.5	8.7	6.9	11	11.4
V6	300-600	2.1	6.1	6.7	6.2	8.8	12.3
V7	0-300	2.3	5.2	11.7	7.5	14	12.7
V7	300-600	5.6	6.3	7.2	6.7	12.8	13
V8	0-300	1.8	4	6.2	11.8	8	15.8
V9	0-300	2.3	6.5	11.9	6.8	14.2	13.3
V10	0-300	2.4	4.7	8.5	7.2	10.9	11.9
V10	300-600	1.7	2.4	7.1	6.7	8.8	9.1
V10	600-900	1.3	2	6.1	6	7.4	8
V11	0-300	5.3	11	7.4	9.6	12.7	20.6
V12	0-300	7.5	6.3	8.5	8.6	16	14.9
V12	300-600	1.8	2.3	6.6	6.7	8.4	9
Average		3.5	4.6	7.9	7.7	11.4	12.4
Minimum		1.3	1.5	5.6	5.7	7.4	8.0
Maximum		9.7	11.0	11.9	12.0	18.1	20.6
Standard deviation		2.6	2.8	1.7	1.9	3.0	3.2
Coefficient of variation		74.6	61.0	21.8	24.1	26.0	26.2

Table 2.d Inorganic N concentrations in single and composite soil samples from the Empangeni study site. Extraction was done with 2.0 M KCl.

Point	Depth (mm)	NO ₃ ⁻ -N (mg/kg)		NH ₄ ⁺ -N (mg/kg)		TIN (mg/kg)	
		Single	Composite	Single	Composite	Single	Composite
V1	0-300	2.7	5.9	7.5	7.7	10.2	13.6
V1	300-600	3.7	5.8	7.1	7.1	10.8	12.9
V1	600-900	3.9	4.1	6.9	7.5	10.8	11.6
V1	900-1200	2.4	2.7	7.3	7.4	9.7	10.1
V2	0-300	4.7	5.9	8.3	8.9	13	14.8
V2	300-600	5.9	8	8	8.5	13.9	16.5
V2	600-900	5.3	6.1	6.8	6.6	12.1	12.7
V3	0-300	4.5	4.3	8.6	9.6	13.1	13.9
V3	300-600	3.1	3.2	6.9	7.2	10	10.4
V3	600-900	3.4	3.2	7	6.5	10.4	9.7
V3	900-1200	3.1	3	6.4	6.5	9.5	9.5
V4	0-300	17.8	8.2	7.9	8.8	25.7	17
V4	300-600	7.4	9.5	8.1	7.1	15.5	16.6
V4	600-900	5.7	7.7	7.2	7	12.9	14.7
V4	900-1200	4.7	4.2	7	7.2	11.7	11.4
V5	0-300	5.9	5.6	8.6	8.7	14.5	14.3
V5	300-600	4.6	7.8	7.6	8.6	12.2	16.4
V5	600-900	4.4	5.8	7.7	7.9	12.1	13.7
V5	900-1200	4	4.7	7.7	7.9	11.7	12.6
V5	1200-1500	3.9	4.3	7.9	7.2	11.8	11.5
V6	0-300	6.6	7	10.2	10.2	16.8	17.2
V6	300-600	5.4	6.7	8.1	9.6	13.5	16.3
V6	600-900	5	5.1	8.1	14.1	13.1	19.2
V6	900-1200	4.8	5.3	8.4	8.2	13.2	13.5
V6	1200-1500	4.6	4.9	8.8	8.2	13.4	13.1
V7	0-300	9.5	12.4	8.5	9.8	18	22.2
V7	300-600	13.1	15.5	8.8	8.2	21.9	23.7
V7	600-900	10.8	14.1	7.9	8	18.7	22.1
V7	900-1200	7.3	11.9	8.5	8.3	15.8	20.2
V7	1200-1500	5.7	10.6	7.8	8.1	13.5	18.7
V8	0-300	6.6	7.7	10.8	13.6	17.4	21.3
V8	300-600	5.7	6.2	16.1	10.5	21.8	16.7
V8	600-900	5.6	5.8	15.1	9.8	20.7	15.6
V8	900-1200	5.4	6.4	9.6	9.7	15	16.1
V8	1200-1500	5.4	5.9	8.8	9.3	14.2	15.2
V9	0-300	21	19.5	17.2	12.8	38.2	32.3
V9	300-600	34.3	15.4	8.6	10.2	42.9	25.6
V9	600-900	31.8	13	8.4	9	40.2	22
V9	900-1200	20.6	10.9	8.5	8.1	29.1	19
V9	1200-1500	9.3	9.4	14.4	16	23.7	25.4
V10	0-300	6.8	15.4	9.1	13.2	15.9	28.6
V10	300-600	7.7	10.9	9.9	10.2	17.6	21.1
V10	600-900	8.2	11.6	15.2	12.5	23.4	24.1
V10	900-1200	7.5	12.1	9.1	9.1	16.6	21.2
V10	1200-1500	7.3	9.7	9.5	8.1	16.8	17.8
V11	0-300	8.4	8.3	12	11.5	20.4	19.8
V11	300-600	7.5	8.1	9.6	16.7	17.1	24.8
V11	600-900	7.1	8	9.5	10.5	16.6	18.5
V12	0-300	8.8	9.6	10.8	11.7	19.6	21.3
V12	300-600	7.9	8.4	10.9	10.1	18.8	18.5
V12	600-900	8.1	7.8	9.5	10.1	17.6	17.9
V12	900-1200	7.9	9.6	8.6	13.7	16.5	23.3
V12	1200-1500	7.5	8.1	8.3	9.8	15.8	17.9
Average		7.9	8.1	9.2	9.5	17.1	17.6
Minimum		2.4	2.7	6.4	6.5	9.5	9.5
Maximum		34.3	19.5	17.2	16.7	42.9	32.3
Standard deviation		6.3	3.7	2.4	2.4	7.2	5.0
Coefficient of variation		79.6	45.0	26.3	25.0	42.0	28.4

Appendix 3. Inorganic N concentrations in 2.0 M KCl and SATe soil extracts

Table 3.a Inorganic N concentrations determined in 2.0 M KCl and SATe at Douglas

Point	Depth	Sample type	NO ₃ ⁻ -N (mg/kg)		NH ₄ ⁺ -N (mg/kg)	
			2.0 M KCl	SATe	2.0 M KCl	SATe
V1	0-300	Single	5.1	1.9	7.9	0.8
V1	300-600	Single	3.9	4.9	7.1	0.6
V1	600-900	Single	3.6	4.1	6.7	0.4
V1	900-1200	Single	3.2	4.2	6.3	0.4
V1	1200-1500	Single	8.2	12.8	6.5	0.9
V1	0-300	Composite	4.4	1.8	6.9	0.6
V1	300-600	Composite	3.6	3.9	7.2	0.3
V1	600-900	Composite	3.7	3.5	6.5	0.4
V1	900-1200	Composite	5.4	6.8	9.4	0.4
V1	1200-1500	Composite	13.6	2.1	6.2	0.4
V2	0-300	Single	6.6	0.7	7.8	0.3
V2	300-600	Single	3.8	0.0	6.3	0.6
V2	600-900	Single	3.0	2.3	6.9	0.3
V2	900-1200	Single	2.8	0.1	6.4	0.6
V2	1200-1500	Single	3.2	2.4	6.8	0.5
V2	0-300	Composite	5.7	0.6	8.1	0.4
V2	300-600	Composite	3.0	2.1	6.8	0.2
V2	600-900	Composite	3.3	1.9	6.7	0.5
V2	900-1200	Composite	2.9	2.1	6.9	0.6
V2	1200-1500	Composite	3.7	0.1	6.9	0.6
V3	0-300	Single	3.9	1.0	7.2	0.3
V3	300-600	Single	3.2	3.9	6.5	0.4
V3	600-900	Single	5.4	0.2	6.7	0.6
V3	0-300	Composite	4.1	0.0	7.4	0.7
V3	300-600	Composite	3.0	3.8	6.4	0.5
V3	600-900	Composite	4.9	0.0	6.4	0.6
V4	0-300	Single	5.5	0.0	7.2	0.3
V4	300-600	Single	4.0	8.8	7.1	0.9
V4	600-900	Single	8.6	3.9	6.5	0.4
V4	900-1200	Single	5.8	1.5	6.1	0.3
V4	1200-1500	Single	3.9	0.1	6.2	0.4
V4	0-300	Composite	5.4	3.1	7.6	0.2
V4	300-600	Composite	5.6	6.2	6.5	0.3
V4	600-900	Composite	7.6	2.7	6.6	0.2
V4	900-1200	Composite	4.8	1.1	6.5	0.4
V4	1200-1500	Composite	3.4	0.3	6.1	0.5
V5	0-300	Single	5.4	0.1	7.6	0.2
V5	300-600	Single	4.0	0.9	7.4	0.3
V5	600-900	Single	3.5	2.0	7.1	0.3
V5	900-1200	Single	4.6	0.0	6.7	0.0
V5	1200-1500	Single	4.4	0.0	6.4	0.3
V5	0-300	Composite	5.9	0.0	7.9	0.0
V5	300-600	Composite	3.8	0.0	7.1	0.2
V5	600-900	Composite	3.8	2.8	6.9	0.3
V5	900-1200	Composite	6.5	3.0	6.6	0.2
V5	1200-1500	Composite	7.4	0.0	5.9	0.5
V6	0-300	Single	7.6	0.0	7.4	0.1
V6	300-600	Single	4.0	2.3	6.0	0.2
V6	600-900	Single	5.6	5.6	5.9	0.2
V6	900-1200	Single	10.7	7.1	6.0	0.2
V6	1200-1500	Single	8.9	0.0	5.9	0.4
V6	0-300	Composite	5.9	0.0	6.8	0.3
V6	300-600	Composite	4.3	1.1	7.1	0.2
V6	600-900	Composite	5.1	3.5	5.2	0.3
V6	900-1200	Composite	7.0	4.3	6.1	0.1
V6	1200-1500	Composite	7.9	0.1	6.3	0.5
V7	0-300	Single	9.7	0.2	7.3	0.9
V7	300-600	Single	5.3	0.5	6.1	0.3
V7	600-900	Single	5.1	0.3	6.5	1.1
V7	900-1200	Single	5.1	1.3	6.8	0.5
V7	1200-1500	Single	5.0	1.1	6.7	0.3
V7	0-300	Composite	7.7	0.1	7.5	0.4
V7	300-600	Composite	5.5	0.3	6.4	0.6
V7	600-900	Composite	5.0	0.2	6.2	0.3
V7	900-1200	Composite	5.9	2.7	5.8	0.9

Table 3.a Continued

V7	1200-1500	Composite	5.4	1.5	6.6	0.4
V8	0-300	Single	7.7	2.1	7.4	0.3
V8	300-600	Single	5.8	0.1	7.0	0.7
V8	600-900	Single	18.4	11.4	6.5	0.4
V8	900-1200	Single	64.4	61.4	6.8	0.7
V8	1200-1500	Single	111.9	78.5	6.4	0.4
V8	0-300	Composite	12.8	1.6	6.3	0.1
V8	300-600	Composite	15.5	8	6.6	0.3
V8	600-900	Composite	47.3	34.1	7.1	0.3
V8	900-1200	Composite	72.6	51.4	6.8	0.3
V8	1200-1500	Composite	64.9	47.4	5.5	0.4
V9	0-300	Single	10.2	1.1	8.7	0.7
V9	300-600	Single	7.9	0.6	6.7	0.9
V9	600-900	Single	21.4	16.9	7.5	1.2
V9	900-1200	Single	6.8	0.7	7.4	1.2
V9	1200-1500	Single	14.4	12.7	7.1	1.3
V9	0-300	Composite	9.6	0.3	7.6	0.6
V9	300-600	Composite	7.7	1.8	7.5	2
V9	600-900	Composite	22	18.1	6.7	0.5
V9	900-1200	Composite	14.4	7.1	6.4	0.3
V9	1200-1500	Composite	14.4	8.1	5.4	0.4
V10	0-300	Single	10.1	0.4	7.9	0.5
V10	300-600	Single	8.5	2.8	6.8	0.3
V10	600-900	Single	20.5	15.5	6.7	0.4
V10	900-1200	Single	14	8	7.2	0.3
V10	0-300	Composite	9.7	0.9	9.7	0.6
V10	300-600	Composite	7.8	2	7.8	0.3
V10	600-900	Composite	19.9	10.7	7.8	0.3
V10	900-1200	Composite	13.4	5	7.8	0.3
V11	0-300	Single	9.7	0.4	8.8	0.6
V11	300-600	Single	7	16.3	8.4	1.1
V11	600-900	Single	13.7	14.9	8.1	1.7
V11	900-1200	Single	26.2	16.2	8.2	0.5
V11	1200-1500	Single	23.2	15.6	7.9	0.6
V11	0-300	Composite	10.4	0.9	8.6	0.6
V11	300-600	Composite	6.1	4.7	7.2	0.8
V11	600-900	Composite	8.1	8.3	6.7	0.8
V11	900-1200	Composite	9.2	6.3	6.7	0.5
V11	1200-1500	Composite	8.5	9	7.1	0.7
V12	0-300	Single	5.2	1.7	8	0
V12	300-600	Single	8.3	7.9	6.7	0.4
V12	600-900	Single	3.7	2	6.6	0.5
V12	900-1200	Single	3.1	2.3	6.2	0.6
V12	1200-1500	Single	4.3	5.1	6	0.7
V12	0-300	Composite	4	0.8	7.5	0
V12	300-600	Composite	2.9	1.2	6.4	0
V12	600-900	Composite	3.8	3	6.2	0.5
V12	900-1200	Composite	2.8	2.4	6.8	0
V12	1200-1500	Composite	4.6	0.6	6.7	0.4
Average			10.2	5.8	6.9	0.5
Minimum			2.8	0	5.2	0
Maximum			111.9	78.5	9.7	2
Standard deviation			14.9	11.8	0.8	0.3
Coefficient of variation			145.3	202	11.3	66.6

Table 3.b Inorganic N concentrations determined in 2.0 M KCl and SATe at Luckhoff

Point	Depth	Sample type	NO ₃ ⁻ -N (mg/kg)		NH ₄ ⁺ -N (mg/kg)	
			2.0 M KCl	SATe	2.0 M KCl	SATe
V1	0-300	Single	30.2	24.5	9.1	0.0
V1	300-600	Single	4.9	4.0	6.8	0.0
V1	600-900	Single	5.9	4.8	7.2	0.4
V1	900-1200	Single	11.9	12.5	6.4	0.6
V1	1200-1500	Single	21.4	21.6	7.0	0.6
V1	0-300	Composite	18.0	15.9	9.0	0.0
V1	300-600	Composite	11.6	10.9	6.9	0.0
V1	600-900	Composite	10.0	10.1	6.2	0.6
V1	900-1200	Composite	13.3	13.2	7.4	0.7
V1	1200-1500	Composite	23.9	29.4	6.5	0.5
V2	0-300	Single	5.1	3.2	8.4	0.0
V2	300-600	Single	4.8	3.9	7.2	0.7
V2	600-900	Single	7.1	6.7	7.0	0.6
V2	900-1200	Single	11.5	12.4	6.7	0.4
V2	1200-1500	Single	7.2	9.2	6.5	0.5
V2	0-300	Composite	9.3	6.4	8.4	0.0
V2	300-600	Composite	8.3	7.4	7.5	0.7
V2	600-900	Composite	12.1	12.7	7.1	0.6
V2	900-1200	Composite	11.2	10.1	6.7	0.6
V2	1200-1500	Composite	10.5	13.3	7.2	0.5
V3	0-300	Single	4.6	2.1	8.0	0.0
V3	300-600	Single	2.2	1.1	7.2	0.7
V3	600-900	Single	5.8	7.7	7.7	1.2
V3	900-1200	Single	12.9	20.2	7.5	0.8
V3	1200-1500	Single	7.8	13.8	6.8	0.8
V3	0-300	Composite	3.5	2.2	9.7	0.0
V3	300-600	Composite	3.3	2.6	6.9	0.0
V3	600-900	Composite	5.0	6.7	7.8	0.0
V3	900-1200	Composite	10.7	11.3	7.4	0.6
V3	1200-1500	Composite	9.0	17.5	6.7	0.9
V4	0-300	Single	4.4	1.6	8.7	0.0
V4	300-600	Single	2.0	0.3	7.5	0.4
V4	600-900	Single	4.5	3.8	7.1	0.7
V4	900-1200	Single	8.9	7.5	6.9	0.0
V4	1200-1500	Single	10.7	13.7	7.5	0.0
V4	0-300	Composite	4.1	1.8	8.9	0.0
V4	300-600	Composite	3.7	2.1	7.2	0.5
V4	600-900	Composite	4.0	3.3	9.2	0.0
V4	900-1200	Composite	4.7	6.2	7.3	0.0
V4	1200-1500	Composite	8.5	10.4	7.0	0.0
V5	0-300	Single	5.1	2.0	10.2	0.0
V5	300-600	Single	5.5	2.8	7.1	0.0
V5	600-900	Single	6.2	6.5	6.6	0.0
V5	900-1200	Single	13.0	15.5	7.5	0.8
V5	1200-1500	Single	14.9	20.1	6.7	0.0
V5	0-300	Composite	5.4	2.0	8.8	0.0
V5	300-600	Composite	4.7	4.4	6.7	0.0
V5	600-900	Composite	7.1	8.0	6.9	0.0
V5	900-1200	Composite	16.2	14.7	7.1	0.0
V5	1200-1500	Composite	13.1	22.0	6.7	0.0
V6	0-300	Single	12.8	9.2	10.3	0.0
V6	300-600	Single	15.9	0.8	7.2	0.4
V6	600-900	Single	7.0	25.2	7.0	0.0
V6	900-1200	Single	7.2	9.1	6.5	1.0
V6	1200-1500	Single	8.3	10.6	7.2	0.6
V6	0-300	Composite	21.6	9.4	10.4	0.5
V6	300-600	Composite	16.0	31.7	7.0	0.3
V6	600-900	Composite	6.1	33.4	7.2	0.7
V6	900-1200	Composite	7.4	7.9	7.0	0.6
V6	1200-1500	Composite	10.4	8.7	8.1	0.5
V7	0-300	Single	4.9	14.6	8.6	0.6
V7	300-600	Single	3.6	4.0	6.9	0.0
V7	600-900	Single	8.1	2.5	7.5	0.0

Table 3.b Continued

V7	900-1200	Single	16	18.1	6.8	0.7
V7	1200-1500	Single	30.6	1.9	8.5	0.2
V7	0-300	Composite	5.1	7.6	8.3	0.3
V7	300-600	Composite	3.4	2.7	6.5	0
V7	600-900	Composite	8.7	2.9	7.3	0
V7	900-1200	Composite	19.9	16.2	7.2	0
V7	1200-1500	Composite	31	46.6	7.1	0
V8	0-300	Single	4.6	50.1	9	0
V8	300-600	Single	2.6	3.4	6.8	0
V8	600-900	Single	3.1	1	8.8	0.9
V8	900-1200	Single	4.8	3.3	8	0
V8	1200-1500	Single	9.1	7	11	0
V8	0-300	Composite	3.7	1.9	9.7	0
V8	300-600	Composite	2.7	3.2	8.5	0
V8	600-900	Composite	4.4	4.8	8	0
V8	900-1200	Composite	7.4	10	7.9	0
V8	1200-1500	Composite	11.3	14.5	7.7	0.4
V9	0-300	Single	4.3	2.3	9.8	0
V9	300-600	Single	3.4	2.5	8.6	0
V9	600-900	Single	3.1	4	8	0.9
V9	900-1200	Single	3.4	4.4	7.7	0.9
V9	1200-1500	Single	13.9	17.6	7.6	0.6
V9	0-300	Composite	4.5	2.1	9.1	0
V9	300-600	Composite	4	2.8	8.1	0
V9	600-900	Composite	5.9	10.9	8	0
V9	900-1200	Composite	14.8	28.5	7.3	0.9
V9	1200-1500	Composite	11.7	19.9	7.4	1.2
V10	0-300	Single	11.1	2.4	7.5	0
V10	300-600	Single	3.6	1.9	8.8	0
V10	600-900	Single	11.1	14.7	7.5	0.3
V10	900-1200	Single	10.8	13.7	7.3	0.4
V10	0-300	Composite	5.3	2.5	10.7	0
V10	300-600	Composite	5	5.5	7.5	0
V10	600-900	Composite	10.2	14.2	8.1	0
V10	900-1200	Composite	8.1	9.1	7.4	0
V11	0-300	Single	6.3	2.3	10.5	0
V11	300-600	Single	8	9.3	7.4	0.6
V11	600-900	Single	11.1	14.4	6.7	0.5
V11	900-1200	Single	10.1	24.2	7.3	0
V11	1200-1500	Single	8.1	14.2	7.2	0.7
V11	0-300	Composite	7.7	5	10.9	0.1
V11	300-600	Composite	5.9	6.8	8.1	0.5
V11	600-900	Composite	9	14.8	7.5	3.2
V11	900-1200	Composite	11.5	13.8	5.7	16.6
V11	1200-1500	Composite	9.3	9.1	6	17.2
V12	0-300	Single	4.1	18.1	7.8	1.9
V12	300-600	Single	6.4	27.2	6.4	1.3
V12	600-900	Single	12.4	17.1	8.3	0
V12	900-1200	Single	14.7	20.3	6	0
V12	1200-1500	Single	21.8	9.5	5.4	0.6
V12	0-300	Composite	5.6	12.7	7.8	0
V12	300-600	Composite	6.1	21.7	6.2	3.3
V12	600-900	Composite	20	22.9	6	0.4
V12	900-1200	Composite	22.5	38.2	5.9	2.8
V12	1200-1500	Composite	21.4	21	6.5	0
Average			9.4	11.1	7.6	0.7
Minimum			2	0.3	5.4	0
Maximum			31	50.1	11	17.2
Standard deviation			6.1	9.4	1.1	2.2
Coefficient of variation			65.1	85	14.9	331

Table 3.c Inorganic N concentrations determined in 2.0 M KCl and SATe at Hofmeyr

Point	Depth	Sample type	NO ₃ ⁻ -N (mg/kg)		NH ₄ ⁺ -N (mg/kg)	
			2.0 M KCl	SATe	2.0 M KCl	SATe
V1	0-300	Single	9.6	52.2	8.5	4.6
V1	300-600	Single	9.7	12.7	5.6	0.0
V1	0-300	Composite	8.5	13.2	8.2	0.0
V1	300-600	Composite	10.8	2.6	5.7	0.2
V2	0-300	Single	4.0	2.8	8.3	0.0
V2	0-300	Composite	2.3	2.6	7.8	0.0
V3	0-300	Single	1.5	1.4	8.8	0.0
V3	300-600	Single	2.0	1.6	8.4	0.2
V3	0-300	Composite	1.5	3.2	11.0	0.6
V3	300-600	Composite	3.4	1.6	7.2	0.1
V4	0-300	Single	2.7	1.5	7.7	0.0
V4	0-300	Composite	3.1	2.9	7.3	0.3
V5	0-300	Single	2.4	3.5	9.8	0.0
V5	300-600	Single	1.7	4.1	5.8	0.4
V5	600-900	Single	2.6	3.9	6.5	0.0
V5	0-300	Composite	2.0	1.1	12.0	1.4
V5	300-600	Composite	2.1	3.6	6.8	0.0
V5	600-900	Composite	2.4	3.5	5.8	0.0
V6	0-300	Single	2.3	2.2	8.7	0.0
V6	300-600	Single	2.1	2.7	6.7	0.2
V6	0-300	Composite	4.5	12.0	6.9	0.0
V6	300-600	Composite	6.1	2.3	6.2	0.1
V7	0-300	Single	2.3	9.2	11.7	0.0
V7	300-600	Single	5.6	4.1	7.2	0.0
V7	0-300	Composite	5.2	7.4	7.5	0.3
V7	300-600	Composite	6.3	3.5	6.7	0.0
V8	0-300	Single	1.8	5.2	6.2	0.2
V8	0-300	Composite	4.0	2.1	11.8	0.1
V9	0-300	Single	2.3	3.2	11.9	0.0
V9	0-300	Composite	6.5	2.0	6.8	0.3
V10	0-300	Single	2.4	4.5	8.5	0.1
V10	300-600	Single	1.7	2.5	7.1	0.0
V10	600-900	Single	1.3	4.1	6.1	0.0
V10	0-300	Composite	4.7	3.1	7.2	0.8
V10	300-600	Composite	2.4	4.0	6.7	0.0
V10	600-900	Composite	2.0	4.0	6.0	0.0
V11	0-300	Single	5.3	4.3	7.4	0.3
V11	0-300	Composite	11.0	2.8	9.6	0.0
V12	0-300	Single	7.5	2.0	8.5	0.0
V12	300-600	Single	1.8	3.0	6.6	0.5
V12	0-300	Composite	6.3	2.5	8.6	0.2
V12	300-600	Composite	2.3	18.3	6.7	0.0
Average			4.0	5.4	7.8	0.3
Minimum			1.3	1.1	5.6	0.0
Maximum			11.0	52.2	12.0	4.6
Standard deviation			2.7	8.2	1.8	0.7
Coefficient of variation			67.7	151.0	22.7	272.6

Table 3.d Inorganic N concentrations determined in 2.0 M KCl and SATe at Empangeni

Point	Depth	Sample type	NO ₃ ⁻ -N (mg/kg)		NH ₄ ⁺ -N (mg/kg)	
			2.0 M KCl	SATe	2.0 M KCl	SATe
V1	0-300	Single	2.7	4.2	7.5	0.7
V1	300-600	Single	3.7	9.5	7.1	1.3
V1	600-900	Single	3.9	4.4	6.9	1.9
V1	900-1200	Single	2.4	0.9	7.3	4.8
V1	0-300	Composite	5.9	0.4	7.7	0.8
V1	300-600	Composite	5.8	9.3	7.1	1.6
V1	600-900	Composite	4.1	1.8	7.5	0.8
V1	900-1200	Composite	2.7	0.7	7.4	5.7
V2	0-300	Single	4.7	1.4	8.3	2.9
V2	300-600	Single	5.9	15.8	8.0	1.8
V2	600-900	Single	5.3	8.2	6.8	0.3
V2	0-300	Composite	5.9	6.3	8.9	2.9
V2	300-600	Composite	8.0	16.5	8.5	0.9
V2	600-900	Composite	6.1	1.1	6.6	2.8
V3	0-300	Single	4.5	1.0	8.6	4.0
V3	300-600	Single	3.1	1.1	6.9	1.4
V3	600-900	Single	3.4	1.8	7.0	2.2
V3	900-1200	Single	3.1	1.2	6.4	3.9
V3	0-300	Composite	4.3	1.0	9.6	1.6
V3	300-600	Composite	3.2	1.1	7.2	1.5
V3	600-900	Composite	3.2	0.9	6.5	1.3
V3	900-1200	Composite	3.0	36.0	6.5	5.2
V4	0-300	Single	17.8	1.6	7.9	2.1
V4	300-600	Single	7.4	12.6	8.1	1.8
V4	600-900	Single	5.7	4.8	7.2	2.7
V4	900-1200	Single	4.7	4.6	7.0	3.4
V4	0-300	Composite	8.2	20.8	8.8	2.1
V4	300-600	Composite	9.5	21.4	7.1	2.0
V4	600-900	Composite	7.7	2.7	7.0	2.0
V4	900-1200	Composite	4.2	3.0	7.2	3.3
V5	0-300	Single	5.9	2.7	8.6	2.9
V5	300-600	Single	4.6	5.9	7.6	2.1
V5	600-900	Single	4.4	3.1	7.7	2.0
V5	900-1200	Single	4.0	1.5	7.7	1.9
V5	1200-1500	Single	3.9	1.2	7.9	7.6
V5	0-300	Composite	5.6	15.5	8.7	1.7
V5	300-600	Composite	7.8	1.8	8.6	2.6
V5	600-900	Composite	5.8	2.6	7.9	2.1
V5	900-1200	Composite	4.7	5.4	7.9	1.7
V5	1200-1500	Composite	4.3	1.5	7.2	0.8
V6	0-300	Single	6.6	11.7	10.2	1.9
V6	300-600	Single	5.4	1.5	8.1	1.9
V6	600-900	Single	5.0	1.4	8.1	1.7
V6	900-1200	Single	4.8	13.8	8.4	0.1
V6	1200-1500	Single	4.6	1.3	8.8	2.7
V6	0-300	Composite	7.0	1.4	10.2	2.4
V6	300-600	Composite	6.7	3.4	9.6	1.1
V6	600-900	Composite	5.1	1.4	14.1	1.7
V6	900-1200	Composite	5.3	1.4	8.2	4.0
V6	1200-1500	Composite	4.9	1.3	8.2	1.7
V7	0-300	Single	9.5	3.6	8.5	1.8
V7	300-600	Single	13.1	2.4	8.8	1.8
V7	600-900	Single	10.8	9.4	7.9	1.7
V7	900-1200	Single	7.3	6.2	8.5	2.0
V7	1200-1500	Single	5.7	19.3	7.8	0.7
V7	0-300	Composite	12.4	25.9	9.8	1.6
V7	300-600	Composite	15.5	23.1	8.2	1.7
V7	600-900	Composite	14.1	18.6	8.0	1.2
V7	900-1200	Composite	11.9	17.6	8.3	0.9
V7	1200-1500	Composite	10.6	2.6	8.1	2.7

Table 3.d Continued

V8	0-300	Single	6.6	1	10.8	1.5
V8	300-600	Single	5.7	1.2	16.1	3.2
V8	600-900	Single	5.6	0.1	15.1	2
V8	900-1200	Single	5.4	0	9.6	1.4
V8	1200-1500	Single	5.4	0.1	8.8	4.6
V8	0-300	Composite	7.7	0.6	13.6	1.4
V8	300-600	Composite	6.2	0	10.5	0
V8	600-900	Composite	5.8	2.2	9.8	0.8
V8	900-1200	Composite	6.4	9.6	9.7	2
V8	1200-1500	Composite	5.9	22.6	9.3	0.3
V9	0-300	Single	21	40.1	17.2	1.2
V9	300-600	Single	34.3	49.3	8.6	1
V9	600-900	Single	31.8	27.9	8.4	1.3
V9	900-1200	Single	20.6	8.3	8.5	1
V9	1200-1500	Single	9.3	8.3	14.4	0
V9	0-300	Composite	19.5	15.8	12.8	0.8
V9	300-600	Composite	15.4	11.9	10.2	1
V9	600-900	Composite	13	8.4	9	1.8
V9	900-1200	Composite	10.9	5.9	8.1	1.4
V9	1200-1500	Composite	9.4	0.2	16	1.9
V10	0-300	Single	6.8	0	9.1	2.9
V10	300-600	Single	7.7	0.8	9.9	1.9
V10	600-900	Single	8.2	3.1	15.2	2
V10	900-1200	Single	7.5	0.3	9.1	1.2
V10	1200-1500	Single	7.3	14.1	9.5	3.1
V10	0-300	Composite	15.4	9.7	13.2	1.6
V10	300-600	Composite	10.9	0.1	10.2	2.9
V10	600-900	Composite	11.6	6.4	12.5	1
V10	900-1200	Composite	12.1	6.7	9.1	1.1
V10	1200-1500	Composite	9.7	0.1	8.1	1.9
V11	0-300	Single	8.4	0	12	0.8
V11	300-600	Single	7.5	0	9.6	0.5
V11	600-900	Single	7.1	0.4	9.5	2.4
V11	0-300	Composite	8.3	0.4	11.5	1.4
V11	300-600	Composite	8.1	1.8	16.7	0.8
V11	600-900	Composite	8	0.3	10.5	1.5
V12	0-300	Single	8.8	0	10.8	2.7
V12	300-600	Single	7.9	0	10.9	3.3
V12	600-900	Single	8.1	0.5	9.5	1.7
V12	900-1200	Single	7.9	0.8	8.6	1.1
V12	1200-1500	Single	7.5	2.6	8.3	0.1
V12	0-300	Composite	9.6	1	11.7	1
V12	300-600	Composite	8.4	0.2	10.1	2.7
V12	600-900	Composite	7.8	2.1	10.1	1.2
V12	900-1200	Composite	9.6	0.4	13.7	2.8
V12	1200-1500	Composite	8.1	0	9.8	0.5
Average			8	6.3	9.3	1.9
Minimum			2.4	0	6.4	0
Maximum			34.3	49.3	17.2	7.6
Standard deviation			5.1	9	2.4	1.2
Coefficient of variation			64	143.2	25.6	63.4

Appendix 4. Single and average EC_a measurements

Table 4.a Single and composite EC_a measurement for the Douglas site

Point	EC _a (mS/m) 0-750 mm depth		EC _a (mS/m) 0-1500 mm depth	
	Single measurement	Composite measurement	Single measurement	Composite measurement
V1	106.41	100.28	149.69	161.76
V2	74.96	73.05	127.93	118.95
V3	60.20		96.33	
V4	59.84	65.74	74.24	89.17
V5	43.09	44.52	146.25	79.17
V6	47.81	47.74	150.94	84.29
V7	75.55	72.99	179.65	90.18
V8	70.94	73.34	129.22	118.26
V9	85.23	84.30	125.31	160.81
V10	61.74	56.09	66.31	72.93
V11	116.37	112.99	172.42	176.73
V12	83.13	92.56	126.95	142.79
Average	73.77	74.87	128.77	117.73
Minimum	43.09	44.52	66.31	72.93
Maximum	116.37	112.99	179.65	176.73
Standard deviation	21.85	21.46	35.26	37.54
Coefficient of variation	29.61	28.66	27.38	31.89

Table 4.b Single and composite EC_a measurement for the Luckhoff site

Point	EC _a (mS/m) 0-750 mm		EC _a (mS/m) 0-1500	
	Single measurement	Composite measurement	Single measurement	Composite measurement
V1	16.06	14.68	24.73	23.62
V2	18.32	17.96	44.81	49.13
V3	13.67	13.92	21.33	23.47
V4	15.59	12.50	31.52	27.01
V5	21.72	23.97	80.16	36.65
V6	18.40	20.81	26.56	28.52
V7	24.02	25.11	38.71	37.72
V8	22.93	22.29	29.14	32.15
V9	20.59	18.91	32.46	33.05
V10	26.06	26.96	40.66	38.52
V11	28.48	29.70	40.82	46.17
V12	27.34	25.95	48.52	41.20
Average	21.10	21.06	38.28	34.77
Minimum	13.67	12.50	21.33	23.47
Maximum	28.48	29.70	80.16	49.13
Standard deviation	4.83	5.55	15.62	8.34
Coefficient of variation	22.89	26.36	40.81	23.99

Table 4.c Single and composite EC_a measurement for the Hofmeyr site

Point	EC _a (mS/m) 0-750 mm depth		EC _a (mS/m) 0-1500 mm depth	
	Single measurement	Composite measurement	Single measurement	Composite measurement
V1	16.06	14.68	24.73	23.62
V2	18.32	17.96	44.81	49.13
V3	13.67	13.92	21.33	23.47
V4	15.59	12.50	31.52	27.01
V5	21.72	23.97	80.16	36.65
V6	18.40	20.81	26.56	28.52
V7	24.02	25.11	38.71	37.72
V8	22.93	22.29	29.14	32.15
V9	20.59	18.91	32.46	33.05
V10	26.06	26.96	40.66	38.52
V11	28.48	29.70	40.82	46.17
V12	27.34	25.95	48.52	41.20
Average	30.63	29.99	19.69	26.10
Minimum	17.34	17.34	0.08	3.33
Maximum	60.63	61.16	36.06	41.18
Standard deviation	16.94	17.17	12.12	12.55
Coefficient of variation	55.32	57.26	61.53	48.09

Appendix 5. EC_a measurements, geometric mean and elevation data used for model development

Table 5.a Douglas EC_a measurements, geometric mean and elevation data

Point	EC _a (mS/m) 0-750 mm depth	EC _a (mS/m) 0-1500 mm depth	Geometric mean EC _a (mS/m) 0-1500 mm	Elevation (m)
V1	103.35	155.72	126.86	1042.76
V2	74.00	123.44	95.58	1014.76
V3	60.20	96.33	76.15	1010.10
V4	62.79	81.70	71.63	1007.26
V5	43.81	112.71	70.27	1012.54
V6	47.78	117.61	74.96	1008.33
V7	74.27	134.91	100.10	1010.80
V8	72.14	123.74	94.48	1011.00
V9	84.77	143.06	110.12	1000.51
V10	58.91	69.62	64.04	994.55
V11	114.68	174.58	141.49	1008.84
V12	87.84	134.87	108.85	1009.01
Average	73.71	122.36	94.54	1010.87
Minimum	43.81	69.62	64.04	994.55
Maximum	114.68	174.58	141.49	1042.76
Standard deviation	21.25	29.87	24.30	11.42
Coefficient of variation	28.84	24.41	25.70	1.13

Table 5.b Luckhoff EC_a measurements, geometric mean and elevation data

Point	EC _a (mS/m) 0-750 mm depth	EC _a (mS/m) 0-1500 mm depth	Geometric mean EC _a (mS/m) 0-1500 mm	Elevation (m)
V1	15.37	24.18	19.27	1210.85
V2	18.14	46.97	29.19	1198.42
V3	13.79	22.40	17.58	1201.17
V4	14.04	29.27	20.27	1208.97
V5	22.84	58.40	36.52	1200.04
V6	19.60	27.54	23.24	1207.70
V7	24.57	38.21	30.64	1205.83
V8	22.61	30.64	26.32	1206.40
V9	19.75	32.75	25.43	1194.16
V10	26.51	39.59	32.40	1198.17
V11	29.09	43.50	35.57	1192.91
V12	26.65	44.86	34.57	1196.64
Average	21.08	36.53	27.58	1201.77
Minimum	13.79	22.40	17.58	1192.91
Maximum	29.09	58.40	36.52	1210.85
Standard deviation	5.13	10.67	6.57	6.01
Coefficient of variation	24.36	29.21	23.83	0.50

Table 5.c Hofmeyr EC_a measurements, geometric mean and elevation data

Point	EC _a (mS/m) 0-375 mm depth	EC _a (mS/m) 0-750 mm depth	Geometric mean EC _a (mS/m) 0-750 mm	Elevation (m)
V1	26.43	34.19	30.06	1234.32
V2	20.46	24.35	22.32	1237.65
V3	21.35	35.67	27.60	1236.91
V4	20.71	21.66	21.18	1231.96
V5	21.05	33.60	26.59	1231.77
V6	60.89	1.70	10.18	1238.07
V7	17.34	29.81	22.74	1227.98
V8	22.01	27.24	24.48	1232.17
V9	20.00	25.50	22.58	1229.18
V10	58.92	7.56	21.10	1243.47
V11	55.08	4.64	15.99	1248.13
V12	19.45	28.86	23.70	1239.77
Average	30.31	22.90	22.38	1235.95
Minimum	17.34	1.70	10.18	1227.98
Maximum	60.89	35.67	30.06	1248.13
Standard deviation	17.05	11.82	5.25	5.94
Coefficient of variation	56.26	51.60	23.45	0.48

Appendix 6. Inorganic N stock in samples at Douglas, Luckhoff and Hofmeyr

Table 6.a Inorganic N in kg/ha for samples taken in 300 mm depth increments

Point	Depth (mm)	Douglas			Luckhoff			Hofmeyr		
		NO ₃ ⁻ -N	NH ₄ ⁺ -N	TIN	NO ₃ ⁻ -N	NH ₄ ⁺ -N	TIN	NO ₃ ⁻ -N	NH ₄ ⁺ -N	TIN
V1	0-300	20	32	52	79	39	118	42	41	83
V1	300-600	16	31	47	51	30	81	54	28	82
V1	600-900	16	28	45	44	27	71			
V1	900-1200	24	41	65	58	32	90			
V1	1200-1500	59	27	86	104	28	133			
V2	0-300	25	35	60	41	37	77	11	38	50
V2	300-600	14	33	47	36	33	69			
V2	600-900	16	33	49	53	31	84			
V2	900-1200	13	30	43	49	29	78			
V2	1200-1500	16	31	47	46	31	77			
V3	0-300	18	32	49	15	42	58	8	56	64
V3	300-600	14	30	44	14	30	45	18	38	55
V3	600-900	20	27	47	22	34	56			
V3	900-1200				47	32	79			
V3	1200-1500				39	29	69			
V4	0-300	25	35	59	18	39	57	15	35	50
V4	300-600	25	29	54	16	31	48			
V4	600-900	31	27	58	17	40	58			
V4	900-1200	21	28	49	21	32	52			
V4	1200-1500	13	24	37	37	31	68			
V5	0-300	26	35	61	24	38	62	10	58	68
V5	300-600	17	31	47	21	29	50	11	35	45
V5	600-900	16	30	46	31	30	61	12	29	41
V5	900-1200	26	26	52	71	31	102			
V5	1200-1500	32	25	57	57	29	87			
V6	0-300	24	28	53	94	45	140	22	33	55
V6	300-600	19	31	50	70	31	100	32	33	66
V6	600-900	22	23	45	27	31	58			
V6	900-1200	29	25	53	32	31	63			
V6	1200-1500	33	27	60	45	35	81			
V7	0-300	32	32	64	22	36	59	25	35	60
V7	300-600	24	27	51	15	28	43	32	34	67
V7	600-900	23	28	51	38	32	70			
V7	900-1200	26	26	52	87	31	118			
V7	1200-1500	23	28	50	135	31	166			
V8	0-300	53	26	79	16	42	59	19	55	74
V8	300-600	67	28	95	12	37	49			
V8	600-900	182	27	209	19	35	54			
V8	900-1200	281	26	308	32	35	67			
V8	1200-1500	262	22	284	49	34	83			
V9	0-300	39	31	70	20	40	59	30	32	62
V9	300-600	33	32	66	17	35	53			
V9	600-900	90	27	118	26	35	61			
V9	900-1200	58	26	83	65	32	97			
V9	1200-1500	55	20	75	51	32	83			
V10	0-300	43	43	86	23	47	70	22	34	56
V10	300-600	36	36	71	22	33	55	12	34	46
V10	600-900	87	34	121	45	35	80	11	32	43
V10	900-1200	53	31	84	35	32	68			
V10	1200-1500									
V11	0-300	44	37	81	34	48	81	55	48	103
V11	300-600	27	32	58	26	35	61			
V11	600-900	36	30	66	39	33	72			
V11	900-1200	38	28	65	50	25	75			
V11	1200-1500	37	31	67	41	26	67			
V12	0-300	17	33	50	24	34	59	32	44	75
V12	300-600	12	27	39	27	27	54	12	36	48
V12	600-900	16	26	41	87	26	114			
V12	900-1200	12	29	41	98	26	124			
V12	1200-1500	20	28	48	93	28	122			
Average		41	30	71	43	33	76	23	39	62
Minimum		12	20	37	12	25	43	8	28	41
Maximum		281	43	308	135	48	166	55	58	103
Standard deviation		52	4	51	27	5	26	14	9	16
Coefficient of variation		125	14	72	62	15	34	61	23	25

Table 6.b Inorganic N in kg/ha for cumulative soil sampling depths

Point	Depth (mm)	Douglas			Luckhoff			Hofmeyr		
		NO ₃ ⁻ -N	NH ₄ ⁺ -N	TIN	NO ₃ ⁻ -N	NH ₄ ⁺ -N	TIN	NO ₃ ⁻ -N	NH ₄ ⁺ -N	TIN
V1	0-300	20	32	52	79	39	118	42	41	83
V1	0-600	36	63	99	129	69	199	96	69	166
V1	0-900	52	91	143	173	97	270			
V1	0-1200	76	133	208	231	129	360			
V1	0-1500	135	160	294	336	157	493			
V2	0-300	25	35	60	41	37	77	11	38	50
V2	0-600	39	68	108	77	69	146			
V2	0-900	56	101	157	130	100	230			
V2	0-1200	68	131	199	179	130	308			
V2	0-1500	85	162	246	225	161	386			
V3	0-300	18	32	49	15	42	58	8	56	64
V3	0-600	31	61	93	30	73	102	25	94	119
V3	0-900	52	88	140	52	107	158			
V3	0-1200				98	139	237			
V3	0-1500				138	168	306			
V4	0-300	25	35	59	18	39	57	15	35	50
V4	0-600	49	63	113	34	70	104			
V4	0-900	80	90	171	52	111	162			
V4	0-1200	101	118	219	72	142	215			
V4	0-1500	114	142	257	109	173	282			
V5	0-300	26	35	61	24	38	62	10	58	68
V5	0-600	43	66	108	44	68	112	20	93	113
V5	0-900	59	95	154	75	98	173	32	122	154
V5	0-1200	85	122	207	146	129	275			
V5	0-1500	117	147	264	203	158	361			
V6	0-300	24	28	53	94	45	140	22	33	55
V6	0-600	43	59	103	164	76	240	54	66	121
V6	0-900	65	82	147	191	107	298			
V6	0-1200	94	107	201	223	138	361			
V6	0-1500	127	133	261	269	173	442			
V7	0-300	32	32	64	22	36	59	25	35	60
V7	0-600	56	59	115	37	65	102	57	70	126
V7	0-900	79	87	166	75	97	172			
V7	0-1200	105	113	217	162	128	290			
V7	0-1500	127	140	268	298	159	457			
V8	0-300	53	26	79	16	42	59	19	55	74
V8	0-600	120	54	174	28	80	107			
V8	0-900	302	82	383	47	114	162			
V8	0-1200	583	108	691	80	149	228			
V8	0-1500	845	130	975	129	183	312			
V9	0-300	39	31	70	20	40	59	30	32	62
V9	0-600	72	63	135	37	75	112			
V9	0-900	162	91	253	63	110	173			
V9	0-1200	220	116	336	128	142	270			
V9	0-1500	275	137	411	179	174	353			
V10	0-300	43	43	86	23	47	70	22	34	56
V10	0-600	79	79	157	202	221	423	34	68	102
V10	0-900	165	112	278	224	254	478	45	100	145
V10	0-1200	218	143	362	268	289	557			
V10	0-1500									
V11	0-300	44	37	81	34	48	81	55	48	103
V11	0-600	71	68	139	59	83	142			
V11	0-900	107	98	205	99	116	215			
V11	0-1200	145	126	270	149	141	290			
V11	0-1500	182	156	338	190	167	356			
V12	0-300	17	33	50	24	34	59	32	44	75
V12	0-600	30	60	89	51	61	112	44	79	123
V12	0-900	45	85	131	138	87	226			
V12	0-1200	57	114	172	237	113	350			
V12	0-1500	77	143	219	330	142	472			
Average		107	89	195	119	110	228	33	60	94
Minimum		17	26	49	15	34	57	8	32	50
Maximum		845	162	975	336	289	557	96	122	166
Standard deviation		135	40	156	87	56	133	21	26	36
Coefficient of variation		126	46	80	73	51	58	62	42	39